CAMILA SILVA BORGES

ASSESSING THE PERFORMANCE OF PROXIMAL SENSORS FOR SOIL AND PLANT ANALYSIS

LAVRAS – MG
2021

CAMILA SILVA BORGES

ASSESSING THE PERFORMANCE OF PROXIMAL SENSORS FOR SOIL AND PLANT ANALYSIS

Doctoral dissertation presented to the Federal University of Lavras as part of the requirements of the Graduate Program in Soil Science, area of concentration in Environmental Resources and Land Use, to obtain the degree of Doctor in Soil Science.

Prof. Dr. Bruno Teixeira Ribeiro

Advisor

LAVRAS-MG
2021

Ficha catalográfica elaborada pelo Sistema de Geração de Ficha Catalográfica da Biblioteca Universitária da UFLA, com dados informados pelo(a) próprio(a) autor(a).

Borges, Camila Silva.
Assessing the performance of proximal sensors for soil and plant analysis / Camila Silva Borges. - 2021.
100 p. : il.

Orientador(a): Bruno Teixeira Ribeiro.

Tese (doutorado) - Universidade Federal de Lavras, 2021.
Bibliografia.

1. Smart sensor. 2. Green chemistry. 3. portable X-Ray Fluorescence Spectrometry (pXRF). I. Ribeiro, Bruno Teixeira. II. Título.

CAMILA SILVA BORGES

ASSESSING THE PERFORMANCE OF PROXIMAL SENSORS FOR SOIL AND PLANT ANALYSIS

Doctoral dissertation presented to the Federal University of Lavras as part of the requirements of the Graduate Program in Soil Science, area of concentration in Environmental Resources and Land Use, to obtain the degree of Doctor in Soil Science.

APPROVED in 16 July 2021.

Dr. Luiz Roberto Guimarães Guilherme	UFLA
Dr. Sérgio Henrique Godinho Silva	UFLA
Dr. José Paulo Molin	ESALQ-USP
Dr. Fábio Luiz Melquiades	UEL

Prof. Dr. Bruno Teixeira Ribeiro
Advisor

LAVRAS - MG
2021

“L'important n'est pas ce qu'on fait de nous,
mais ce que nous faisons nous-mêmes de ce que
l'on fait de nous”

(O importante não é aquilo que fazem de nós,
mas o que nós mesmos fazemos do que os
outros fizeram de nós)

Jean-Paul Sartre

ACKNOWLEDGMENT

To God, for life and for all the opportunities it comes with.

To my husband Rooges, for his love, presence, support, encouragement and patience.

To my parents, Clara and Josimar and my sister, Gabriela, for their love, encouragement and the example to be followed.

To dear professor Dr. Bruno Teixeira Ribeiro, for once again guiding and encouraging me in scientific research. To you, my eternal thanks and respect.

To my dear friends Thalita and Ruby, for their affection and friendship.

To the professors who directly contributed to this thesis, especially professors Guilherme Lopes and Luiz Roberto (Bebeto).

To professor David C. Weindorf and to the Texas Tech University for the partnership and support in conducting this work.

To the incredible Betânia (Beth) and Geila (Geilinha) for their affection, friendship, promptness and for the incredible moments lived in the Laboratory of X-Ray Fluorescence and Environmental Chemistry at UFLA.

To the Department of Soil Science at UFLA and its employees for their support in carrying out this project, especially Dirce.

To Geraldo and to the CAMPO team (Center for Technological and Environmental Agriculture) for all their support in conventional foliar analyses.

To my dear Júlia (in memoriam) and Bolotinha (Loló) for their ability to bring joy to the most difficult moments.

To the Brazilian people, for another three years to finance my studies.

This work was conducted with the support of the National Council for Scientific and Technological Development (CNPq) or the Research Support Foundation of Minas Gerais (FAPEMIG).

This study was financed in part by the Coordenação de Aperfeiçoamento de Pessoal de Nível Superior – Brasil (CAPES) – Finance Code 001

RESUMO GERAL

A caracterização do solo e de plantas tem sido muito beneficiada pelo uso de sensores portáteis. Esta tese de doutorado empregou dois sensores: equipamento portátil de fluorescência de raios X (pXRF) e *Nix™ Pro Color Sensor* para caracterização de solos e plantas. O pXRF pode ser considerado um dos avanços mais importantes na análise de solos e plantas em todo o mundo. Já o *Nix™ Pro* é um sensor de bolso com conexão para smartphones via Bluetooth lançado recentemente no mercado que permite obter parâmetros de cor em diferentes sistemas (e.g., RGB, CMYK, CIELab) de qualquer superfície sólida. Para avaliar o desempenho desses sensores, este trabalho foi dividido em duas partes distintas: Solo e Planta. Na seção Solo, o pXRF foi empregado para obter a composição elementar total de solos de Veredas. Os resultados obtidos com pXRF foram comparados aos obtidos pelo método de digestão ácida. Na seção Planta, o pXRF foi usado para analisar mais de 600 amostras de folhas secas e moídas de diferentes culturas brasileiras. Os resultados foram correlacionados com o método convencional para análise foliar. Por fim, foi verificada a sensibilidade do *Nix™ Pro Color Sensor* para obter a cor de folhas intactas de plantas. Para isso, um atributo correlacionado à cor de folhas de plantas (índice SPAD) foi utilizado como variável dependente. O pXRF revelou grande potencial para caracterização elementar de solos de Veredas. Vários elementos foram determinados com sucesso via pXRF em condições de laboratório. Outras investigações em campo podem ser grandemente beneficiadas pelo pXRF, contribuindo para o inventário ainda escasso dos solos de Veredas do Cerrado. Para análise foliar, o pXRF revelou ser um método alternativo e ambientalmente amigável para determinar macro- e micronutrientes em materiais vegetais secos e moídos. O *Nix™ Pro Color Sensor* revelou-se sensível e como uma forma eficaz para determinação da cor de folhas de plantas. A partir deste estudo piloto, várias outras aplicações e calibrações podem ser realizadas para diferentes espécies de plantas e condições ambientais em todo o mundo, por exemplo, para estimar o conteúdo real de clorofila, N e Mg, e muitos fatores que influenciam o estado nutricional das plantas, baseado exclusivamente em parâmetros de cor obtidos com o sensor *Nix™ Pro*.

Palavras-chave: Sensores inteligentes. Química verde. pXRF.

GENERAL ABSTRACT

The characterization of soil and plants has been greatly benefited by the use of portable and in-field sensors. This doctoral thesis employed two sensors: portable X-ray fluorescence spectrometry (pXRF) and Nix™ Pro Color Sensor for soil and plant characterization. The pXRF can be considered one of the most important advances for soil and plant analysis worldwide. Nix™ Pro is a pocket-sized sensor with smartphone connection via Bluetooth recently launched in the market that allows to obtain color parameters in different systems (RGB, CMYK, CIELab) of any solid surface. To assess the performance of the above-mentioned sensors, this work was split into two distinct parts: Soil and Plant. In the Soil section, pXRF was employed to obtain the total elemental composition of wetland soils from Brazilian Savannah ("*Veredas*"). The pXRF results were compared to those obtained after wet digestion method. In the Plant section, pXRF was used to analyse more than 600 samples from different Brazilian crops. Also, the pXRF results were correlated to the conventional and standard method for foliar analysis. Finally, the sensibility of the Nix™ Pro Color Sensor to measure the greenness of intact plant leaves was verified. For that, a color-dependent parameter (SPAD index) was used as dependent variable. The pXRF revealed great potential for characterization of Cerrado wetland soils. Several elements were successfully determined via pXRF under lab conditions. Further in-field investigations may be greatly benefited by pXRF contributing to still scarce inventory of Cerrado wetland soils. For plant analysis, pXRF revealed to be an alternative environmental-friendly method to determine macro- and micronutrients in dried and ground plant materials. The Nix™ Pro Color Sensor revealed to be sensible and an effective way to determine the color of intact plant leaves. From this pilot study, several other applications and calibrations can be performed for different plant species and environmental conditions worldwide, for example, to estimate the real chlorophyll content, N and Mg contents, and many factors influencing the nutritional status of plants, based exclusively on color parameters from Nix™ Pro color sensor.

Keywords: Smart sensor. Green chemistry. pXRF.

CONTENTS

FIRST PART

GENERAL INTRODUCTION

The characterization of earth materials samples has been greatly benefited by the use of proximal sensors (Weindorf et al., 2014; Oyedotun, 2018). In Soil Science, several sensors have contributed to the advance of many subareas (e.g., Pedology, Physics, Chemistry, Mineralogy, and Soil Fertility). Proximal soil sensing can be defined as all technologies that use sensors close to or in direct contact to the soil in order to measure some property (Adamchuk et al., 2017). The main advantages of proximal sensing compared with laboratory-based methods include time and cost savings, non-destructive analysis and environmentally-friendly methods (Viscarra Rossel et al., 2011; Lima et al., 2019; Mancini et al., 2019; Tavares et al., 2019; Silva et al., 2020). Also, substantial data can be easily obtained via proximal sensors for modelling purposes (Viscarra Rossel et al., 2010), contributing to precision agriculture and smart farming (Molin et al., 2020; Bolfe et al., 2020). Currently, there are several sensors with different principles and technology to assess many soil properties (Viscarra Rossel et al., 2010; Viscarra Rossel et al., 2011).

This doctoral dissertation employed the portable X-ray fluorescence spectrometry (pXRF) and the Nix™ Pro for soil and plant characterization. Over the last ten years, pXRF can be considered one of the most important advances for soil and plant characterization worldwide (Weindorf et al., 2014; Ribeiro et al., 2017; Silva et al., 2021). In Brazil, an expressive increase of pXRF applications for characterization of tropical soils occurred over the last five years (Ribeiro et al., 2017; Silva et al., 2021). There is a great potential to analyze plant material via pXRF (McLaren et al., 2012; Reidinger et al., 2012; Guerra et al., 2018; Kalcsits et al., 2016; McGladdery et al., 2018) Recently, a pocket-sized color sensor known as Nix Pro (www.nixsensor.com) was launched in the market. Small, light and with Bluetooth connectivity to smartphones via Android and iOS operating systems, this sensor is able to measure instantaneously the color in different systems (CMYK, RGB, CIELab) of any solid surface. It has been successfully applied in Soil Science, for example, replacing the traditional Munsell Color Chart (Stiglitz et al., 2016). In Plant Science, it has not been used yet. Part one presents a brief overview of portable X-ray fluorescence spectrometry and Nix™ Pro Color Sensor.

In order to contribute to pXRF applications and methodology in tropical conditions, article 1 brings the characterization of wetland soils from Brazilian Savannah ("*Veredas*") via

pXRF. This work compares pXRF results with wet digestion methods. In chapter 4, a comprehensive assessment of the elemental composition (macro- and micronutrients) of dried and ground plant material via pXRF was performed. More than 600 samples across Brazil were used. Finally, article 3 for the first time assessed the performance and sensibility of the Nix™ Pro Color Sensor to measure the greenness of leaves from different crops. A color-dependent parameter (SPAD index) was used as dependent variable.

Two papers from this doctoral dissertation have been published and another one is currently under review:

Article 1 - Comparison of portable X-ray fluorescence spectrometry and laboratory-based methods to assess the soil elemental composition: Applications for wetland soils
Journal: Environmental Technology & Innovation
JCR: 5.263
DOI: 10.1016/j.eti.2020.100826

Article 2 - Foliar Elemental Analysis of Brazilian Crops via Portable X-ray Fluorescence Spectrometry
Journal: Sensors
JCR: 3.576
DOI: 10.3390/s20092509

Article 3 - Pocket-sized sensor to assess the color of plant leaves
Submitted to Journal of Plant Physiology
JCR: 3.549

REFERENCES

ADAMCHUK, V.; ALLRED, B.; DOOLITTLE, J.; GROTE, K.; VISCARRA ROSSEL, R. Tools for Proximal Soil Sensing. in: C. Ditzler, K. Scheffe, and H.C. Monger (Eds.), **Soil Survey Manual. Handbook** 18. Government Printing Office, Washington, D.C. p. 355-387 2016.

BOLFE, E.L.; JORGE, L.A.D.C.; SANCHES, I.D.; LUCHIARI JÚNIOR, A.; DA COSTA, C.C.; VICTORIA, D.D.C.; INAMASU, R.Y.; GREGO, C.R.; FERREIRA, V.R.; RAMIREZ, A.R. Precision and Digital Agriculture: Adoption of Technologies and Perception of Brazilian Farmers. **Agriculture,** v. 10, n. 653, 2020. https://doi.org/10.3390/agriculture10120653

GUERRA, M.B.B.; ADAME, A.; DE ALMEIDA, E.; BRASIL, M.A.S.; SCHAEFER, C.E.G.R.; KRUG, F.J. In situ determination of k, ca, s and si in fresh sugar cane leaves by handheld energy dispersive X-Ray fluorescence spectrometry. **Journal of the Brazilian Chemical Society**, v. 29, p.1086–1093, 2018. https://doi.org/10.21577/0103-5053.20170229

KALCSITS, L.A. Non-destructive measurement of calcium and potassium in apple and pear using handheld X-ray fluorescence. **Frontiers in Plant Science**, v. 7, p.1–8, 2016.

LIMA, T.M.; WEINDORF, D.C.; CURI, N.; GUILHERME, L.R.G.; LANA, R.M.Q.; RIBEIRO, B.T. Elemental analysis of Cerrado agricultural soils via portable X-ray fluorescence spectrometry: Inferences for soil fertility assessment. **Geoderma**, v. 353, p. 264–272, 2019. https://doi.org/10.1016/j.geoderma.2019.06.045

MANCINI, M.; WEINDORF, D. C.; CHAKRABORTY, S.; SILVA, S.H.G.; DOS SANTOS, A.F.T.; GUILHERME, L.R.G.; CURI, N. Tracing tropical soil parent material analysis via portable X-ray fluorescence (pXRF) spectrometry in Brazilian Cerrado**. Geoderma**, v. 337, p. 718–728, 2019. https://doi.org/10.1016/j.geoderma.2018.10.026.

MCGLADDERY, C.; WEINDORF, D.C.; CHAKRABORTY, S.; LI, B.; PAULETTE, L.; PODAR, D.; PEARSON, D.; KUSI, N.Y.O.; DUDA, B. Elemental assessment of vegetation via portable X-ray fluorescence (PXRF) spectrometry. **Journal of Environmental Management**, v. 210, p. 210–225, 2018. https://doi.org/10.1016/j.jenvman.2018.01.003

MCLAREN, T.I.; GUPPY, C.N.; TIGHE, M.K. A Rapid and Nondestructive Plant Nutrient Analysis using Portable X-Ray Fluorescence. **Soil Science Society of America Journal**, v. 76, n. 1446, 2012. https://doi.org/10.2136/sssaj2011.0355

MOLIN, J.P.; BAZAME, H.C.; MALDANER, L.; CORREDO, L.P.; MARTELLO, M.; CANATA, T.F. Precision agriculture and the digital contributions for site-specific management of the fields. **Revista Ciência Agronômica**, v. 51, 2020. https://doi.org/10.5935/1806-6690.20200088

OYEDOTUN, T. D. T. X-ray fluorescence (XRF) in the investigation of the composition of earth materials: a review and an overview. **Geology, Ecology, and Landscapes**, v. 2, p. 148-154, 2018. https://doi.org/10.1080/24749508.2018.1452459

REIDINGER, S.; RAMSEY, M.H.; HARTLEY, S.E. Rapid and accurate analyses of silicon and phosphorus in plants using a portable X-ray fluorescence spectrometer. **New Phytologist**, v. 195, p. 699–706, 2012. https://doi.org/10.1111/j.1469-8137.2012.04179.x

RIBEIRO, B.T.; SILVA, S.H.G.; SILVA, E.A.; GUILHERME, L.R.G. Aplicações da fluorescência de raios-X portátil (pXRF) na Ciência do Solo tropical. **Ciência e Agrotecnologia**, v. 41, p. 245–254, 2017. https://doi.org/10.1590/1413-70542017413000117

SILVA, S.H.G.; SILVA, E.A.; POGGERE, G.C.; PÁDUA JUNIOR, A.L.; GONÇALVES, M.G.M.; GUILHERME, L.R.G.; CURI, N. Modeling and prediction of sulfuric acid digestion analyses data from PXRF spectrometry in tropical soils. **Scientia Agricola**, v. 77, n. 12, 2020. https://doi.org/dx.doi.org/10.1590/1678-992X-2018-0132

SILVA, S. H. G.; RIBEIRO, B. T.; GUERRA, M. B. B.; DE CARVALHO, H. W. P.; LOPES, G.; CARVALHO, G. S.; GUILHERME, L.R.G.; RESENDE, M.; MANCINI, M.; CURI, N.; RAFAEL, R.B.A.; CARDELLI, V.; COCCO, S.; CORTI, G.; CHAKRABORTY, S.; LI, B.; WEINDORF, D. C. pXRF in tropical soils: Methodology, applications, achievements and challenges. **Advances in Agronomy**, v. 167, p. 1-62, 2021. https://doi.org/10.1016/bs.agron.2020.12.001

STIGLITZ, R.; MIKHAILOVA, E.; POST, C.; SCHLAUTMAN, M.; SHARP, J. Evaluation of an inexpensive sensor to measure soil color. **Computers and Electronics in Agriculture**, v. 121, p. 141–148, 2016. https://doi.org/10.1016/j.compag.2015.11.014

TAVARES, T.R.; NUNES, L.C.; ALVES, E.E.N.; ALMEIDA, E.; MALDANER, L.F.; KRUG, F.J.; CARVALHO, H.W.P.; MOLIN, J.P. Simplifying Sample Preparation for Soil Fertility Analysis by X-ray Fluorescence Spectrometry. **Sensors**, v. 19, n. 5066, 2019. https://doi.org/10.3390/s19235066

VISCARRA ROSSEL, R.A.; ADAMCHUK, V.I.; SUDDUTH, K.A.; MCKENZIE, N.J.; LOBSEY, C. Proximal Soil Sensing: An Effective Approach for Soil Measurements in Space and Time, in: Sparks, D.L. (Ed.), **Advances in Agronomy**. Elsevier Inc., San Diego, CA, USA, p. 243–291, 2011. https://doi.org/10.1016/b978-0-12-386473-4.00005-1

VISCARRA ROSSEL, R.A.; MCBRATNEY, A.B.; MINASNY, B. **Proximal Soil Sensing**. Springer, Dordrecht, The Netherlands. 2010. https://doi.org/10.1007/978-90-481-8859-8

WEINDORF, D.C.; BAKR, N.; ZHU, Y. Advances in portable X-ray fluorescence (PXRF) for environmental, pedological, and agronomic applications, in: Sparks, D.L. (Ed.), **Advances in Agronomy**. Elsevier, San Diego, CA, USA, p. 1–45, 2014. https://doi.org/10.1016/B978-0-12-802139-2.00001-9

BRIEF HISTORICAL AND DESCRIPTION OF X-RAY FLUORESCENCE SPECTROMETRY AND NIX™ PRO COLOR SENSOR

X-ray fluorescence spectrometry

X-ray fluorescence spectrometry (XRF) is an analytical technique based on the fluorescence emitted from a sample (e.g., soil, rocks, metal alloys, plant, sediments, and fossils) when atoms are struck with a primary X-ray source (Weindorf et al., 2014). When that occurs, a vacancy in the innermost layers (K or L shell) of the electrosphere is created (Jenkins, 2006; Weindorf et al., 2014). To fill this vacancy, outer shell electrons move towards the inner orbitals (L to K or M to K shell), a process that emits energy (X-ray photons) equal to the energy difference between the two orbitals (Kalnicky and Singhvi, 2001). Therefore, since the fluorescent energy is typically element specific, it allows elemental identification and quantification (Weindorf et al., 2014).

The first X-ray fluorescence spectrometer was a floor-standing research equipment built in 1950 (Glanzman and Closs, 2007). Only in 1959 the early XRF application was described, when G. Roger Webber reported a geochemical prospecting in sediment samples (Webber, 1959; Glanzman and Closs, 2007). Portable X-ray fluorescence spectrometers (pXRF) in turn were developed only in 1965 (Bowie, Darnley and Rhodes, 1965) being commercially available in 1979 for mining applications. By this time, elemental identification was performed one at a time and the instrument weighted about 20 pounds (Glanzman and Closs, 2007). Latter, in 1990's with the X-MET 880 (Outokumpu Electronics and Columbia Scientific Instruments) and the SPECTRACE 9000 (TN Technologies) spectrometers, pXRF instruments gain popularity and became purchase and rental available (Glanzman and Closs, 2007). At that time, pXRF already provided near real-time multi-elemental analysis (Cr, Mn, Fe, Ni, Cu, Zn, As, Se, Pb, Cd, and Sn) and could be hand-held operated (Bernick and Campagna, 1995). Furthermore, it was around the 1980s that the first in situ analyzes of the chemical composition of the planet Mars were obtained, by miniaturized X-ray fluorescence spectrometers on rovers (Clark et al., 1982; Rieder et al., 1997; Gellert et al., 2015). A complete historical overview of pXRF usage can be found in Weindorf et al. (2014) and Shackley (2010).

Since then, significant and constant improvements both in the physical structure of the device and in data processing have led to the development of the models in use today (Tracer 5, Bruker; Niton, Thermo Fisher; Vanta Series, Olympus Corporation). These sensors are able to simultaneously measure a wide range of elements with reduced limit of detection, high

accuracy, no sample preparation requirements, onsite, and so on (Weindorf et al., 2014; Ribeiro et al., 2017).

As mentioned, the first pXRF applications have focused on mining prospecting (Bowie, 1968). However, beyond this use (Durance et al., 2014; Gazley et al., 2011; Lemiere et al., 2018) pXRF fits for a broader range of scientific applications, such as: forensic science (Trombka et al., 2002; Schweitzer et al., 2005; Appoloni and Melquiades, 2014; Woods et al., 2014; Shutic et al., 2017), archaeology/paleontology/anthropology research (Forster et al., 2011; Perrone et al., 2014; Zimmerman et al., 2015; Lubos et al., 2016; Fanti et al., 2018), medicine (Khuder et al., 2007; Khuder et al., 2012), environmental (Rouillon and Taylor, 2016; Al Maliki et al., 2017; Urritia-Goyes et al., 2018; Ribeiro et al., 2019), pedological (Stockmann et al., 2016; Mancini et al., 2019; Silva et al., 2019; Sun et al., 2020), agronomic (Sharma et al., 2015; Rawal et al., 2019; Lima et al., 2019; Andrade et al., 2020; Teixeira et al., 2020) and many others.

In fact, pXRF is already a standard method for soil and sediment analyses (USEPA, 2007; Weindorf and Chakraborty, 2016). However, despite its great potential for several research areas (West et al., 2011), its applicability for analysis of plant material is still scarce (Marguí et al., 2009; McLaren et al., 2012; Reidinger et al., 2012; Guerra et al., 2018; McGladdery et al., 2018; Montanha et al., 2019; Bachiega et al., 2019; Sapkota et al., 2019), and the absence of a standardized method makes it difficult to compare the results.

Nix™ Pro Color Sensor

The Nix™ Pro is a pocket-sized, portable and inexpensive color sensor controlled by smartphone through a bluetooth connection (Nix Team, Ontario, Canada). It is a spectrophotometer that, in contact with any surface (e.g., walls, food, powders, water) produces scanning results in various color codes (RGB, CMYK, CIElab, HEX, etc.) (Nix Team, Canada). The equipment has an internal LED light source that is activated at the time of the measurement. Then, the equipment captures the reflected color and translates it into color codes.

In the visible spectrum (380 - 750 nm), color can mainly be distinguished in the following hues: indigo, violet, blue, green, yellow, orange and red. However, human color perception can substantially vary from person to person, within a single group of people, and among different groups of people (Webster and Webster, 2002). The Nix Pro in turn, unlike human eyes, can quantitatively describe color, avoiding the subjectivity of measurement.

Soil color is basically developed by a mixture of water content, organic matter, phyllosilicates and oxides. It is such an important attribute that is used as a key attribute for soil classification (Santos et al., 2018). Traditionally, soil color has been qualitatively determined using the Munsell chart.

Plant leaves are another kind of matrix that changes in color, which is of great relevance for soil fertility and crop management. Foliar color and nutritional status are directly related (Yao and Lou, 2012; Barbedo, 2019), and the chlorophyll content has a key role on it (Singh et al., 2002). Thus, foliar color can be used to estimate other related properties, such as nutritional status (Pasuquin et al., 2012; Prilianti et al., 2014), senescence, diseases (Singh et al., 2020), water content (Ge et al., 2016), etc. Additionally, just like soil color, foliar color has been qualitatively determined by a leaf color chart (LCC) (Singh et al., 2002; Prilianti et al., 2014), such as the Munsell Plant Tissue Color Chart (Raese et al., 2007; Oliveira; Santana, 2020) and the Globe Plant Color Chart (Thompson et al., 2013).

The Nix Pro^{TM} was not specifically developed for color measurement of soil or plants, but it seems to be extremely promising for that (Stiglitz et al., 2016; Mukhopadhyay et al., 2020; Raeesi et al., 2019).

REFERENCES

AL MALIKI, A.; AL-LAMI, A.K.; HUSSAIN, H.M.; AL-ANSARI, N. Comparison between inductively coupled plasma and X-ray fluorescence performance for Pb analysis in environmental soil samples. **Environmental Earth Sciences**, v. 76, p. 1–7, 2017. http://dx.doi.org/10.1007/s12665-017-6753-z.

ANDRADE, R.; SILVA, S.H.G.; WEINDORF, D.C.; CHAKRABORTY, S.; FARIA, W.M.; MESQUITA, L.F.; GUILHERME, L.R.G.; CURI, N. Assessing models for prediction of some soil chemical properties from portable X-ray fluorescence (pXRF) spectrometry data in Brazilian Coastal Plains. **Geoderma**, v. 357, n. 113957, 2020. https://doi.org/10.1016/j.geoderma.2019.113957

APPOLONI, C.R.; MELQUIADES, F.L. Portable XRF and principal component analysis for bill characterization in forensic science. **Applied Radiation and Isotopes**, v. 85, p. 92–95, 2014. https://doi.org/10.1016/j.apradiso.2013.12.004

BACHIEGA, P.; DE ALMEIDA, E.; SALGADO, J.M.; ARRUDA, M.A.Z.; LEHMANN, E.L.; MORZELLE, M.C.; DE CARVALHO, H.W.P. Benchtop and Handheld Energy-Dispersive X-Ray Fluorescence (EDXRF) as Alternative for Selenium Concentration Measurement in Biofortified Broccoli Seedling. **Food Analytical Methods**, v. 12, p. 1520–1527, 2019. https://doi.org/10.1007/s12161-019-01489-5

BARBEDO, J.G.A. Detection of nutrition deficiencies in plants using proximal images and machine learning: **A review. Computers and Electronics in Agriculture**, v. 162, p. 482–492, 2019. https://doi.org/10.1016/j.compag.2019.04.035

BERNICK, M.B.; CAMPAGNA, P.R. Application of field-portable X-ray fluorescence spectrometers for field-screening air monitoring filters for metals. **Journal of Hazardous Materials**, p. 91–99, 1995

BOWIE, S.H.U.; DARNLEY, A.G.; RHODES, J.R. Portable Radioisotope X-Ray Fluorescence Analyzer: **Trans. Instn. Mining and Metall**., v. 74, p. 361-379 and p. 557-563, 1965.

BOWIE, S.H.U. Portable X-Ray Fluorescence analyzers in the Mining Industry. **Mining Magazine**, v. 118, n. 4, p. 230-239, 1968.

CLARK, B..C.; BAIRD, A.K.; WELDON, R.J.; TSUSAKI, D.M.; SCHNABEL, L.; CANDELARIA, M.P. Chemical composition of Martian fines. **Journal of Geophysical Research: Solid Earth**, v. 87, p. 10059-10067, 1982. https://doi.org/10.1029/JB087iB12p10059

DURANCE, P.; JOWITT, S.M.; BUSH, K. An assessment of portable X-ray fluorescence spectroscopy in mineral exploration , Kurnalpi Terrane , Eastern Goldfields Superterrane, Western Australia. **Applied Earth Science**, v. 123, p. 150–163, 2014. https://doi.org/10.1179/1743275814Y.0000000052

FANTI, F.; BELL, P.R.; TIGHE, M.; MILAN, L.A.; DINELLI, E. Geochemical fingerprinting as a tool for repatriating poached dinosaur fossils in Mongolia: A case study for

the Nemegt Locality, Gobi Desert. **Palaeogeography, Palaeoclimatology, Palaeoecology,** v. 494, p. 51–64, 2018. https://doi.org/10.1016/j.palaeo.2017.10.032

FORSTER, N.; GRAVE, P.; VICKERY, N.; KEALHOFER, L. Non-destructive analysis using PXRF: Methodology and application to archaeological ceramics. **X-Ray Spectrometry**, v. 40, p. 389–398, 2011. https://doi.org/10.1002/xrs.1360

GAZLEY, M.F.; VRY, J.K.; DU PLESSIS, E.; HANDLER, M.R. Application of portable X-ray fluorescence analyses to metabasalt stratigraphy , Plutonic Gold Mine , Western Australia. **Journal of Geochemical Exploration**, v. 110, p. 74–80, 2011. https://doi.org/10.1016/j.gexplo.2011.03.002

GE, Y.; BAI, G.; STOERGER, V.; SCHNABLE, J.C. Temporal dynamics of maize plant growth, water use, and leaf water content using automated high throughput RGB and hyperspectral imaging. **Computers and Electronics in Agriculture**, v. 127, p. 625–632, 2016. https://doi.org/10.1016/j.compag.2016.07.028

GELLERT, R.; CLARK, B.C.; MSL, MER SCIENCE TEAMS. In Situ Compositional Measurements of Rocks and Soils with the Alpha Particle X-ray Spectrometer on NASA's Mars Rovers. **Element**s, v. 11, p. 39-44, 2015. https://doi.org/10.2113/gselements.11.1.39

GLANZMAN, R.K.; CLOSS, L.G. Field Portable X-Ray Fluorescence Geochemical Analysis – Its Contribution to Onsite Real-time Project Evaluation, in: Milkereit, B. (Ed.), **Proceedings of Exploration 07: Fifth Decennial International Conference on Mineral Exploration, Advances in Prospect-Scale Geochemical Methods**. Toronto, Canada, p. 291–301, 2007.

GUERRA, M.B.B.; ADAME, A.; DE ALMEIDA, E.; BRASIL, M.A.S.; SCHAEFER, C.E.G.R.; KRUG, F.J. In situ determination of k, ca, s and si in fresh sugar cane leaves by handheld energy dispersive X-Ray fluorescence spectrometry. **Journal of the Brazilian Chemical Society**, v. 29, p. 1086–1093, 2018. https://doi.org/10.21577/0103-5053.20170229

JENKINS, R. **X-ray Techniques : Overview, Encyclopedia of Analytical Chemistry**. John Wiley & Sons, Chichester, UK. 2006. https://doi.org/10.1002/9780470027318.a6801

KALNICKY, D.J.; SINGHVI, R. Field portable XRF analysis of environmental samples. **Journal of Hazardous Materials**, v. 83, p. 93–122, 2001. https://doi.org/10.1016/S0304-3894(00)00330-7

KHUDER, A.; BAKIR, M.A.; KARJOU, J.; SAWAN, M.K. XRF and TXRF techniques for multi-element determination of trace elements in whole blood and human hair samples. **Journal of Radioanalytical and Nuclear Chemistry**, v. 273, p. 435–442, 2007. https://doi.org/10.1007/s10967-007-6869-9

KHUDER, A.; BAKIR, M.A.; SOLAIMAN, A.; ISSA, H.; HABIL, K.; MOHAMMAD, A. Major, minor, and trace elements in whole blood of patients with different leukemia patterns. **Nukleonika**, v. 57, p. 389–399, 2012.

LEMIÈRE, B. A review of pXRF (Field Portable X-ray Fluorescence) Applications for Applied Geochemistry. **Journal of Geochemical Exploration**, v. 188, p. 350–363, 2018. https://doi.org/10.1016/j.gexplo.2018.02.006

LIMA, T.M.; WEINDORF, D.C.; CURI, N.; GUILHERME, L.R.G.; LANA, R.M.Q.; RIBEIRO, B.T. Elemental analysis of Cerrado agricultural soils via portable X-ray fluorescence spectrometry: Inferences for soil fertility assessment. **Geoderma**, v. 353, p. 264–272, 2019. https://doi.org/10.1016/j.geoderma.2019.06.045

LUBOS, C.; DREIBRODT, S.; BAHR, A. Analysing spatio-temporal patterns of archaeological soils and sediments by comparing pXRF and different ICP-OES extraction methods. **Journal of Archaeological Science: Reports**, v. 9, p. 44–53, 2016. https://doi.org/10.1016/j.jasrep.2016.06.037

MANCINI, M.; WEINDORF, D.C.; CHAKRABORTY, S.; SILVA, S.H.G.; DOS SANTOS TEIXEIRA, A.F.; GUILHERME, L.R.G.; CURI, N. Tracing tropical soil parent material analysis via portable X-ray fluorescence (pXRF) spectrometry in Brazilian Cerrado. **Geoderma**, v. 337, p. 718–728, 2019. doi:10.1016/j.geoderma.2018.10.026.

MARGUÍ, E.; QUERALT, I.; HIDALGO, M. Application of X-ray fluorescence spectrometry to determination and quantitation of metals in vegetal material. **TrAC - Trends in Analytical Chemistry**, v. 28, p. 362–372, 2009. https://doi.org/10.1016/j.trac.2008.11.011

MCGLADDERY, C.; WEINDORF, D.C.; CHAKRABORTY, S.; LI, B.; PAULETTE, L.; PODAR, D.; PEARSON, D.; KUSI, N.Y.O.; DUDA, B. Elemental assessment of vegetation via portable X-ray fluorescence (PXRF) spectrometry. **Journal of Environmental Management**, v. 210, p. 210–225, 2018. https://doi.org/10.1016/j.jenvman.2018.01.003

MCLAREN, T.I.; GUPPY, C.N.; TIGHE, M.K. A Rapid and Nondestructive Plant Nutrient Analysis using Portable X-Ray Fluorescence. **Soil Science Society of America Journal**, v. 76, n. 1446, 2012. https://doi.org/10.2136/sssaj2011.0355

MONTANHA, G.S.; RODRIGUES, E.S.; MARQUES, J.P.R.; ALMEIDA, E.; REIS, A.R.; CARVALHO, H.W.P. X-ray fluorescence spectroscopy (XRF) applied to plant science: challenges towards in vivo analysis of plants. **Metallomics**, v. 12, p. 183-192, 2019. https://doi.org/10.1039/c9mt00237e

MUKHOPADHYAY, S.; CHAKRABORTY, S.; BHADORIA, P.B.S.; LI, B.; WEINDORF, D.C. Assessment of heavy metal and soil organic carbon by portable X-ray fluorescence spectrometry and NixPro^{TM} sensor in landfill soils of India. **Geoderma Regional**, v. 20, n. e00249, 2020. https://doi.org/10.1016/j.geodrs.2019.e00249

OLIVEIRA, L.F.R.; SANTANA, R.C. Exploratory analysis of nutrient concentrations in Eucalyptus leaf color patterns. **Advances in Forestry Science**, v. 7, p. 973-979, 2020.

PASUQUIN, J.M.; SAENONG, S.; TAN, P.S.; WITT, C.; FISHER, M.J. Evaluating N management strategies for hybrid maize in Southeast Asia. **Field Crops Research**, v. 134, p. 153–157, 2012. https://doi.org/10.1016/j.fcr.2012.06.004

PERRONE, A.; FINLAYSON, J.E.; BARTELINK, E.J.; DALTON, K.D. Application of Portable X-ray Fluorescence (XRF) for Sorting Commingled Human Remains, in: Adams, B.J., Byrd, J.E. (Eds.), **Commingled Human Remains: Methods in Recovery, Analysis,**

and Identification. Elsevier Inc., p. 145–166. 2014. https://doi.org/10.1016/B978-0-12-405889-7.00007-1

PRILIANTI, K.R.; YUWONO, S.P.; ADHIWIBAWA, M.A.S.; PRIHASTYANTI, M.N.P.; LIMANTARA, L.; BROTOSUDARMO, T.H.P. Automatic leaf color level determination for need based fertilizer using fuzzy logic on mobile application: A model for soybean leaves, in: **6th International Conference on Information Technology and Electrical Engineering (ICITEE)**. Institute of Electrical and Eletronics Engineers, Yogyakarta, Indonesia, p. 1–6. 2014. https://doi.org/10.1109/ICITEED.2014.7007895

RAEESI, M.; ZOLFAGHARI, A.A.; YAZDANI, M.R.; GORJI, M.; SABETIZADE, M. Prediction of soil organic matter using an inexpensive colour sensor in arid and semiarid areas of Iran. **Soil Research**, v. 57, p. 276–286, 2019. https://doi.org/10.1071/SR18323

RAESE, J.T.; DRAKE, S.R.; CURRY, E.A. Nitrogen Fertilizer Influences Fruit Quality, Soil Nutrients and Cover Crops, Leaf Color and Nitrogen Content, Biennial Bearing and Cold Hardiness of 'Golden Delicious', **Journal of Plant Nutrition**, v. 30, p. 1585-1604, 2007. https://doi.org/10.1080/01904160701615483

RAWAL, A.; CHAKRABORTY, S.; LI, B.; LEWIS, K.; GODOY, M.; PAULETTE, L.; WEINDORF, D.C. Determination of base saturation percentage in agricultural soils via portable X-ray fluorescence spectrometer. **Geoderma**, v. 338, p. 375–382, 2019. doi:10.1016/j.geoderma.2018.12.032.

RIBEIRO, B.T.; SILVA, S.H.G.; SILVA, E.A.; GUILHERME, L.R.G. Aplicações da fluorescência de raios-X portátil (pXRF) na Ciência do Solo tropical. **Ciencia e Agrotecnologia**, v. 41, p. 245–254, 2017. https://doi.org/10.1590/1413-70542017413000117

RIBEIRO, B.T.; NASCIMENTO, D.C.; CURI, N.; GUILHERME, L.R.G.; COSTA, E.T.S.; LOPES, G.; CARNEIRO, J.P. Assessment of trace element contents in soils and water from cerrado wetlands, triângulo mineiro region. **Revista Brasileira de Ciencia do Solo**, v. 43, p. 1–17, 2019. https://doi.org/10.1590/18069657rbcs20180059

RIEDER, R.; ECONOMOU, T.; WANKE, H.; TURKEVICH, A.; CRISP, J.; BRUCKNER, J.; DREIBUS, G.; MCSWEEN JR., H.Y. The Chemical Composition of Martian Soil and Rocks Returned by the Mobile Alpha Proton X-ray Spectrometer: Preliminary Results from the X-ray Mode. **Science**, v. 278, p. 1771-1774, 1997. https://doi.org/10.1126/science.278.5344.1771

REIDINGER, S.; RAMSEY, M.H.; HARTLEY, S.E. Rapid and accurate analyses of silicon and phosphorus in plants using a portable X-ray fluorescence spectrometer. **New Phytologist**, v. 195, p. 699–706, 2012. https://doi.org/10.1111/j.1469-8137.2012.04179.x

ROUILLON, M.; TAYLOR, M.P. Can field portable X-ray fluorescence (pXRF) produce high quality data for application in environmental contamination research? **Environmental Pollution**, v. 214, p. 255–264, 2016. doi:10.1016/j.envpol.2016.03.055.

SANTOS, H.G.; JACOMINE, P.K.T.; ANJOS, L.H.C.; OLIVEIRA, V.A.; LUMBRERAS, J.F.; COELHO, M.R.; ALMEIDA, J.A.; ARAÚJO FILHO, J.C.; OLIVEIRA, J.B.; CUNHA, T.J.F. **Sistema Brasileiro de Classificação de Solos**, 5th ed. 2018. Embrapa, Brasília, DF.

SAPKOTA, Y.; MCDONALD, L.M.; GRIGGS, T.C.; BASDEN, T.J.; DRAKE, B.L. Portable X-Ray fluorescence spectroscopy for rapid and cost-effective determination of elemental composition of ground forage. **Frontiers in Plant Science**, v. 10, p. 1–9, 2019. https://doi.org/10.3389/fpls.2019.00317

SCHWEITZER, J.S.; TROMBKA, J.I.; FLOYD, S.; SELAVKA, C.; ZEOSKY, G.; GAHN, N.; MCCLANAHAN, T.; BURBINE, T. Portable generator-based XRF instrument for non-destructive analysis at crime scenes. **Nuclear Instruments and Methods in Physics Research B**, v. 241, p. 816–819, 2005. https://doi.org/10.1016/j.nimb.2005.07.137

SHACKLEY, M.S. An Introduction to X-Ray Fluorescence (XRF) Analysis in Archaeology, in: Shackley, M.S. (Ed.), **X-Ray Fluorescence Spectrometry (XRF) in Geoarchaeology**. Springer, New York, NY, p. 7–44. 2011. https://doi.org/10.1007/978-1-4419-6886-9_2

SHARMA, A.; WEINDORF, D.C.; WANG, D.D.; CHAKRABORTY, S. Characterizing soils via portable X-ray fluorescence spectrometer: 4. Cation exchange capacity (CEC). **Geoderma**, v. 239, p. 130–134, 2015. https://doi.org/10.1016/j.geoderma.2014.10.001

SHUTIC, S.; CHAKRABORTY, S.; LI, B.; WEINDORF, D.C.; SPERRY, K.; CASADONTE, D. Forensic identification of pharmaceuticals via portable X-ray fluorescence and diffuse reflectance spectroscopy. **Forensic Science International**, v. 279, p. 22–32, 2017. https://doi.org/10.1016/j.forsciint.2017.08.008

SILVA, E.A.; WEINDORF, D.C.; SILVA, S.H.G.; RIBEIRO, B.T.; POGGERE, G.C.; CARVALHO, T.; GONÇALVES, M.G.M.; GUILHERME, L.R.G.; CURI, N. Advances in Tropical Soil Characterization via Portable X-Ray Fluorescence Spectrometry. **Pedosphere**, v. 29, p. 468–482, 2019. https://doi.org/10.1016/S1002-0160(19)60815-5

SINGH, B.; SINGH, Y.; LADHA, J.K.; BRONSON, K.F.; BALASUBRAMANIAN, V.; SINGH, J.; KHIND, C. Chlorophyll Meter - and leaf color chart-based nitrogen management for rice and wheat in Northwestern India. **Agronomy Journal**, v. 94, p. 821–829, 2002.

SINGH, J.P.; PRADHAN, C.; DAS, S.C. Image Processing and Machine Learning Techniques to Detect and Classify Paddy Leaf Diseases: A Review, in: Swain, D., Pattnaik, P.K., Gupta, P.. (Eds.), **Machine Learning and Information Processing**. Springer Nature Singapore Pte Ltd., Singapore, p. 161–172. 2020. https://doi.org/10.1007/978-981-15-1884-3_4

STIGLITZ, R.; MIKHAILOVA, E.; POST, C.; SCHLAUTMAN, M.; SHARP, J. Evaluation of an inexpensive sensor to measure soil color**. Computers and Electronics in Agriculture**, v. 121, p. 141–148, 2016. https://doi.org/10.1016/j.compag.2015.11.014

STOCKMANN, U.; CATTLE, S.R.; MINASNY, B.; MCBRATNEY, A.B. Utilizing portable X-ray fluorescence spectrometry for in-field investigation of pedogenesis. **Catena**, v. 139, p. 220–231, 2016. https://doi.org/10.1016/j.catena.2016.01.007

SUN, F.; BAKR, N.; DANG, T.; PHAM, V.; WEINDORF, D.C.; JIANG, Z.; LI, H.; WANG, Q. Geoderma Enhanced soil profile visualization using portable X-ray fluorescence (PXRF) spectrometry. **Geoderma**, v. 358, n. 113997, 2020. https://doi.org/10.1016/j.geoderma.2019.113997

TEIXEIRA, A.F.S.; PELEGRINO, M.H.P.; FARIA, W.M.; SILVA, S.H.G.; GONÇALVES, M.G.M.; ACERBI JUNIOR, F.W.; GOMIDE, L.R.; PÁDUA JUNIOR, A.L.; SOUZA, I.A.; CHAKRABORTY, S. et al. Tropical soil pH and sorption complex prediction via portable X-ray fluorescence spectrometry. **Geoderma**, v. 361, n. 114132, 2020.

THOMPSON, J.A.; POLLIO,A.R.; TURK, P.J. Comparison of Munsell Soil Color Charts and the GLOBE Soil Color Book. **Soil Science Society of America Journal**, v. 77, p. 2089-2093, 2013. https://doi.org/ 10.2136/sssaj2013.03.0117n

TROMBKA, J.I.; SCHWEITZER, J.; SELAVKA, C.; DALE, M.; GAHN, N.; FLOYD, S.; MARIE, J.; HOBSON, M.; ZEOSKY, J.; MARTIN, K.; MCCLANNAHAN, T.; SOLOMON, P.; GOTTSCHANG, E. Crime scene investigations using portable, non-destructive space exploration technology. **Forensic Science International**, v. 129, p. 1–9, 2002.

URRUTIA-GOYES, R.; ARGYRAKI, A.; ORNELAS-SOTO, N. Characterization of soil contamination by lead around a former battery factory by applying an analytical hybrid method. **Environmental Monitoring and Assessment**, v. 190, 2018. https://doi.org/10.1007/s10661-018-6820-2

US EPA (2007) Method 6200: **Field portable X-ray fluorescence spectrometry for determination of elemental concentrations in soil and sediment**. https://www.epa.gov/sites/production/%0Afiles/2015-12/ documents/6200.pdf.

WEBBER, G.R. Application of X-ray Spectrometric Analysis to Geochemical Prospecting: **Economic Geology**, v. 54, n. 5, p. 816-828, 1959.

WEBSTER, M.A.; WEBSTER, S.M.; BHARADWAJ, S.; VERMA, R.; JAIKUMAR, J.; MADAN, G.; VAITHILINGHAM, E. Variations in normal color vision III Unique hues in Indian and United States observers. **Journal of the Optical Society of America A**, v. 19, n. 10, p. 1951-1962, 2002. https://doi.org/10.1364/josaa.19.001951

WEINDORF, D.C.; BAKR, N.; ZHU, Y. Advances in portable X-ray fluorescence (PXRF) for environmental, pedological, and agronomic applications, in: Sparks, D.L. (Ed.), **Advances in Agronomy**. Elsevier, San Diego, CA, USA, p. 1–45, 2014. https://doi.org/10.1016/B978-0-12-802139-2.00001-9

WEINDORF, D.C.; CHAKRABORTY, S. Portable X-ray Fluorescence Spectrometry Analysis of Soils. **Methods of Soil Analysis** 1, 0. 2016. https://doi.org/10.2136/methods-soil.2015.0033

WEST, M.; ELLIS, A.T.; POTTS, P.J.; STRELI, C.; VANHOOF, C.; WEGRZYNEK, D.; WOBRAUSCHEK, P. Atomic spectrometry update-X-ray fluorescence spectrometry**.** **Journal of Analytical Atomic Spectrometry**, v. 26, n. 10, 1919–1963, 2011. https://doi.org/10.1039/c1ja90038b

WOODS, B.; KIRKBRIDE, K.P.; LENNARD, C.; ROBERTSON, J. Soil examination for a forensic trace evidence laboratory – Part 2: Elemental analysis. **Forensic Science International**, v. 245, p. 195–201, 2014. https://doi.org/10.1016/j.forsciint.2014.10.018

YAO, X.; LUO, W. Foliar image color features for rubber nitrogen deficiency status analysis. **Advanced Materials Research**, v. 488–489, p. 1674–1679, 2012. https://doi.org/10.4028/www.scientific.net/AMR.488-489.1674

ZIMMERMAN, H.A.; SCHULTZ, J.J.; SIGMAN, M.E. Preliminary Validation of Handheld X-Ray Fluorescence Spectrometry : Distinguishing Osseous and Dental Tissue from Nonbone Material of Similar Chemical Composition. **Journal of Forensic Sciences**, v. 60, p. 382–391, 2015. https://doi.org/10.1111/1556-4029.12690

SECOND PART – ARTICLES

ARTICLE 1: COMPARISON OF PORTABLE X-RAY FLUORESCENCE SPECTROMETRY AND LABORATORY-BASED METHODS TO ASSESS THE SOIL ELEMENTAL COMPOSITION: APPLICATIONS FOR WETLAND SOILS

(Article published in Environmental Technology & Innovation)

DOI: 10.1016/j.eti.2020.100826

Camila Silva Borges [a], David C. Weindorf [b], Diogo Costa Nascimento [c], Nilton Curi [a], Luiz Roberto Guimarães Guilherme [a], Geila Santos Carvalho [a], Bruno Teixeira Ribeiro [a*]

[a] Department of Soil Science, Federal University of Lavras – UFLA, Doutor Sylvio Menicucci Avenue, Lavras, Minas Gerais State, 37200-900, Brazil

[b] Department of Plant and Soil Science, Texas Tech University, Bayer Plant Science Building, Room 211A, 2911 15th Street, Lubbock, TX 79409-2122, United States of America

[c] Federal Center of Technological Education of Minas Gerais State, 900 Raymundo Mattoso Street, Curvelo, 35790-000, Brazil

Abstract: The portable X-ray fluorescence spectrometry (pXRF) can be considered one of the most novelty for soil characterization. In tropical regions (e.g., Brazil), some studies have showed a consistent correlation between pXRF and laboratory-based methods. However, there is no work dedicated exclusively for hydromorphic soils (gley or organic-rich soils). This study aims to assess the total elemental composition reported by portable X-ray fluorescence (pXRF) spectrometry and to compare it to laboratory-based wet digestion method and wavelength dispersive X-ray (WDXRF) spectrometry. A collection of 144 hydromorphic soil samples from six wetlands located in the Cerrado biome (Savannah), Brazil, was used for this investigation. Soil samples were disaggregated and passed through a 150-μm nylon mesh and subjected to wet digestion (US EPA 3051a) followed by elemental determination via atomic absorption spectrometry (AAS). Subsamples of each ground soil were also directly analyzed via both pXRF and WDXRF. Linear regressions were performed to establish the relationship between methods. Several elements (Pb, Cu, Zn, Cr, Fe, Ti, Sr, and Y) determined via pXRF were successfully correlated to other methods (USEPA 3051a and WDXRF). Specially for Pb, a very strong correlation ($R > 0.90$) was observed between pXRF, WDXRF and US EPA 3051a methods. The pXRF revealed also to be a useful tool for characterization of hydromorphic soils and future studies should be conducted directly in the field to assess the elemental composition of Cerrado wetland soils.

Keywords: XRF analysis. Soil chemistry. Proximal sensors.

Introduction

Traditionally, the assessment of the total elemental composition of soil has been performed by wet digestion methods (e.g., US EPA 3051a, US EPA 3052) followed by the determination via atomic absorption spectrometry (AAS) or inductively coupled plasma optical emission spectrometry (ICP-OES), for instance. These methods are considered non-environmentally friendly and have been gradually replaced by fast and non-destructive methods such as portable X-ray fluorescence (pXRF) spectrometry (Weindorf et al., 2014; Ribeiro et al., 2017). Nowadays, the pXRF method can be considered one of the most important innovations in Soil Science (USEPA, 2007a; Soil Survey Staff, 2014; Weindorf et al., 2014; Weindorf and Chakraborty, 2016).

The pXRF method has been applied worldwide for different purposes (e.g., agronomic, pedological, geological and environmental) (Weindorf et al., 2014). The pXRF reports the total elemental concentration and the results have been well correlated to those obtained via laboratory-based methods (Kilbride et al., 2006; Radu and Diamond, 2009; Hu et al., 2014; Rouillon and Taylor, 2016). Further, it facilitates in-field investigation of large areas and high sample throughput (Chakraborty et al., 2019; Mancini et al., 2019). Based on pXRF data and prediction models several soil properties have been successfully estimated (Zhu et al., 2011; Weindorf et al., 2012; Andrade et al., 2020a,b; Lima et al., 2019; Rawal et al., 2019). Others have used pXRF data visualization tools to augment traditional morphological profile description (Sun et al., 2020).

In tropical regions (e.g., Brazil) some studies using pXRF method started few years ago (Ribeiro et al., 2017). Until now, the correlation between pXRF and conventional methods was assessed by a very few studies. For soils from Southern of Minas Gerais State, Brazil, a strong correlation between pXRF and wet digestion-ICP method was observed for Ca, Cu, Fe, Mn, Cr, Ni, and V (Silva et al., 2019). However, for others elements like Al, K, Ti, and Zr a poor correlation was obtained. These differences are related to the intrinsic characteristics of each method and the performance of wet digestion procedure which depends on soil properties. For Fe_2O_3, a very strong correlation between pXRF and laboratory-based methods has always been found (Santana et al., 2018; Silva et al., 2020). These studies were performed using always samples from non-hydromorphic soils. To date, there is no work which evaluated the pXRF performance exclusively for hydromorphic soils compared to laboratory-based methods.

In this work, an important wet ecosystem (wetlands) occurring in the Cerrado Biome (Brazilian Savannah) (Junk et al., 2014; Hu et al., 2017) was selected. In this environment, the total elemental composition and hazardous pollutants have scarcely been studied (Ramos et al., 2006; Moraes and Horn, 2013; Rosolen et al., 2015a,b; Ribeiro et al., 2019). Also, the elemental assessment has always been performed via wet digestion method. This analysis is time consuming and non-environmentally friendly. The pXRF technology has been not applied on Cerrado wetland soils yet. It was hypothesized that the pXRF method may be a useful tool to improve the characterization of wetland soils. Thus, this work aimed to verify the pXRF performance compared to benchtop wavelength dispersive X-ray fluorescence spectrometry (WDXRF), and to correlate it to standard method employed in Brazil for soil metal assessment (US EPA 3051a).

Material and methods

Sampling site description

Six representative wetlands (W1, W2, W3, W4, W5 and W6) were selected around Uberlândia city, Triângulo Mineiro region, Minas Gerais State, Brazil (Fig. 1). According to the Köppen classification, the climate is Aw and the historical annual average rainfall is 1472 mm (Ribeiro et al., 2013). Most rainfall (86%) occurs during spring-summer, with 14% during fall-winter. Mean elevation is 819 m amsl (ranging from 745 to 892 m). The selected wetlands are located in two geomorphic-geologic units: the Chapada Plateau surface composed of clayey sediments, and the lower surface composed of sandstones of the Bauru Group (Nishiyama, 1989; Ramos et al., 2006).

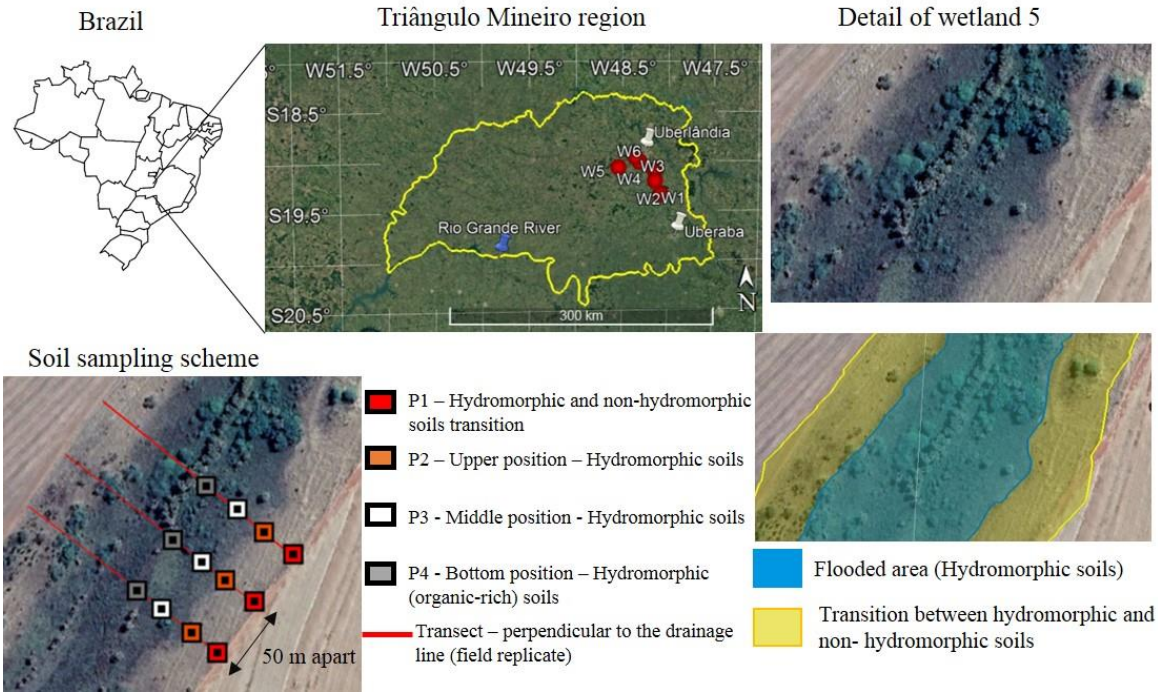

Fig. 1. Location of selected wetlands (W1, W2, W3, W4, W5, and W6) around Uberlândia city, Triângulo Mineiro region, Minas Gerais State, Brazil.

In each wetland, three transects 50 m apart were established perpendicularly to the drainage line (Fig. 1). Each transect was considered as a field replicate and divided in four portions: P1, P2, P3, and P4 (bottom). P1 position is a transition between hydromorphic and non-hydromorphic soils. P2, P3, and P4 are located in the seasonally or permanently flooded area. Per Nascimento et al. (2018), the bottom portion and the subsurface (40–70 cm) layer of the middle portion (P2 and P3) remain flooded during the entire year. According to the Brazilian System of Soil Classification (Santos et al., 2018), Gleissolo Háplico occurs in the P2 position, and Gleissolo Melânico occurs in the P3 and P4 positions. Gleissolo Háplico and Gleissolo Melânico correspond to Entisols and Gleysols per US Soil Taxonomy and FAO, respectively. Composite soil samples were collected from 0–20 cm (organic-rich) and 40–70 cm depth (gley horizon) at the upper (P1 and P2), middle (P3), and bottom position (P4). Each composite soil sample was constituted by mixture of four single samples. The soil samples were collected using a stainless hand auger or by excavation of a soil pit (Fig. 2). Thus, in each wetland, 24 soil samples were collected totalizing 144 samples (full dataset). The soil samples were air dried and ground to pass through a 2-mm sieve for further analysis. Coarse fragments (> 2 mm) were not found in all soil samples.

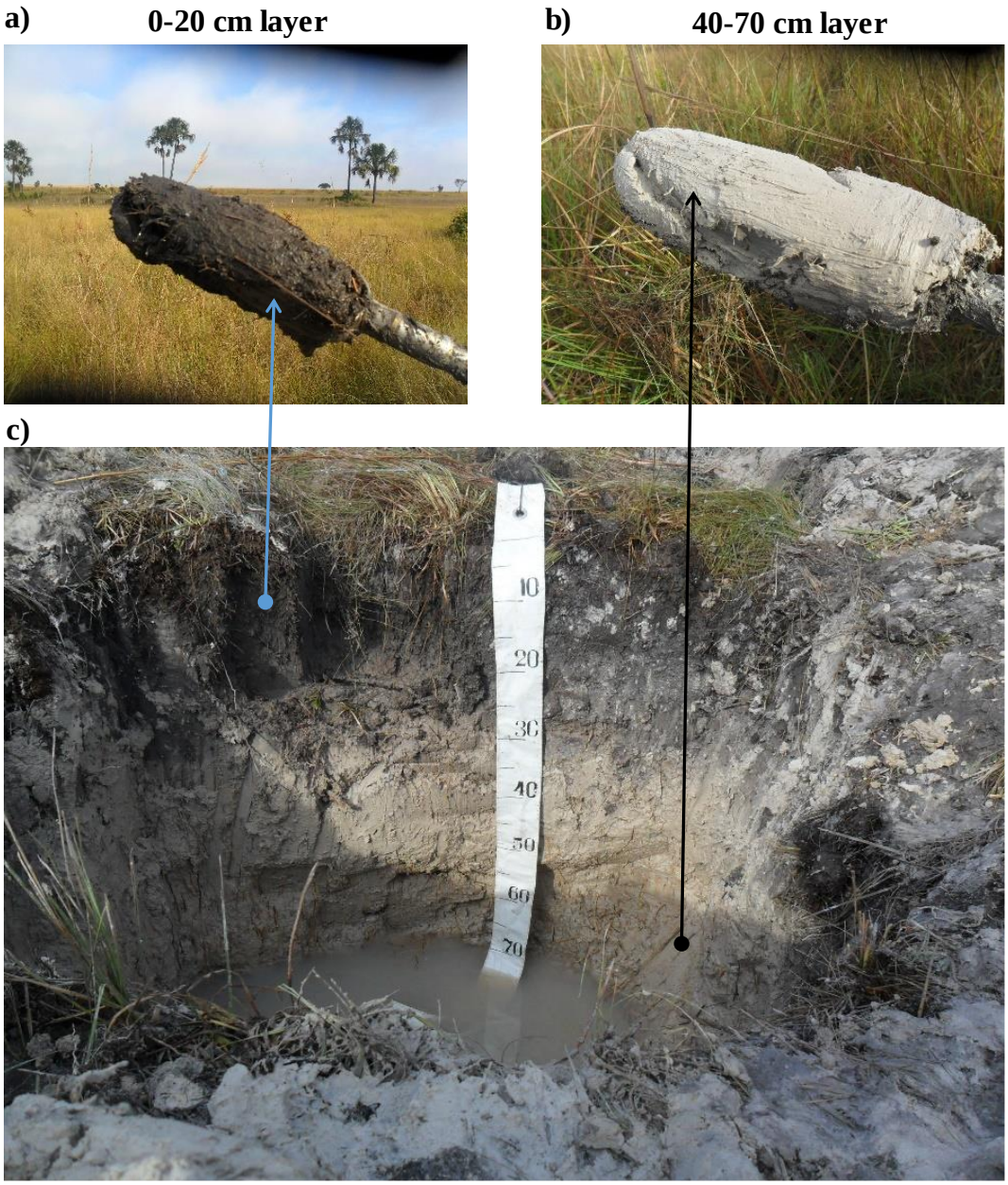

Fig. 2. Sampling details of soil samples from 0-20 cm layer (organic-rich) (a) and 40-70 cm layer (gley horizon) (b), and detail of the soil pit showing the typical occurrence of Gleysols in the studied Cerrado wetlands (Veredas). Source: Photos: Bruno T. Ribeiro.

USEPA 3051a method

A homogeneous portion of the soil samples passed through a 2 mm sieve was totally ground in an agate mortar and passed through a 150-µm nylon mesh sieve. Using 50-mL Teflon® vessels, 1.0 g of soil was weighed and combined with 10 ml of HNO_3 (Sigma-Aldrich®). Soil digestion was performed by microwave following the USEPA 3051a protocol (USEPA, 2007a). After digestion, samples were filtered using Whatmann No. 40 filter paper,

rinsing with 10 ml of ultrapure water. In the obtained extract, elemental composition was assessed via either graphite-furnace atomic absorption spectrometry (GFAAS) or flame atomic absorption spectrometer (FAAS). To verify the accuracy of the digestion procedure and the performance of the AAS equipment, blank samples and National Institute of Standards and Technology (NIST) Standard Reference Material® (SRM) 2710a (Montana I soil) were used. Recovery percentages (AAS determined/NIST certified) were as follows: Fe (95); Pb (92); Mn (80); Cu (117); Ni (78); Zn (98); As (110); and Cd (100). The US EPA 3051a method was referenced in this work as acid digestion (AD) method for further discussion.

pXRF analyses

Portable X-ray fluorescence analyses were also performed on soil samples passed through a 150-µm nylon mesh sieve following the USEPA Method 6200 (USEPA, 2007b) and Weindorf and Chakraborty (2016). Samples were scanned using a Vanta series (Olympus, Waltham, MA, USA) pXRF. The equipment operates with Li ion batteries and contains a Rh X-ray tube (8–50 kV) as the primary X-ray excitation source. Instrument calibration was via 316 stainless steel calibration alloy. The operational conditions were: Geochem mode and dwell time of 60 s (30 s per beam). Prolene® thin-film (Chemplex, Industries, INC) (63.5 mm diameter) was placed on the X-ray source and detector aperture (~2 cm). After that, approximately 10 g of soil was massed over the circle film ensuring at least 10 mm thickness of sample prior to scanning. For quality assurance and control (QA/QC), NIST SRM 2711a was used. Recovery percentages (pXRF determined/NIST certified) were as follows: Si (95); Al (86); Fe (92); Ti (108); Cr (76); Mn (94); Cu (108); Y (—); Th (133); Zn (101); Pb (103); Sr (93); As (130); and Rb (95).

WDXRF analyses

Using the 150-µm soil samples, pressed flat dies (3.4 cm of diameter and 0.7 cm of thickness) were obtained using an automatic press machine applying 2 ton cm^{-2}. Each flat die was obtained by mixing 9.0 g of soil plus 1.0 g of Hoechst wax C micropowder (Merck®). The dies were screened using a wavelength dispersive X-ray (WDXRF) spectrometer Bruker® (Kennewick, WA, USA) S8 Tiger 4 kW model. The operational conditions were: (i) Rh X-ray tube (60 kV maximum) with 75 µm Be window; (ii) analyzer crystals - XS-55, PET, LiF (200): 20–60 kV, 5–170 mA, and 4 kW. The analyses were performed using the Bruker® Quant-

Express method. For this standardless method, after internal calibration-check the following recoveries (%) were found: Na_2O (99), Al_2O_3 (99), SiO_2 (100), SO_3 (98), Cl (104), K_2O (100), CaO (100), Fe_2O_3 (114), SrO (98), and Sb_2O_3 (98). For data spectral acquisition, processing, identification and quantification of the elements, the software Spectraplus (*Geo-quant mode*) was used.

Statistical analysis

Data from all three methods (USEPA 3051a, pXRF, and WDXRF) were subjected to descriptive statistics: minimum, maximum, mean, median, and standard deviation values. Comparisons between USEPA 3051a, pXRF, and WDXRF results were performed for the same elements determined by all methods. Linear regressions and graphs were obtained using both Sigma Plot 14.0 (Systat Software Inc., San Jose, CA, USA) and R software (RStudio Team, 2016). R and R^2 values were considered as statistical parameters.

Results and discussion

Methodological comparison for elemental analysis

After soil digestion (USEPA 3051a method) the following elements were determined via AAS: Fe≫Pb > Mn > Cu > Ni > Zn > As ≫ Cd (Table 1). Ribeiro et al. (2019) previously noted the concentrations and associated correlations with soil depth and other soil attributes. Summarily, cationic elements (e.g., Pb, Mn, Cu, Ni, and Zn) were correlated to soil organic matter content and its fractions (fulvic acid, humic acid, and humin); furthermore, Fe and As were correlated with each other (Ribeiro et al., 2019). The values obtained via AD did not exceed Brazilian threshold values (Conama Resolution 420, 2009; Cetesb, 2014; Copam Normative Deliberation 166, 2011).

Table 1

Elemental composition of studied Cerrado wetland soils after acid digestion (USEPA 3051a method) and determination via atomic absorption spectrometry (FAAS or GFAAS).

Element	Mean	Median	Minimum	Maximum	s.d. (%)
Fe (g kg^{-1})	13.0	11.8	0.4	39.7	10.0
Pb (mg kg^{-1})	21.8	12.2	6.3	93.4	18.0

Mn (mg kg^{-1})	16.4	10.9	2.9	151.0	17.3
Cu (mg kg^{-1})	13.4	9.5	1.1	71.2	13.5
Ni (mg kg^{-1})	6.8	5.5	0.6	39.1	5.7
Zn (mg kg^{-1})	6.0	4.6	1.4	29.7	4.2
As (mg kg^{-1})	5.4	4.3	0.6	15.7	3.4
Cd (µg kg^{-1})	28.5	23.4	1.7	103.5	68.1

s.d: standard deviation; recoveries (%): Fe (95); Pb (92); Mn (80); Cu (117); Ni (78); Zn (98); As (110); Cd (100); determination via FAAS: Fe, Mn, Cu, and Zn; determination via GFAAS: Pb, Ni, As, and Cd.

By comparison, thirteen elements were quantified via WDXRF and ranked from the highest to lowest concentration (Table 2). Titanium and Fe were the major elements followed by V, Ce, Cr, Ba, Nb, Cu, Ni, Y, Zn, Pb, and Sr. Similarly, fourteen elements were quantified via pXRF and ranked: Si, Al, Fe, and Ti (major elements), Cr, Mn, Cu, Y, Th, Zn, Pb, Sr, As, and Rb (trace elements) (Table 3). The content of elements reported by the three methods was different, as expected. This is due to the intrinsic characteristic of each method/equipment, calibration, detection limits, etc. Comparing WDXRF and pXRF, the elements Si, Al, Mn, Th, As, and Rb were not detected by WDXRF; and V, Ce, Ba, Nb, and Ni were not reported by pXRF. However, the elements detected by both WDXRF and pXRF were ranked according to their concentrations as the same way: Fe and/or Ti followed by Cr, Cu, Y, Zn, Pb, and Sr.

Table 2

Elemental composition of studied Cerrado wetland soils via wavelength dispersive energy (WDXRF) method.

Element	Mean	Median	Minimum	Maximum	s.d. (%)
Ti (g kg^{-1})	32.4	30.9	14.2	55.1	7.1
Fe (g kg^{-1})	31.8	23.9	4.2	85.2	24.2
V (mg kg^{-1})	280.3	285.0	119.0	472.0	51.5
Ce (mg kg^{-1})	258.3	160.0	31.0	1,132.0	228.7
Cr (mg kg^{-1})	178.9	121.0	58.0	1,252.0	173.2
Ba (mg kg^{-1})	64.3	53.0	37.0	229.0	30.3
Nb (mg kg^{-1})	60.2	58.0	21.0	131.0	16.0
Cu (mg kg^{-1})	37.0	33.0	10.0	132.0	20.4
Ni (mg kg^{-1})	33.2	30.0	14.0	145.0	19.5
Y (mg kg^{-1})	31.0	25.0	10.0	194.0	23.0
Zn (mg kg^{-1})	22.9	21.0	11.0	51.0	9.0
Pb (mg kg^{-1})	22.7	18.0	5.0	84.0	14.5
Sr (mg kg^{-1})	19.7	17.0	10.0	58.0	9.6

Table 3

Elemental composition of studied Cerrado wetland soils via portable X-ray fluorescence analysis (pXRF).

Element	Mean	Median	Minimum	Maximum	s.d. (%)
Si (g kg^{-1})	169.7	163.9	75.9	342.8	59.5
Al (g kg^{-1})	160.3	165.3	56.0	270.1	48.6
Fe (g kg^{-1})	32.0	27.6	4.8	83.5	21.6
Ti (g kg^{-1})	17.6	17.1	6.5	30.7	4.2
Cr (mg kg^{-1})	145.0	67.0	25.0	1142.0	183.6
Mn (mg kg^{-1})	127.1	102.0	23.0	465.0	85.6
Cu (mg kg^{-1})	48.2	41.0	10.0	181.0	31.2
Y (mg kg^{-1})	40.1	30.0	8.0	325.0	41.6
Th (mg kg^{-1})	35.1	36.0	12.0	65.0	9.7
Zn (mg kg^{-1})	28.2	27.0	13.0	81.0	10.7
Pb (mg kg^{-1})	22.7	17.0	5.0	97.0	17.1
Sr (mg kg^{-1})	14.5	12.0	4.0	48.0	9.0
As (mg kg^{-1})	11.8	10.0	2.0	30.0	7.1
Rb (mg kg^{-1})	3.3	3.0	1.0	12.0	2.1

s.d.: standard deviation; Recoveries (%): Si (66); Al (86); Fe (92); Ti (108); Cr (76); Mn (94); Cu (108); Y (---); Th (133); Zn (101); Pb (103); Sr (93); As (130); and Rb (95).

Conversely to non-hydromorphic soils from Cerrado biome, the major and trace elements geochemistry of Cerrado wetlands soils has been assessed by a very few studies. Also, there are no specific background reference values for Cerrado wetlands soils (Ribeiro et al., 2019). Rosolen et al. (2015a) also determined the concentration of 18 elements (As, Ba, Ca, Cr, Cu, Fe, K, Mg, Mn, Na, Ni, P, Pb, Sr, Ti, V, Zn, and Zr) after digestion with Aqua Regia (HCl/HNO_3) followed by determination via ICP-OES in some wetland soils from Triângulo Mineiro region, Minas Gerais state. The authors found high concentrations for As, Cr and Cu attributed to agricultural practices in higher surrounding areas.

The mean concentrations of total Cr via WDXRF and pXRF were 178.9 and 145.0 mg kg^{-1}, respectively (Tables 2 and 3). When the soil samples were analyzed via both WDXRF and pXRF, 95% of total soil samples had total Cr concentration > 75.0 mg kg^{-1}. For non-hydromorphic soils of the Cerrado biome the total Cr concentration ranges from 85 to 118 mg kg^{-1} (Marques et al., 2004). Brazilian environmental legislation (Conama Resolution 420, 2009; Cetesb, 2014; Copam Normative Deliberation 166, 2011) establishes the semi-total concentration of 75 mg kg^{-1} as threshold value for Cr. Thus, the total Cr concentration values found here do not allow the assessment of contamination level. In wetlands soils impacted by

agricultural practices, Rosolen et al. (2015a) found Cr concentration up to 155 mg kg^{-1} after wet digestion (Aqua Regia).

Even the WDXRF or pXRF reporting total Cu concentration, the mean value did not exceed the threshold value (60 mg kg^{-1}) established by the Brazilian regulation considering the semi-total concentration. Moreover, only 8% of total soil samples had total concentration of Cu > 60 mg kg^{-1} (semi-total threshold reference value). The mean total concentration found for V was 280.3 mg kg^{-1} (Table 2) whereas the background value (semi-total) established for Minas Gerais State in Brazil after wet digestion (USEPA 3051a) is 129 mg kg^{-1} (Copam Normative Deliberation 166, 2011). In Brazil, there are no threshold values established for V yet. For non-hydromorphic soils from Cerrado biome, the total V concentration ranged from 161 to 802 mg kg^{-1} (Marques et al., 2004). In the wetlands studied by Rosolen et al. (2015a) the V concentration ranged from 19.6 to 291.6 mg kg^{-1}.

The Ce concentration obtained via WDXRF (Table 2) ranged from 31.0 to 1132 mg kg^{-1} (mean = 258.3 mg kg^{-1} and median = 160 mg kg^{-1}). Via pXRF Ce was not reported. Cerium is the most abundant rare earth element in the lithosphere and its mean concentration is ~65 mg kg^{-1}. According to Ramos et al. (2016), Ce concentration in Brazilian soils ranges from 15 to 286 mg kg^{-1}. Marques et al. (2004) studied the trace element geochemistry of Cerrado soils and found background concentration values for Ce up to 250 mg kg^{-1}. High Ce concentration in wetland soils may be explained by the agricultural use in surrounding higher areas. Due to the position of wetlands in the landscape (depressions), they are susceptible to accumulating contamination by eroded sediments, fertilizers and agrochemicals (Rosolen et al., 2015a). For instance, high Ce concentration can be found in some fertilizers (up to 24,100 mg kg^{-1}) (Ramos et al., 2016).

The mean (64.3 mg kg^{-1}) and median (58.0 mg kg^{-1}) values for WDXRF Ba are close to the background values (64 mg kg^{-1}) for Cerrado soils reported by Marques et al. (2004). For impacted wetlands soils the semi-total concentrations for Ba ranged from 9.0 to 190.3 mg kg^{-1} (Rosolen et al., 2015a). The WDXRF Ni concentration was close to the legislative semi-total threshold value (30 mg kg^{-1}) even considering the total concentration. The total concentration values for Pb via both WDXRF (Table 2) and pXRF (Table 3) can be considered safe. For Pb, the Brazilian legislation establishes the semi-total concentration values of 19.5 and 72 mg kg^{-1} for background reference and threshold values, respectively. The mean and median values for total Pb via WDXRF were 22.7 and 18.0 mg kg^{-1}, respectively (Table 2). Similar results were found for Pb when it was analyzed via pXRF (Table 3). Low Pb concentration was also observed in the wetlands soils studied by Rosolen et al. (2015a). The mean Zn concentration

(WDXRF/pXRF) was 22.9/28.2 mg kg^{-1}, whereas the background concentration for Cerrado soils is 38 mg kg^{-1}. The mean As total concentration (11.8 mg kg^{-1}) obtained via pXRF (Table 3) was lesser than the semi-total concentration (15.0 mg kg^{-1}) established as threshold value. For wetlands soils influenced by agricultural activities, the As concentration after Aqua Regia digestion ranged from 10 to 30 mg kg^{-1} (Rosolen et al., 2015a). The concentrations found for Ti, Fe, Nb, Y, and Sr are reported in Table 2, however there are no reference values established for these elements considering either total or semi-total concentration for Brazilian soils.

Correlations between USEPA 3051a, pXRF, and WDXRF methods

Linear regressions were performed between pXRF and WDXRF for Pb, Cu, Zn, Cr, Fe, Ti, Sr, and Y (Fig. 3). These elements were quantified by both pXRF and WDXRF methods, and significant and strong correlations were observed with R and R^2 values ranging from 0.91-0.96 and 0.89–0.92, respectively.

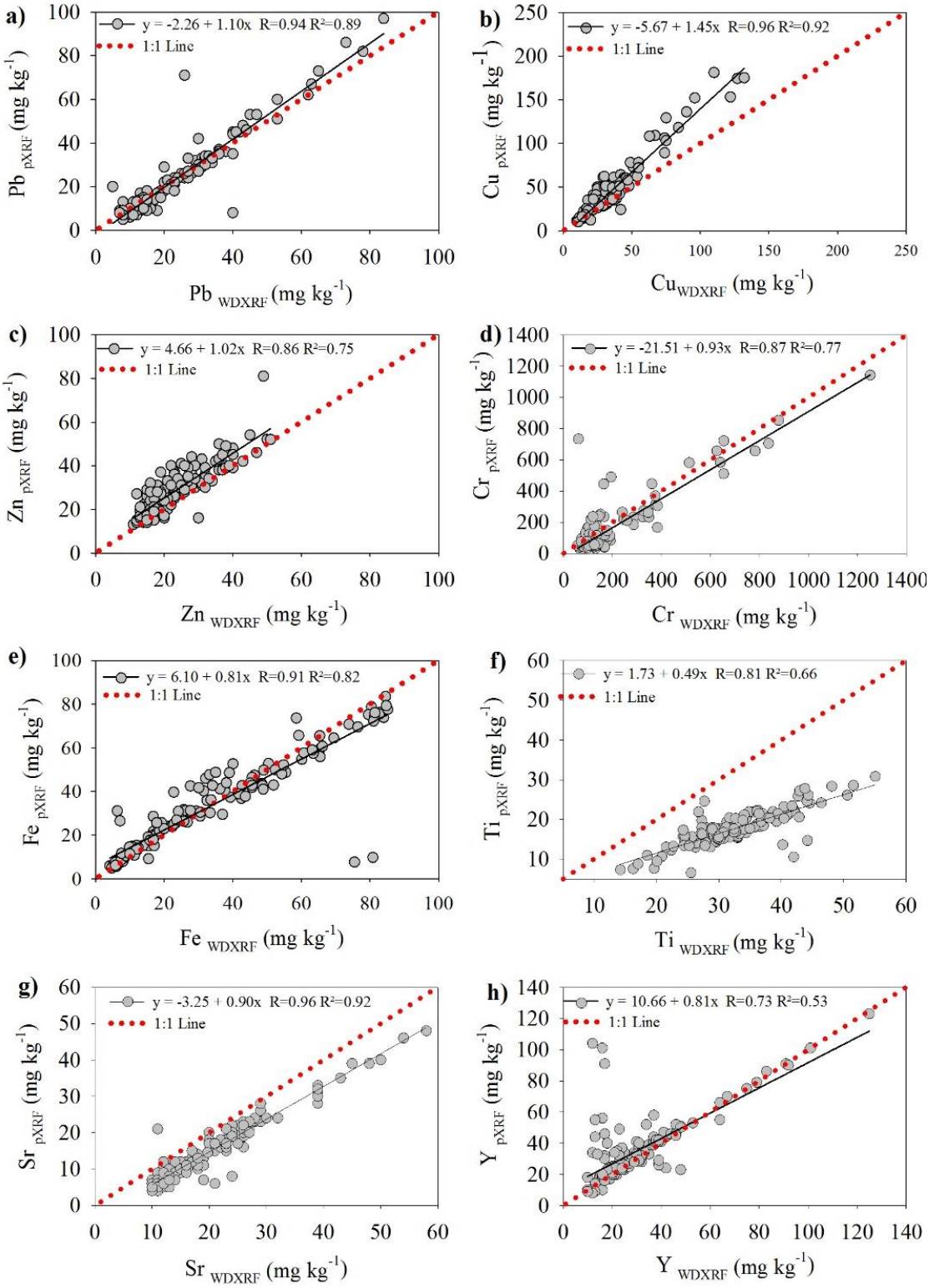

Fig. 3. Linear regression between portable X-ray fluorescence (pXRF) and wavelength dispersive X-ray fluorescence (WDXRF) methods for Pb (a), Cu (b), Zn (c), Cr (d), Fe (e), Ti (f), Sr (g), and Y (h) concentrations in Cerrado wetland soils. Red dotted line indicates the 1:1 line.

All three methods were used to assess Pb, Cu, Fe and Zn (Fig. 4). As expected, the pXRF and WDXRF results were higher than the results obtained via AD, except for Pb. The

AD Pb was strongly correlated to both pXRF and WDXRF with high R and R^2 values, corroborating the results obtained by Al Maliki et al. (2017) and Lee et al. (2016). The lowest values found for AD can be attributed to the incomplete digestion of soil samples underestimating the results (Suh et al., 2016). Explicitly, AD results are considered semi-total. A total digestion of soil samples can be reached via USEPA method 3052 using both HNO_3 and HF (Silva et al., 2014).

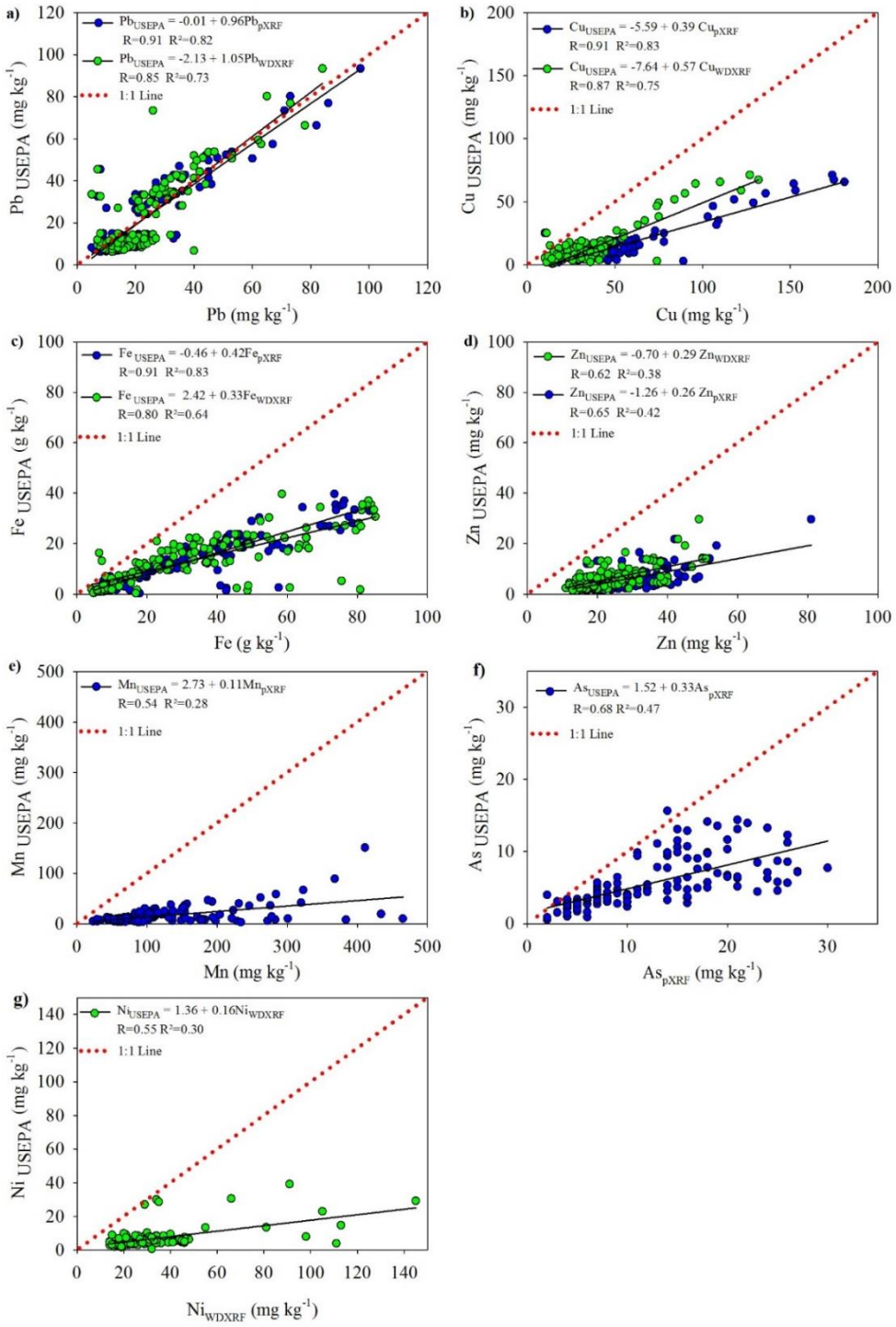

Fig. 4. Linear regression between acid digestion, portable X-ray fluorescence (pXRF) and wavelength dispersive X-ray fluorescence (WDXRF) methods for Pb, Cu, Fe and Zn (a, b, c, d); Linear regression

between acid digestion and portable X-ray fluorescence (pXRF) methods for Mn and As (e, f); Linear regression between acid digestion and wavelength dispersive X-ray fluorescence (WDXRF) methods for Ni (g) in the studied Cerrado wetland soils. Red dotted line indicates the 1:1 line.

According to Parsons et al. (2013) a perfect straight line would be obtained comparing the XRF data and the elemental concentrations after complete soil digestion (e.g., US EPA 3052 method). For instance, a strong correlation was observed between WDXRF data and the elemental concentrations obtained after wet digestion (HNO_3 + HCl + HF) (Arenas et al., 2011). A non-straight 1:1 line observed for Cu, Fe and Zn (Fig. 4) may be attributed to the occurrence of these elements as constituents of silicate minerals which are difficult to be totally digested by semi-total AD.

The AD/pXRF and AD/WDXRF concentration ratios were both 0.99 for Pb (Fig. 5). Based on this result the pXRF can be considered suitable for Pb concentration assessment in wetland soils. For Zn, Fe, Cu, Mn, As and Ni the AD/XRF concentration ratio was <0.50. The lowest ratio was observed for Mn (AD/pXRF). For this element, the AD concentration corresponds to 12% of total concentration. Silva et al. (2014) compared the metal concentration after soil digestion by three USEPA methods (3050b, 3051a, and 3052). No differences were observed between 3051a (semi-total) and 3052 (total) methods for Pb and Cu; significant differences were observed for Hg, Ni, Cu, Cd, and especially Zn (see Fig. 5).

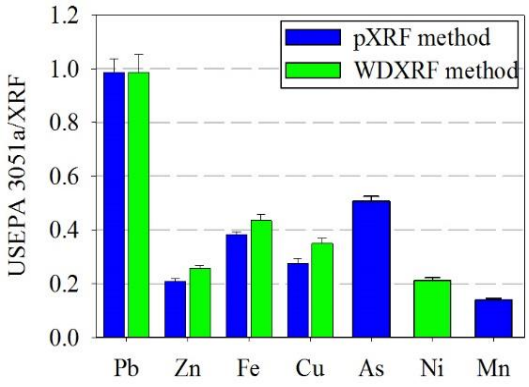

Fig. 5. Acid digest/X-ray fluorescence concentration ratio for Pb, Cu, Fe, Zn, Mn, As e Ni in the studied Cerrado wetland soils. Error bars means the standard error (n=144).

The pXRF method has been considered worldwide as a powerful tool for environmental, agronomic and pedological purposes (Weindorf et al., 2014). Its main advantage is the simultaneous and fast determination of various elements in seconds in the field or under

laboratory conditions. Also, this method can be considered environmentally-friendly. Of course, some limitations are expected like detection limits compared to AAS, ICP-OES and ICP-MS. The WDXRF method has high spectral resolution and low background interference allowing the determination of the light elements down to Be (Weindorf et al., 2014). However, the cost of the WDXRF equipment is very high.

Regarding the pXRF methods, several works have found strong correlation with standard methods in different soils and environments. Radu and Diamond (2009) found a strong correlation between the pXRF and AAS measurements for As, Cu, and Zn using soil samples from silver mines and abandoned mining sites in North Tipperary, Ireland. Bilo et al. (2019) found a strong correlation between XRF and ICP-OES measurements for Pb, Zn, and Cd. Working in Australian soils, Rouillon and Taylor (2016) observed very high correlation coefficients for Pb, Cu, and Fe, comparing pXRF and wet digestion methods. Compared to aqua regia digestion followed by ICP-OES determination, two pXRF instruments satisfactorily quantified the total concentration of Cu, Pb, As, Cd, Zn, Fe, Ni, and Mn in 81 soil samples (Kilbride et al., 2006).

The results of this study reinforce the pXRF technology as a powerful and accurate tool for fast characterization of soils (Weindorf et al., 2014). Regarding Cerrado wetlands soils, the total elemental composition can be obtained rapidly, allowing the determination of background reference values and identification of contaminated hotspots. The mapping of chemical properties of Cerrado wetlands areas will be greatly benefited by pXRF. Further studies are still needed prior to use pXRF in-situ, for example, to assess the effect of wet conditions on pXRF performance in hydromorphic soils (Ribeiro et al., 2018). Also, consideration should be given to combining pXRF data with auxiliary input data from other portable sensors, such as Vis-NIR, LIBS, Nix^{TM} and others to predict soil properties.

Conclusions

Portable X-ray fluorescence (pXRF) revealed great potential for fast characterization of Cerrado wetland soils. Several elements were successfully determined via pXRF and well correlated to other methods (e.g., AD and WDXRF). Since the XRF methods (pXRF and WDXRF) report the total elemental concentration, the results were higher than AD results, except for Pb. For Pb, a straight 1:1 correlation was observed between AD and XRF methods. Elements like Cu, Fe, Zn, Mn, As, and Ni had a low AD/XRF concentration ratio. Strong

correlations were observed between pXRF and WDXRF for Pb, Cu, Zn, Cr, Fe, Ti, Sr, and Y, reinforcing the accurate performance of pXRF.

Acknowledgments

The authors thank the following Brazilian universities and research funding agencies: Federal University of Lavras, Brazil; Federal University of Uberlândia, Brazil; National Council for Scientific and Technological Development (CNPq), Brazil; Coordination for the Improvement of Higher Education Personnel (CAPES), Brazil; and Research Foundation of Minas Gerais State (FAPEMIG), Brazil. Our thanks to B.L. Allen Endowment in Pedology at Texas Tech University in conducting this research. Also, Dr. Bruno T. Ribeiro thanks the PrInt-Capes Program (Process number 888887.363577/2019-00) for the opportunity to write this paper during his stay at Texas Tech University as visiting professor.

References

Al Maliki, A., Al-lami, A.K., Hussain, H.M., Al-Ansari, N., 2017. Comparison between inductively coupled plasma and X-ray fluorescence performance for Pb analysis in environmental soil samples. Environ. Earth Sci. 76, 1–7. http://dx.doi.org/10.1007/s12665-017-6753-z.

Andrade, R., Faria, W.M., Silva, S.H.G., Chakraborty, S., Weindorf, D.C., Mesquita, L.F., Guilherme, L.R.G., Curi, N., 2020a. Prediction of soil fertility via portable X-ray fluorescence (pXRF) spectrometry and soil texture in the Brazilian coastal plains. Geoderma 357, 113960. http://dx.doi.org/10. 1016/j.geoderma.2019.113960.

Andrade, R., Silva, S.H.G., Weindorf, D.C., Chakraborty, S., Faria, W.M., Mesquita, L.F., Guilherme, L.R.G., Curi, N., 2020b. Assessing models for prediction of some soil chemical properties from portable X-ray fluorescence (pXRF) spectrometry data in Brazilian coastal plains. Geoderma 357, 113957. http://dx.doi.org/10.1016/j.geoderma.2019.113957.

Arenas, L., Ortega, M., García-Martínez, M.J., Querol, E., Llamas, J.F., 2011. Geochemical characterization of the mining district of Linares (Jaen, Spain) by means of XRF and ICP-AES. J. Geochem. Explor. 108, 21–26. http://dx.doi.org/10.1016/j.gexplo.2010.09.002.

Bilo, F., Borgese, L., Pardini, G., Marguí, E., Zacco, A., Dalipi, R., Federici, S., Bettinelli, M., Volante, M., Bontempi, E., Depero, L.E., 2019. Evaluation of different quantification modes for a simple and reliable determination of Pb, Zn and Cd in soil suspensions by total reflection X-ray fluorescence spectrometry. J. Anal. At. Spectrom. 34, 930–939. http://dx.doi.org/10.1039/c9ja00040b.

Chakraborty, S., Li, B., Weindorf, D.C., Deb, S., Acree, A., De, P., Panda, P., 2019. Use of portable X-ray fluorescence spectrometry for classifying soils from different land use land

cover systems in India. Geoderma 338, 5–13. http://dx.doi.org/10.1016/j.geoderma.2018.11.043.

Companhia de Tecnologia de Saneamento Ambiental - Cetesb, 2014. Decisão de Diretoria 045/2014/E/C/I, de 20-02-2014. Dispõe sobre a aprovação dos Valores Orientadores para Solos e Águas Subterrâneas no Estado de São Paulo - 2014, em substituição aos Valores Orientadores de 2005 e dá outras providências. Diário Oficial Estado de São Paulo, São Paulo, Available online at: http://www.Cetesb.sp.gov.br/wp-content/uploads/sites/ 11/2013/11/DD-045-2014-P53.pdf.

Conselho Estadual de Política Ambiental - Copam, Deliberação Normativa Copam n◦ 166, de 29 de junho de 2011. Altera o Anexo I da Deliberação Normativa Conjunta Copam CERH no 2 de 6 de setembro de 2010, estabelecendo os Valores de Referência de Qualidade dos Solos. Belo Horizonte. Available online at: http://www.siam.mg.gov.br/sla/download.pdf?idNorma=18414.

Conselho Nacional do Meio Ambiente - Conama, 2009. Resolução Conama n◦ 420, de 28 de dezembro de 2009: Dispõe sobre critérios e valores orientadores de qualidade do solo quanto à presença de substâncias químicas e estabelece diretrizes para o gerenciamento ambiental de áreas contaminadas por essas substâncias em decorrência de atividades antrópicas [internet]. Brasília, DF. Available online at: http://www.mma.gov.br/ port/conama/res/res09/res42009.pdf.

Hu, W., Huang, B., Weindorf, D.C., Chen, Y., 2014. Metals analysis of agricultural soils via portable X-ray fluorescence spectrometry. Bull. Environ. Contam. Toxicol. 92, 420–426. http://dx.doi.org/10.1007/s00128-014-1236-3.

Hu, S., Niu, Z., Chen, Y., Li, L., Zhang, H., 2017. Global wetlands: Potential distribution, wetland loss, and status. Sci. Total Environ. 586, 319–327. http://dx.doi.org/10.1016/j.scitotenv.2017.02.001.

Junk, W.J., Piedade, M.T.F., Lourival, R., Wittmann, F., Kandus, P., Lacerda, L.D., Bozelli, R.L., Esteves, F.A., Nunes da Cunha, C., Maltchik, L., Schöngart, J., Schaeffer-Novelli, Y., Agostinho, A.A., 2014. Brazilian wetlands: Their definition, delineation, and classification for research, sustainable management, and protection. Aquat. Conserv. Mar. Freshw. Ecosyst. 24, 5–22. http://dx.doi.org/10.1002/aqc.2386.

Kilbride, C., Poole, J., Hutchings, T.R., 2006. A comparison of Cu, Pb, As, Cd, Zn, Fe, Ni and Mn determined by acid extraction/ICP-OES and ex situ field portable X-ray fluorescence analyses. Environ. Pollut. 143, 16–23. http://dx.doi.org/10.1016/j.envpol.2005.11.013.

Lee, H., Choi, Y., Suh, J., Lee, S.H., 2016. Mapping copper and lead concentrations at abandoned mine areas using element analysis data from ICP-AES and portable XRF instruments: A comparative study. Int. J. Environ. Res. Public Health 13, http://dx.doi.org/10.3390/ijerph13040384.

Lima, T.M., Weindorf, D.C., Curi, N., Guilherme, L.R.G., Lana, R.M.Q., Ribeiro, B.T., 2019. Elemental analysis of Cerrado agricultural soils via portable X-ray fluorescence spectrometry: Inferences for soil fertility assessment. Geoderma 353, 264–272. http://dx.doi.org/10.1016/j.geoderma.2019.06.045.

Mancini, M., Weindorf, D.C., Chakraborty, S., Silva, S.H.G., dos Santos Teixeira, A.F., Guilherme, L.R.G., Curi, N., 2019. Tracing tropical soil parent material analysis via portable X-ray fluorescence (pXRF) spectrometry in Brazilian Cerrado. Geoderma 337, 718–728. http://dx.doi.org/10.1016/j.geoderma.2018.10.026.

Marques, J.J., Schulze, D.G., Curi, N., Mertzman, S.A., 2004. Trace element geochemistry in Brazilian Cerrado soils. Geoderma 121, 31–43. http://dx.doi.org/10.1016/j.geoderma.2003.10.003.

Moraes, P.P.F., Horn, A.H., 2013. Teores dos metais pesados Cr, Cd e Zn em perfis de solos de Veredas da bacia do rio Formoso, município de Buritizeiro, Minas Gerais. Geonomos 18, 78–85. http://dx.doi.org/10.18285/geonomos.v18i2.75.

Nascimento, D.C., Berbert, C.P., Ribeiro, B.T., 2018. Electrochemical attributes of water from Cerrado wetlands (Veredas), Triângulo Mineiro region, Brazil. Rev. Cienc. Agron. 49, 11–21. http://dx.doi.org/10.5935/1806-6690.20180002.

Nishiyama, L., 1989. Geologia do Município de Uberlândia e áreas adjacentes. Soci. Nat. 1, 9–16.

Parsons, C., Margui Grabulosa, E., Pili, E., Floor, G.H., Roman-Ross, G., Charlet, L., 2013. Quantification of trace arsenic in soils by field-portable X-ray fluorescence spectrometry: Considerations for sample preparation and measurement conditions. J. Hard Mater. 262, 1213–1222. http://dx.doi.org/10.1016/j.jhazmat.2012.07.001.

Radu, T., Diamond, D., 2009. Comparison of soil pollution concentrations determined using AAS and portable XRF techniques. J. Hard Mater. 171, 1168–1171. http://dx.doi.org/10.1016/j.jhazmat.2009.06.062.

Ramos, M.V.V., Curi, N., da Motta, P.E.F., Vitorino, A.C.T., Ferreira, M.M., Silva, M.L.N., 2006. Veredas do triângulo mineiro: solos, água e uso. Ciência e Agrotecnologia 30, 283–293. http://dx.doi.org/10.1590/s1413-70542006000200014.

Ramos, S.J., Dinali, G.S., Oliveira, C., Martins, G.C., Moreira, C.G., Siqueira, J.O., Guilherme, L.R.G., 2016. Rare earth elements in the soil environment. Curr. Pollut. Rep. 2, 28–50. http://dx.doi.org/10.1007/s40726-016-0026-4.

Rawal, A., Chakraborty, S., Li, B., Lewis, K., Godoy, M., Paulette, L., Weindorf, D.C., 2019. Determination of base saturation percentage in agricultural soils via portable X-ray fluorescence spectrometer. Geoderma 338, 375–382. http://dx.doi.org/10.1016/j.geoderma.2018.12.032.
Ribeiro, B.T., Júnior, D. da C.F., da Silva, C.R., 2013. 10-day probable rainfall for Uberlândia, Minas Gerais State, Brazil. Biosci. J. 29, 536–542.

Ribeiro, B.T., Nascimento, D.C., Curi, N., Guilherme, L.R.G., Costa, E.T. de S., Lopes, G., Carneiro, J.P., 2019. Assessment of trace element contents in soils and water from Cerrado wetlands, triângulo mineiro region. Rev. Bras. Cienc. Solo 43, 1–17. http://dx.doi.org/10.1590/18069657rbcs20180059.

Ribeiro, B.T., Silva, S.H.G., Silva, E.A., Guilherme, L.R.G., 2017. Portable X-ray fluorescence (pXRF) applications in tropical soil science. Ciência e Agrotecnologia 41, 245–254. http://dx.doi.org/10.1590/1413-70542017413000117.

Ribeiro, B.T., Weindorf, D.C., Silva, B.M., Tassinari, D., Amarante, L.C., Curi, N., Guimarães Guilherme, L.R., 2018. The influence of soil moisture on oxide determination in tropical soils via portable X-ray fluorescence. Soil Sci. Am. J. 0, 0. http://dx.doi.org/10.2136/sssaj2017.11.0380.

Rosolen, V., De-Campos, A.B., Govone, J.S., Rocha, C., 2015a. Contamination of wetland soils and floodplain sediments from agricultural activities in the Cerrado Biome (State of Minas Gerais, Brazil). Catena 128, 203–210. http://dx.doi.org/10.1016/j.catena.2015.02.007.

Rosolen, V., de Oliveira, D.A., Bueno, G.T., 2015b. Vereda and murundu wetlands and changes in Brazilian environmental laws: challenges to conservation. Wetlands Ecol. Manage. 23, 285–292. http://dx.doi.org/10.1007/s11273-014-9380-4.

Rouillon, M., Taylor, M.P., 2016. Can field portable X-ray fluorescence (pXRF) produce high quality data for application in environmental contamination research? Environ. Pollut. 214, 255–264. http://dx.doi.org/10.1016/j.envpol.2016.03.055.

RStudio Team, 2016. Rstudio: Integrated development environment for R. RStudio, Inc. www.rstudio.com. (Accessed 9 Nov. 2019).

Santana, M.L.T., Ribeiro, B.T., Silva, S.H.G., Poggere, G.C., Guilherme, L.R.G., Curi, N., 2018. Conditions affecting oxide quantification in unknown tropical soils via handheld X-ray fluorescence spectrometer. Soil Res. 56, 648–655. http://dx.doi.org/10.1071/SR18099.

Santos, H.G., Jacomine, P.K.T., Anjos, L.H.C., Oliveira, V.A., Lumbreras, J.F., Coelho, M.R., Almeida, J.A., Araújo Filho, J.C., Oliveira, J.B., Cunha, T.J.F., 2018. Sistema brasileiro de classificação de solos, 5. ed. rev. e ampl. Embrapa, Brasília, DF, (ebook).

Silva, Y.J.A.B., Nascimento, C.W.A., Biondi, C.M., 2014. Comparison of USEPA digestion methods to heavy metals in soil samples. Environ. Monit. Assess. 186, 47–53. http://dx.doi.org/10.1007/s10661-013-3354-5.

Silva, S.H.G., Silva, E.A, Poggere, G.C., Pádua Junior, A., Gonçalves, M.G.M., Guilherme, L.R.G., Curi, N., 2020. Modeling and prediction of sulfuric acid digestion analyses data from PXRF spectrometry in tropical soils. Sci. Agricola 77, 12. http://dx.doi.org/10.1590/1678-992X-2018-0132.

Silva, E.A., Weindorf, D.C., Silva, S.H.G., Ribeiro, B.T., Poggere, G.C., Carvalho, T.S., Gonçalves, M.G.M., Guilherme, L.R.G., Curi, N., 2019. Advances in tropical soil characterization via portable X-ray fluorescence spectrometry. Pedosphere 29, 468–482. http://dx.doi.org/10.1016/S1002-0160(19)60815-5.

Soil Survey Staff, 2014. Soil Survey Field and Laboratory Methods Manual. Soil Survey Investigations Report No. 51. Version 2.0, USDA-NRCS, Available at: https://www.nrcs.usda.gov/wps/PA_NRCSConsumption/download?cid=stelprdb1244466&ext=pdf. (verified 06 Dec. 2019).

Suh, J., Lee, H., Choi, Y., 2016. A rapid, accurate, and efficient method to map heavy metal-contaminated soils of abandoned mine sites using converted portable XRF data and GIS. Int. J. Environ. Res. Public Health 13, http://dx.doi.org/10.3390/ijerph13121191.

Sun, F., Bakr, N., Dang, T., Pham, V., Weindorf, D.C., Jiang, Z., Li, H., Wang, Q., 2020. Geoderma enhanced soil profile visualization using portable X-ray fluorescence (PXRF) spectrometry. Geoderma 358, 113997. http://dx.doi.org/10.1016/j.geoderma.2019.113997.

USEPA, 2007a. Method 3051a (SW-846): Microwave assisted acid digestion of sediments, sludges, soils, and oils. US EPA. https://www.epa.gov/sites/production/files/2015-12/documents/3051a.pdf. (Acessed 6 Dec. 2019).

USEPA, 2007b. Method 6200: Field portable X-ray fluorescence spectrometry for the determination of elemental concentrations in soil and sediment. US EPA. https://www.epa.gov/sites/production/files/2015-12/documents/6200.pdf. (Accessed 9 Nov. 2019).

Weindorf, D.C., Bakr, N., Zhu, Y., 2014. Advances in portable X-ray fluorescence (PXRF) for environmental, pedological, and agronomic applications. In: Advances in Agronomy. Elsevier, http://dx.doi.org/10.1016/B978-0-12-802139-2.00001-9.

Weindorf, D.C., Chakraborty, S., 2016. Portable X-ray fluorescence spectrometry analysis of soils. Methods Soil Anal. 1, http://dx.doi.org/10.2136/methods-soil.2015.0033.

Weindorf, D.C., Zhu, Y., McDaniel, P., Valerio, M., Lynn, L., Michaelson, G., Clark, M., Ping, C.L., 2012. Characterizing soils via portable X-ray fluorescence spectrometer: 2. Spodic and Albic horizons. Geoderma 189–190, 268–277. http://dx.doi.org/10.1016/j.geoderma.2012.06.034.

Zhu, Y., Weindorf, D.C., Zhang, W., 2011. Characterizing soils using a portable X-ray fluorescence spectrometer: 1. Soil texture. Geoderma 167–168, 167–177. http://dx.doi.org/10.1016/j.geoderma.2011.08.010.

ARTICLE 2: FOLIAR ELEMENTAL ANALYSIS OF BRAZILIAN CROPS VIA PORTABLE X-RAY FLUORESCENCE SPECTROMETRY

(Article published in Sensors)

DOI: 10.3390/s20092509

Camila S. Borges[1], David C. Weindorf [2], Geila S. Carvalho[1], Luiz R. G. Guilherme[1], Thalita Takayama[1], Nilton Curi[1], Geraldo J. E. O. Lima[3] and Bruno T. Ribeiro [1,2,*]

[1] Department of Soil Science, Federal University of Lavras – UFLA, Doutor Sylvio Menicucci Avenue, Lavras 37200-900, Minas Gerais State, Brazil; camila.borges@estudante.ufla.br (C.S.B.); geilacarvalho@ufla.br (G.S.C.); guilherm@ufla.br (L.R.G.G.); thalita.takayama@estudante.ufla.br (T.T.); niltcuri@ufla.br (N.C.)

[2] Department of Plant and Soil Science, Texas Tech University, Bayer Plant Science Building, Room 211A, 2911 15th Street, Lubbock, TX 79409-2122, USA; david.weindorf@ttu.edu

[3] Campo – Environmental and Technological Agricultural Center, Lindolfo Garcia Adjuto Street, 1000, Paracatu 38600-000, Minas Gerais State, Brazil; geraldo.lima@campoanalises.com.br

***** Correspondence: bruno.ribeiro@ttu.edu or brunoribeiro@ufla.br

Abstract: Foliar analysis is very important for the nutritional management of crops and as a supplemental parameter for soil fertilizer recommendation. The elemental composition of plants is traditionally obtained by laboratory-based methods after acid digestion of ground and sieved leaf samples. This analysis is time-consuming and generates toxic waste. By comparison, portable X-ray fluorescence (pXRF) spectrometry is a promising technology for rapid characterization of plants, eliminating such constraints. This worked aimed to assess the pXRF performance for elemental quantification of leaf samples from important Brazilian crops. For that, 614 samples from 28 plant species were collected across different regions of Brazil. Ground and sieved samples were analyzed after acid digestion (AD), followed by quantification via inductively coupled plasma optical emission spectroscopy (ICP-OES) to determine the concentration of macronutrients (P, K, Ca, Mg, and S) and micronutrients (Fe, Zn, Mn, and Cu). The same plant nutrients were directly analyzed on ground leaf samples via pXRF. Four certified reference materials (CRMs) for plants were used for quality assurance control. Except for Mg, a very strong correlation was observed between pXRF and AD for all plant-nutrients and crops. The relationship between methods was nutrient- and crop-dependent. In particular, eucalyptus displayed optimal correlations for all elements, except for Mg. Opposite to eucalyptus, sugarcane showed the worst correlations for all the evaluated elements, except for S, which had a very strong correlation coefficient. Results demonstrate that for many crops, pXRF can reasonably quantify the concentration of macro- and micronutrients on ground and sieved leaf samples. Undoubtedly, this will contribute to enhance crop management strategies concomitant with increasing food quality and food security.

Keywords: foliar analysis; plant nutrition; proximal sensors

Introduction

The nutritional status of crops is crucial for assuring high productivity, food quality, and food security [1,2]. Well-nourished plants are more resilient to pests and diseases [3–5] and to adverse environmental conditions (e.g., dry season, soil water deficiency) [6,7]. At present, Brazil is widely recognized as a global food supplier [8] and for being one of the last agricultural frontiers. According to current world rankings [8,9], Brazil is the number 1 producer of soybean, sugarcane, and coffee; the number 2 producer of oilseeds (sunflower seed, peanuts (in shell), cottonseed, and rapeseed); and the number 3 producer of maize. Suitable management of soil fertility and plant mineral nutrition in Brazilian agriculture is one of the main factors responsible for increasing productivity and achieving food security goals in highly weathered-leached soils of Brazil [10].

The technical recommendation of fertilizers is frequently comprised of results from soil fertility analysis [11,12]. Additionally, chemical foliar analysis can be used as a complementary parameter for recommendation of fertilizers [13,14] to confirm observed visual deficiency of a given plant nutrient in the field and for temporal monitoring of the nutritional status of crops [15,16]. In sum, soil and foliar analyses are fundamental for successful fertilization and management of crops [17–19].

Foliar analysis of crops has been traditionally performed by wet digestion of oven-dried and ground leaf samples under laboratory conditions [20,21]. This analysis is time and labor consumptive and requires numerous chemicals. In the last two decades, portable X-ray fluorescence (pXRF) spectrometry has been an important and innovative tool in soil science [22,23]. At present, the pXRF method is recognized as an official method for soil analysis [22–26]. In a few seconds, under laboratory conditions or directly in the field, the total elemental composition of soils can be easily and adequately obtained. Furthermore, pXRF methods require no chemicals and are thus environmentally friendly. Based on pXRF spectra, prediction models of many soil properties (e.g., pH, texture, soil organic matter, macro and micronutrients) have been established [27–31]. Several pXRF soil studies have been successfully conducted in tropical environments [32,33].

pXRF approaches can also be used for chemical analysis of plant tissues and seeds [34–36]. However, there is no standard method for this and more investigations are still needed. Some previous works have successfully employed the pXRF to assess the elemental composition of vegetation [37–43]. The concentrations of Cu, Zn, Pb, K, and Fe from different plant species growing in polluted mines were obtained via pXRF and were well correlated to

laboratory-based methods [44]. For grasses, a strong correlation between pXRF and acid digestion was obtained for P, K, Ca, and Fe [45]. Sulfur, K, and Ca were reliably measured in cowpea, croton, mango, and maize leaves [40]. However, in Brazil, very few studies using pXRF for foliar analysis have been performed. The performance of pXRF was tested for soybean leaves [35] and for some varieties of sugarcane [46].

Given the lack of extensive research on pXRF elemental characterization of Brazilian crops, a study of such seems timely. Thus, the objective of this research was to compare the concentrations of macro- (P, K, Ca, Mg, and S) and micronutrients (Cu, Fe, Zn, and Mn) obtained via pXRF with those obtained via nitro-perchloric digestion, followed by inductively coupled plasma emission spectroscopy (ICP-OES) quantification. It was hypothesized that the pXRF will accurately quantify plant nutrients, showing strong correlations with conventional acid digestion and lab-based methods. These correlations are expected to be crop-dependent. If suitable correlations are obtained, the pXRF can be proposed as a fast, accurate, and environmentally friendly method for foliar analysis.

Material and Methods

Plant Material Collection from Brazilian Crops

Diagnostic leaves from 28 plant species were collected in different regions of Brazil (Southern, Southeastern, and Northeast) (Figure 1). The procedures for sampling the diagnostic leaves in the field were specific for each crop (Table S1) [11]. A total of 614 composite leaf samples were collected for this work. Table 1 shows the number of samples for each crop. The samples were sent to an ISO/IEC Standard 17025 Laboratory of Soil and Plant Analysis located in Minas Gerais State, Brazil. In the laboratory, the samples were carefully washed with distilled water, oven-dried (60ºC), and ground (30 mesh). The ground leaf material was stored in cold chamber at 4ºC for further analysis.

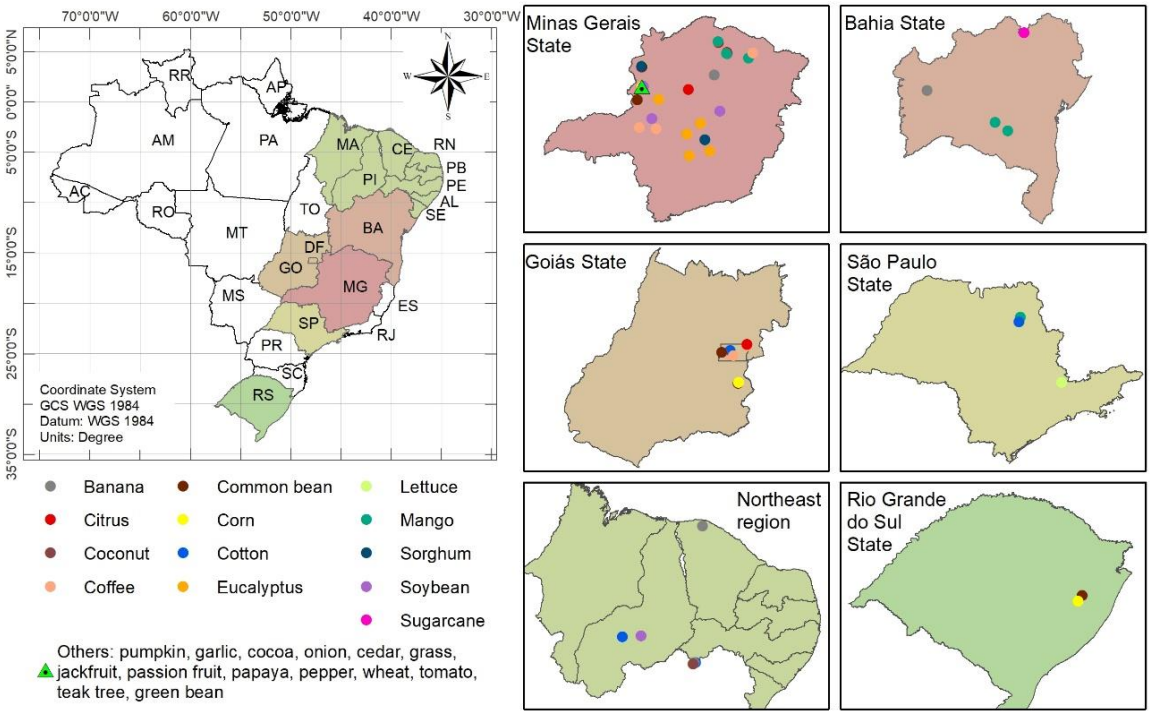

Figure 1. Location of crops in different regions of Brazil selected for this study.

Table 1. Plant species (Brazilian crops) selected for this work

Crop		Number of samples (n)
Cereals and oilseeds (n = 157)		
Bean	*Phaseolus vulgaris*	45
Corn	*Zea mays*	14
Soybean	*Glycine max*	11
Sorghum	*Sorghum bicolor L.*	24
Wheat	*Triticum* spp	1
Cotton	*Gossypium hirsutum L.*	62
Fruits (n = 186)		
Banana	*Musa spp.*	96
Coconut	*Cocos nucifera L.*	53
Jackfruit	*Artocarpus heterophyllus*	1
Mango	*Mangifera indica*	26
Passion fruit	*Passiflora edulis*	2
Papaya	*Carica papaya*	8
Vegetables (n = 28)		
Garlic	*Allium sativum*	2
Green bean	*Phaseolus vulgaris L.*	1
Onion	*Allium cepa*	2
Tomato	*Solanum lycopersicum*	1
Lettuce	*Lactuca sativa*	14
Pumpkin	*Cucurbita* spp	7
Pepper	*Capsicum annuum*	1
Citrus (n = 46)		
Orange	*Citrus sinensis L. Osbeck*	7

Lemon	*Citrus limon*	39
Forest trees (n = 84)		
Cedar	*Cedrela fissilis*	5
Eucalyptus	*Eucalyptus globulus Labill*	78
Teak trees	*Tectona grandis L.f.*	1
Perennials and semi-perennials (n = 113)		
Coffee	*Coffea ssp.*	96
Cocoa	*Theobroma cacao*	1
Sugarcane	*Saccharum officinarum*	12
Grass	*Poaceae*	4

Conventional Analysis of Plant Leaves: Acid Digestion (AD) Method

For determination of P, K, Ca, Mg, S, Fe, Cu, Mn, and Zn, the ground samples were wet digested (using the nitro-perchloric acid method) [20,47] with modifications. The samples (0.5 g) were transferred to 50-mL glass digestion tubes and treated with 6 mL of acid solution (HNO3:HClO4 2:1 v/v). Using a heating block digestion system, the samples were digested in three steps: i) heating at 120 ºC for 30 min; ii) heating at 160 ºC for 40 min; and iii) heating at 210 ºC for 20 min. After digestion, the samples were cooled under laboratory conditions to room temperature (22 ºC). After cooling, the samples were transferred to 50 mL volumetric flasks, then brought to volume with ultrapure water. Sub-samples were analyzed using a Ciros Vision ICP-OES (Spectro Analytical Instruments Inc., Kleve, Germany).

pXRF Analysis

Plant nutrients (P, K, Ca, Mg, S, Fe, Cu, Mn, and Zn) were also quantified via pXRF using an Olympus Vanta analyzer (Olympus®, Waltham, MA) equipped with a Rh tube (10–40 keV), silicon drift detector, and operated in the Geochem Mode on line power (115 VAC). Homogenized sub-samples of ground plant material (30 mesh) were packed into 23-mL plastic vials (48.9 mm high and 27.6 mm diameter). Inside the plastic vials, at least 1 cm thickness of plant material was assured for analysis. The vials were covered using Prolene® X-ray thin film (Chemplex Industries Inc., Palm City, FL, USA) and placed on the pXRF aperture. The X-ray thin film was held in place externally by latex rubber (Figure 2). The diameter of plastic vials was sufficient to cover the entire X-ray source and detector area without any influence of vial walls. The samples were scanned for 60 s as follows: beam 1 (first 30 s) for Fe, Cu, Mn, and Zn; beam 2 (last 30 s) for P, K, Ca, Mg, and S.

Figure 2. Details of portable X-ray fluorescence (pXRF) measurements. (**a**) Detail of ground leaf sample into the plastic vial and placed on X-ray source and detector aperture; (**b**) samples covered by a proper cap for protection against the X-ray; (**c**) data acquisition in real-time using a laptop connected to pXRF equipment.

For quality assurance and quality control (QA/QC), the following materials were used: Olympus® stainless calibration coin; blank sample (pure SiO_2) and three certified reference materials (CRMs) from the National Institute of Standards and Technology (NIST 1547 peach leaves, NIST 1573a tomato leaves, and NIST 1515 apple leaves). Additionally, an internal standard prepared from soybean leaves was also employed. For each studied element, the recoveries (pXRF value/certified value) were obtained and linear regressions were made. The obtained equations were used as corrections factors (CF) of pXRF measurements. The limits of detection (LOD) considered for low-density sample types were (mg kg^{-1}): P (50); K (25); Ca (25); Mg (3000); S (50); Mn (5); Fe (5); Cu (5); and Zn (5).

Statistical Analyses

Descriptive statistics (maximum, minimum, median, average, and standard deviation) for the results obtained via both acid digestion (AD) and pXRF were calculated. For comparison between methods, correlations and simple linear regressions were performed for each crop. The crops with fewer than 10 samples (Table 1) were grouped and collectively termed "others" (e.g.,

vegetables, fruits, etc.). For the full data set (n = 614), 70% of data were randomly selected to obtain linear regressions between AD and pXRF for each plant nutrient. The obtained equations were then validated using the remaining 30% of the data. The statistical significance of correlations and regressions was assessed based on Pearson's correlation coefficient (R), determination coefficient of regression (R^2), root mean square error (RMSE), and mean absolute error (MAE) (Equations (1) to (4), respectively). The linear regression analysis was performed using Sigma Plot Software version 14.0.

$$R = \frac{\sum_{i=1}^{n} x_i\, y_i - \bar{x}\bar{y}}{\sqrt{[\sum_{i=1}^{n} x_i^2 - n\bar{x}^2][\sum_{i=1}^{n} y_i^2 - n\bar{y}^2]}} \quad (1)$$

where n, $\bar{x}$ and $\bar{y}$ indicates the number of samples and the respective mean of each x_i and y_i variable.

$$R^2 = 1 - \frac{\sum_{i=1}^{n}(Y_i - \hat{Y}_i)^2}{\sum_{i=1}^{n}(Y_i - \bar{Y}_i)^2} \quad (2)$$

$$RMSE = \sqrt{\sum_{i=1}^{n} \frac{(\hat{Y}_i - Y_i)^2}{n}} \quad (3)$$

where, Y_i, $\hat{Y}_i$ and $\bar{Y}_i$ indicates the observed, the predicted and the mean of the target variable.

$$MAE = \frac{\sum_{i=1}^{n}|\hat{y}_i - y|}{n} \quad (4)$$

where n, $\hat{y}_i$ and y indicates the number of samples and the pXRF and AD values.

Results and Discussion

Recoveries of Elements

For all elements, pXRF measurements were higher than certified values (Figure 3), supporting previous results [42]. A 1:1 straight correlation was not reached. However, the pXRF results were very reliable, since significant linear regressions between pXRF measurements and CRM values were obtained with very high R2 values (from 0.96 to 0.99) (Figure 3). The pXRF recoveries for each element were almost the same, independent of CRMs. The worst linear

regression (R^2 = 0.88) was obtained for Mg (Figure 3d), which produces low fluorescence energy and can be influenced by spectral interference. This limitation for Mg has been reported and its quantification via pXRF should be conducted under vacuum conditions [40].

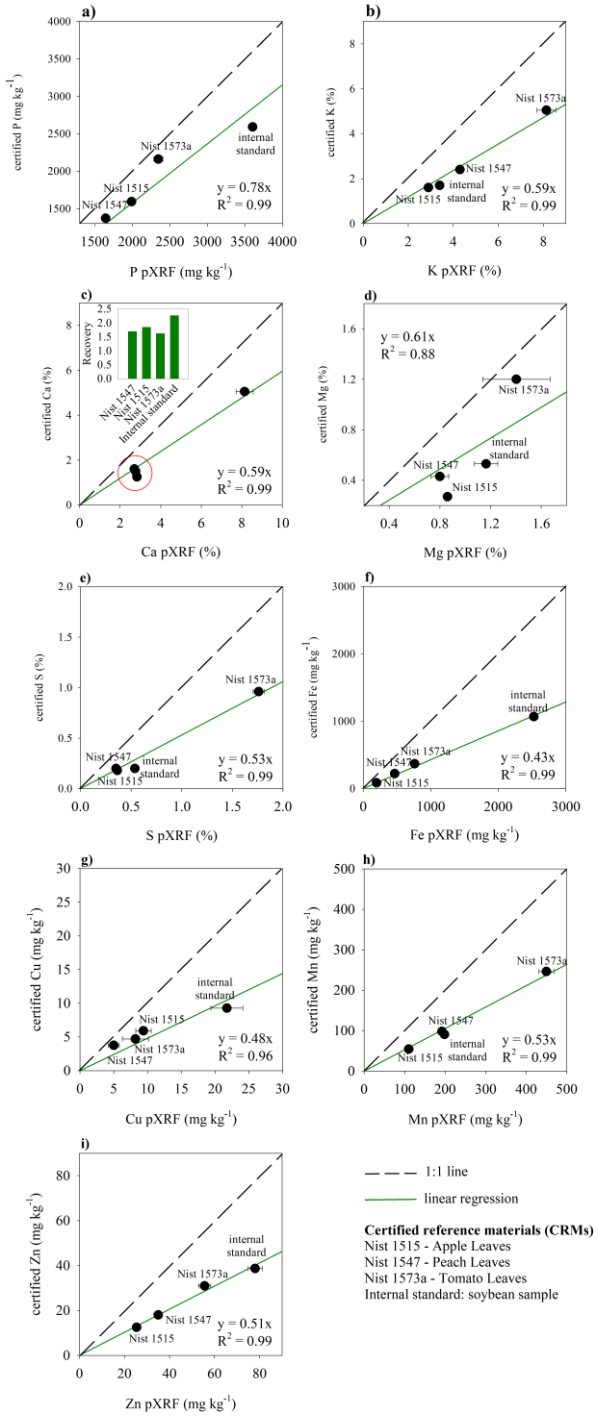

Figure 3. Calibration curve for obtained concentrations via pXRF and certified values for NIST 1515 (apple leaves), NIST 1547 (peach leaves), NIST 1537a (tomato leaves), and an internal standard (soybean sample): (a) Phosphorus; (b) Potassium; (c) Calcium; (d) Magnesium; (e) Sulfur; (f) Iron; (g) Copper; (h) Manganese; (i) Zinc.

For quality assurance and control, calibration routine on specific matrices can be performed for X-ray fluorescence analysis of plants [48]. Here, a calibration curve was obtained (Figure 3). The b parameter of linear equations (y = bx) (Figure 3) was used as the correction factor (CF) of pXRF measurements. The CF values represent the mean recoveries for four CRMs (NIST 1547; NIST 1573a; NIST 1515; and the internal standard for soybean leaves). For elemental assessment of thatch, deciduous leaves, grasses, tree bark, and herbaceous plants, CF values were considered as a mean of recoveries obtained for NIST 1515 and NIST 1547 [42]. The recovery assessment of CRMs is an important analytical procedure for quality assurance control of analysis [48], allowing a suitable interpretation and discussion of obtained results.

General Description of AD and pXRF Data

For all nutrients, the pXRF measurements were higher than LOD considered for low-density powder samples. The pXRF concentrations were higher than AD (Table 2). These results were expected, since the pXRF reports the total elemental concentration rather than the acid extractable concentration. The performance of AD methods is influenced by the digestion procedure and dilutions before quantification via ICP-OES [49–51]. Conversely, AD results higher than pXRF were found [35]. However, in Reference [35], they compared the AD method using ground and sieved leaf samples with the pXRF measurements performed directly on fresh leaves. The authors attributed the difference between pXRF and AD to the irregular distribution of nutrients in the leaves. The water content of fresh leaves can also be another factor influencing the results, since the water can attenuate X-rays [52]
and underestimates the results [40].

Many factors can influence the plant analysis via X-ray fluorescence techniques [53]. The performance of pXRF is related to particle size distribution, uniformity, homogeneity, thickness, and water content [40,42,54,55]. In this work, the pXRF measurements were performed on ground (30 mesh) and sieved samples. A perfect uniformity of plant material size distribution was not expected. However, the size uniformity of plant materials had a minimal effect on chemical analysis via X-ray fluorescence techniques [54].

For all macro- and micronutrients, the mean values were higher than the mean adequate concentrations for plants (MACP) [55,56] (Table 2). Regarding the macronutrients, except for P, the percentage of samples with concentrations higher than the MACP ranged from 81% (Ca) to 90% (Mg). For P, only 38% of samples were higher than the MACP. For the micronutrients,

the percentage of samples with concentrations exceeding the MACP ranged from 53% (Fe) to 67% (Zn). The most limiting nutrient was P, corroborating the very high P-adsorption capacity of highly-weathered leached soils (e.g., Oxisols) of Brazil [10,57,58], mainly by Fe oxides minerals. However, other facts that should be considered for this result is the fertility management and the differentiated nutritional need of P of the different evaluated crops. The mean concentrations of macronutrients decreased as K > Ca > Mg > S = P. For the micronutrients, concentrations were observed as Mn > Fe > Zn > Cu. In general, these results corroborate the expected uptake of nutrients by plants [55,56,59,60]. Plant mineral nutrition varies between species and from old to young leaves [55,56]. It is worthy to mention that in this work standard diagnostic leaves for nutritional status assessment were employed.

After N (not detectable by pXRF), Ca and K are the most abundant elements in plant dry matter, with concentrations ranging from 1 to 80 g kg^{-1} [56]. For Ca, both pXRF and AD methods (Table 2) resulted in similar mean values (13.64 and 14.15 g kg^{-1}, respectively), and 81% of samples had Ca concentrations higher than the MACP [55]. The mean K concentrations varied slightly more between methods (24.20 and 18.12 g kg^{-1} for pXRF and AD, respectively), but both reported concentrations were considered appropriate. For K, 83% of samples exceeded the MACP (Table 2). Similar Ca and K concentrations in cowpea, maize, and mango leaves were also obtained via pXRF [40]. Sulfur is the macronutrient found in lower concentrations in plant dry matter, ranging from 1 to 15 g kg^{-1} [56,59]. The obtained results by both AD and pXRF (2.24 and 2.95 g kg^{-1}, respectively) support this average concentration. These values were very similar to mean P concentrations (2.46 and 2.23 g kg^{-1}, respectively, for AD and pXRF methods), which were below the adequacy level (3 to 5 g kg^{-1}) [60].

High concentrations were observed for Mn, ranging from 21.73 to 4170 mg kg^{-1} when analyzed via pXRF and from 0.34 to 3273 mg kg^{-1} when analyzed via AD (Table 2). Adequate concentrations for foliar Mn in plants range from 30 to 500 mg kg^{-1}, with a deficiency from 20 to 30 mg kg^{-1} and toxicity between 200 and 5300 mg kg^{-1}, depending on the species [61]. The mean and median concentrations obtained for Fe via both AD and pXRF were within the range expected for plants (50 to 250 mg kg^{-1}) but values up to 792 mg kg^{-1} were found via pXRF. Normally, Fe deficiency occurs at concentrations below 50 mg kg^{-1} [59]. Zinc concentration in plant dry matter is commonly at least five times higher than Cu [56]. Yet in this work, Cu concentrations in the leaves were much higher than those of Zn. It is possible that the low levels of Zn in the leaves are related to the antagonistic effect of Cu, which causes a reduction in Zn uptake [62].

Table 2. Descriptive statistics (minimum, maximum, median, mean, and standard deviation) for pXRF and acid digestion (AD) data.

Nutrient	Minimum		Maximum		Median		Mean		s.d.		MACP	**%**
	pXRF	AD	pXRF	AD	pXRF	AD	pXRF	AD	pXRF	AD		
P (g kg^{-1})	0.52	0.32	8.99	10.96	1.67	1.64	2.46	2.23	1.75	1.71	2	38
K (g kg^{-1})	2.56	0.83	91.68	49.18	21.27	17.56	24.20	18.12	15.41	9.48	10	83
Ca (g kg^{-1})	2.08	0.48	55.49	58.74	13.96	10.80	13.64	14.15	9.94	10.96	5	81
Mg (g kg^{-1})	4.34	0.79	19.34	15.09	8.36	3.89	8.62	4.30	2.35	2.34	2	90
S (g kg^{-1})	0.65	0.51	14.96	15.46	2.53	1.86	2.95	2.24	1.68	1.61	1	86
Fe (mg kg^{-1})	43.00	6.90	792.06	687.13	143.62	104.30	194.14	131.59	121.76	93.49	100	53
Cu (mg kg^{-1})	0.00	0.18	795.84	719.40	8.16	7.39	20.76	18.03	61.55	54.53	6	63
Mn (mg kg^{-1})	21.73	0.34	4170.04	3273.00	183.33	97.50	282.58	220.76	440.31	355.79	50	61
Zn (mg kg^{-1})	7.65	2.38	376.89	345.58	24.48	23.79	35.25	31.32	35.70	33.32	20	67

Mean adequate concentration for plant growth (MACP) [55]; ** The pXRF did not detect Mg in 36% of samples. For Mg, the descriptive statistic represents 64% of full data set. %: percentage of samples with concentration higher than MACP.

Correlation between AD and pXRF

The obtained equations from linear regression (70% of full dataset) between AD and pXRF are shown in Table 3. Considering that AD methods are still a standard method for plant analysis, the AD data were plotted as a function of pXRF (AD = **a** + pXRF**x**). Except for Mg, high R values were obtained, ranging from 0.81 (K) to 0.98 (Cu). The R^2 values ranged from 0.66 (K, S, and Fe) to 0.97 (Cu).

Table 3. Linear equations obtained for 70% of the full dataset correlating to pXRF and AD data.

Plant-Nutrient	Equation	R	R^2
P	AD = 0.80pXRF + 0.27*	0.84	0.70
K	AD = 0.49pXRF + 6.23*	0.81	0.66
Ca	AD = 1.01pXRF - 2.24*	0.92	0.84
Mg	AD = 0.13pXRF + 3.26^{ns}	0.12	0.01
S	AD = 0.79pXRF - 0.08*	0.81	0.66
Cu	AD = 0.87pXRF + 0.09*	0.98	0.97
Fe	AD = 0.63pXRF + 7.76*	0.82	0.66
Zn	AD = 0.59pXRF + 0.52*	0.92	0.85
Mn	AD = 0.69pXRF + 18.73*	0.91	0.83

* $p<0.01$; ns: non-significant.

The non-significant correlation observed for Mg is related to the limitations for its determination via XRF techniques, as discussed before [40]. The validation of the obtained equations (Table 3) using 30% of the data revealed a very accurate prediction for all plant nutrients, with high R and R^2 values (Figure 4). The best prediction was observed for Cu (R and R^2 = 0.99; RMSE = 6.47 mg kg^{-1}). Based on R and R^2 values, the accuracy of predictions decreased in the following order: Cu > Mn > Zn > Ca > Fe > P > K > S.

Except for Ca, the micronutrients (heaviest elements) were better predicted than macronutrients (lightest elements). The ability of the X-ray fluorescence techniques to detect a particular element is directly related to its atomic number (Z) [63]. As the atomic number increases, so does the fluorescence energy. Thus, the so-called light elements (lighter than Ca; e.g., K, P, S, and Mg) are generally weakly identified and quantified via X-ray fluorescence techniques, while the heavier elements (Z > 20, e.g., Cu, Zn, Fe, and Mn) can be easily measured [22]. For the lightest elements (Mg, P, and S), the best performance of pXRF would be reached under vacuum conditions and without a Prolene® film [40]. Even without specific and intricate vacuum conditions, suitable correlations between AD and pXRF were obtained (Figure 4). A

strong correlation was obtained (R = 0.99) between pXRF and AD for S using pressed pellets of sugarcane leaves [46]. For P, a strong correlation between pXRF data and AD using CRMs for plants was also obtained [64].

The concentration of a given element in the sample can also influence the pXRF performance. For instance, Mn and Fe feature similar atomic numbers (Z = 25 and Z = 26, respectively), yet the prediction for Mn was better than Fe. As seen in Table 2, the Mn concentrations were higher than Fe. Similarly, Zn and Cu have similar atomic numbers (30 and 29, respectively). Better correlation was observed for Cu, as Cu concentrations were higher than Zn (Table 2). The adequate performance observed for Ca can also be related to its high concentration (Table 2). Similarly, a better correlation for Ca and K compared to Mn and Fe was found, where the total concentration within the plant was the compelling factor [65].

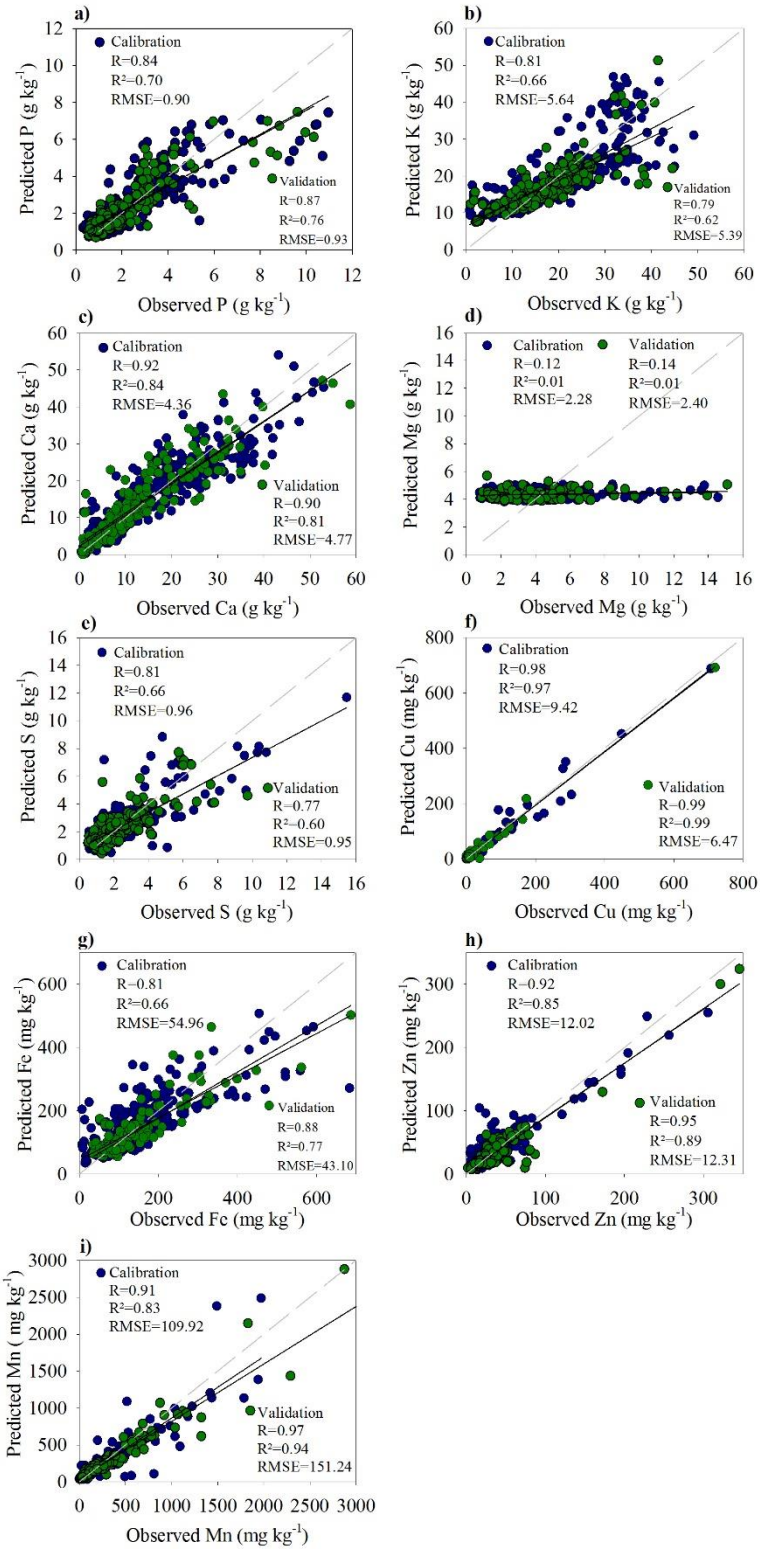

Figure 4. Prediction of macro- and micronutrients concentration in leaf samples from Brazilian crops (n = 614) using pXRF: (a) Phosphorus; (b) Potassium; (c) Calcium; (d) Magnesium; (e) Sulfur; (f) Copper; (g) Iron; (h) Zinc; (i) Manganese.

Correlation between pXRF and AD for Each Crop

The correlation between pXRF and AD was nutrient- and crop-dependent (Figure 5). For P (Figure 5a), a very strong correlation between methods was observed for coconut, cotton, lettuce, soybean, and eucalyptus. Sugarcane showed no correlation for P. For K (Figure 5b), a very strong correlation was observed for eucalyptus, cotton, corn, banana, and sorghum and a weak correlation was shown for lettuce. Regarding Ca (Figure 5c), the correlation was strong and very strong for most crops and a weak correlation was also observed for sugarcane. As expected, the worst correlations were observed for Mg (Figure 5d), where only citrus had a strong correlation. For this nutrient, moderate correlations were observed for banana, soybean, common bean, and lettuce; weak correlations were observed for sorghum and eucalyptus; and no significant correlations were observed for coconut, cotton, and coffee. For S (Figure 5e), contrary to P and Ca, a very strong correlation was
observed for sugarcane and no significant correlations were observed for sorghum and corn.

Regarding the micronutrients, very strong and strong correlations were observed for most crops, mainly for Fe, Mn, and Cu (Figure 5f–h). Corroborating the results for P and Ca, for all micronutrients, the worst correlation was observed in sugarcane. Regarding the macronutrients, the mean absolute errors (MAEs) were quite low (Table 4). The highest MAE values were observed for K (corn, lettuce, sorghum, and sugarcane), ranging from 14.57 to 35.39 mg kg^{-1} for these crops. For the micronutrients and considering all crops, the mean MAE decreased as Fe (74 mg kg^{-1}) > Mn (56 mg kg^{-1}) > Zn (7.4 mg kg^{-1}) > Cu (5.1 mg kg^{-1}).

Table 4. The mean absolute error (MAE) between pXRF and AD methods for each nutrient and crop.

Crop	P	K	Ca	Mg	S	Cu	Fe	Zn	Mn
	----------(g kg^{-1}) ----------					---------- (mg kg^{-1})----------			
Banana	0.19	6.3	0.75	4.41	0.49	1.56	41.28	1.72	106.07
Citrus	0.24	0.24	2.94	1.55	0.01	0.37	66.22	1.58	30.39
Coconut	0.65	5.94	1.99	1.84	1.27	1.92	50.83	2.23	54.39
Coffee	0.01	4.73	4.5	3.49	0.67	5.91	44.13	3.2	48.86
Common bean	0.45	2.68	6.45	1.71	0.74	2.98	80.16	7.72	33.7
Corn	1.29	18.41	4.61	*	2.12	7.43	102.52	23.91	52.75
Cotton	0.37	0.51	1.43	5.73	1.02	1.45	26.89	1.64	33.08
Eucalyptus	0.58	3.37	3.65	5.64	0.52	1.77	96.6	5.55	153.14
Lettuce	2.16	32.59	3.63	2.49	1.82	17.37	91.2	14.24	56.18
Mango	0.33	0.76	5.19	*	0.24	4.28	31.75	1.51	40.31
Sorghum	2.17	35.39	4.24	8.17	1.95	5.69	194.55	22.42	32.72
Soybean	0.81	3.5	6.05	0.9	0.88	15.78	99.18	10.27	55.21
Sugarcane	0.41	14.57	2.96	*	0.18	2.16	67.59	6.13	50.29
Others	0.42	6.85	0.7	6.39	0.45	3.34	47.64	1.14	30.79
Mean	0.72	9.70	3.51	3.85	0.88	5.14	74.32	7.38	55.56

Citrus: orange and lemon. Others: pumpkin, garlic, cocoa, onion, cedar, grass, jackfruit, passion fruit, papaya, pepper, wheat, tomato, teak tree, and green bean. *For Mg, there was no sufficient data for corn, mango, or sugarcane.

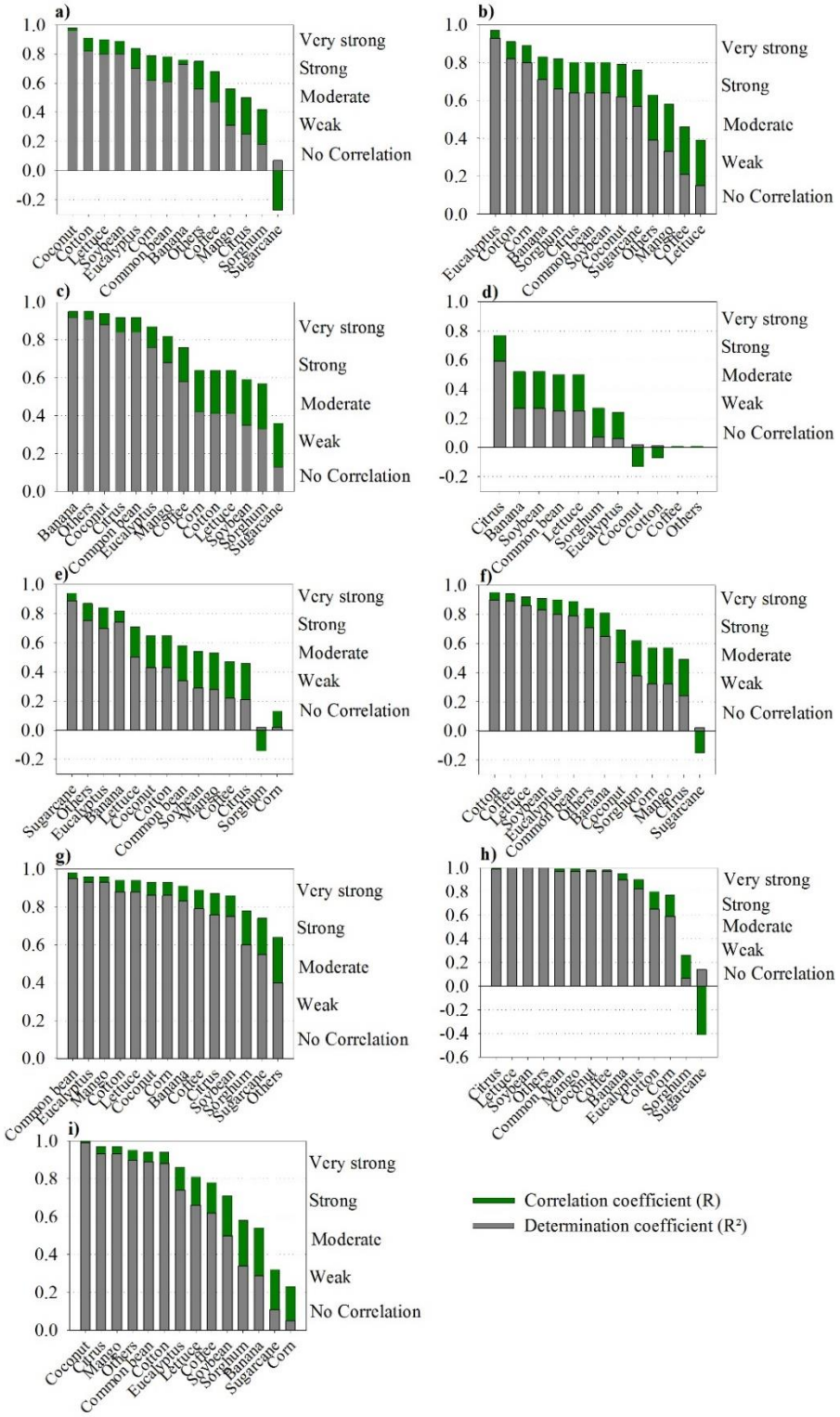

Figure 5. Correlation coefficient (R) and determination coefficient (R^2) from the linear regression between pXRF and AD methods for each nutrient and crop. Citrus: orange and lemon. Others: pumpkin, garlic, cocoa, onion, cedar, grass, jackfruit, passion fruit, papaya, pepper, wheat, tomato, teak tree, and green bean. For Mg, there was no sufficient data for corn, mango, or sugarcane: (**a**) Phosphorus; (**b**) Potassium; (**c**) Calcium; (**d**) Magnesium; (**e**) Sulfur; (**f**) Iron; (**g**) Manganese; (**h**) Copper; (**i**) Zinc.

Supporting the results found in this work, a strong correlation between pXRF and AD was also observed for Ca, Mn, Zn, and Cu in different plant species [44]. Assessing the

elemental composition of plants (thatch, deciduous leaves, grasses, tree bark, and herbaceous plants) in mining-impacted areas, a significant correlation for Cu, Fe, Zn, Mn, Cd, Pb, and K was found [42]. Conversely, a poor correlation was observed for Cu in lettuce plants [41]. The results found that Ca, Cu, Zn, and Mn corroborate the performance of pXRF for soybean, wheat, corn, and cotton samples [37].

Different correlations between methods can be related to the intrinsic characteristics of plant materials, which will determine the performance of AD procedures [66]. The pXRF performance may be related to the anatomic characteristics of each plant species influencing the X-ray absorption and emission of the fluorescent energy. Further studies involving plant anatomy (e.g., epidermis, adaxial and abaxial surfaces, cuticle, stomata, and mesophyll) are still needed to elucidate the diverse performance of pXRF for plant analysis. After that, in-field measurements will be greatly benefited. It is hypothesized here that plant materials with higher cellulose and lignin contents may be more difficult to digest. In general, grasses usually feature higher cellulose and lignin contents [67]. The acid digestion of a lettuce leaf or even the penetration of X-rays may be quite different when compared to more lignified leaves.

The accurate performance of pXRF to assess the elemental composition of plants will very likely contribute to fast and in-field diagnostic of nutritional status, improving the suitable management of soil fertility properties, food quality, and food security. Based on the results of this work, the foliar elemental composition can be analyzed via pXRF on ground and sieved leaf samples, eliminating the need for AD. For in-field applications, further studies are still needed to assess the other factors that can influence the pXRF results, such as water content, anatomy of leaves, cellulose, and lignin contents. Additionally, the nutritional status should be assessed combining pXRF with other proximal sensors (e.g., Vis-NIR, NixPro), as such techniques have been proven to enhance predictive models in coal and soils [68,69]. Especially for crops in which foliar fertilization is necessary, the pXRF can be a useful tool for decision-making. The assessment of fruit quality and nutritive value via pXRF is also promising [70] and worthy of additional study.

Conclusions

Except for Mg, pXRF spectrometry successfully quantified macro- and micronutrients in several leaf samples from important Brazilian crops. For many nutrients, a very strong correlation was observed between pXRF and the most traditional method for foliar analysis (nitro-perchloric digestion). The correlation between pXRF and acid digestion was nutrient-

and crop-dependent. Except for Mg, a very strong correlation was always observed for eucalyptus leaves. Conversely, except for S and K, a weak or non-significant correlation was observed for sugarcane leaves.

pXRF measurements made directly on ground and sieved leaf samples has a great potential to replace conventional foliar analysis based on acid digestion, dispensing the use of chemicals, acquisition, and maintenance of high-cost equipment (e.g., an atomic absorption spectrometer, an inductively coupled plasma-optical emission spectrometer). Measurements in the field directly on intact and fresh leaves still need more studies to elucidate all factors that can influence the pXRF performance for plant analysis.

Acknowledgments

The authors gratefully acknowledge the BL Allen Endowment in Pedology at Texas Tech University in conducting this research. Our thanks to the following Brazilian research funding agencies: CNPq, CAPES, and FAPEMIG. We really appreciate the precious help of Maria E.C. Monteiro (PPGCS/UFLA), to create the map of selected crop distribution in Brazil, and CAMPO (Environmental and Technological Agriculture Center) for all their support for conventional foliar analysis.

References

1. FAO. Plant Nutrition for Food Security. A Guide for Integrated Nutrient Management; Food and Agriculture Organization of The United Nations (FAO): Rome, Italy, 2006.

2. White, P.J.; Broadley, M.R.; Gregory, P.J. Managing the nutrition of plants and people. Appl. Environ. Soil Sci. **2012**, 2012, 104826.

3. Dordas, C. Role of nutrients in controlling plant diseases in sustainable agriculture: A review. Agron. Sustain. Dev. **2009**, 28, 33–46.

4. Spann, T.M.; Schumann, A.W. The Role of Plant Nutrients in Disease Development with Emphasis on Citrus and Huanglongbing. Proc. Fla. State Hortic Soc. **2009**, 122, 169–171.

5. Huber, D.; Römheld, V.; Weinmann, M. Relationship between Nutrition, Plant Diseases and Pests. In Marschner's Mineral Nutrition of Higher Plants, 3rd ed.; Marschner, P., Ed.; Elsevier: London, UK, 2012; pp. 283–298.

6. Wang, M.; Zheng, Q.; Shen, Q.; Guo, S. The critical role of potassium in plant stress response. Int. J. Mol. Sci. **2013**, 14, 7370–7390.

7. Ahanger, M.A.; Tyagi, S.R.;Wani, M.R.; Ahmad, P. Drought Tolerance: Role of Organic Osmolytes, Growth Regulators, and Mineral Nutrients. In Physiological Mechanisms

and Adaptation Strategies in Plants Under Changing Environment; Ahmad, P.,Wani, M.R., Eds.; Springer: New York, NY, USA, 2014; Volume 1, pp. 16–43.

8. United States Department of Agriculture, Foreing Agricultural Service Home Page. Available online: https://apps.fas.usda.gov/psdonline/circulars/production.pdf (accessed on 20 January 2020).

9. United States Department of Agriculture, Foreing Agricultural Service Home Page. Available online: https://apps.fas.usda.gov/psdonline/circulars/co_ee.pdf (accessed on 20 January 2020).

10. Lopes, A.S.; Guilherme, L.G. A career perspective on soil management in the Cerrado region of Brazil. Adv. Agron. **2016**, 137, 1–72.

11. Ribeiro, A.C.; Guimarães, P.T.G.; Alvarez, V.V.H. Recomendaç*ã*o Para o uso de Corretivos e Fertilizantes em Minas Gerais; CFSEMG/UFV: Viçosa, Brazil, 1999.

12. Blaylock, A.D.; Belden, K.; Hough, H.W. Guide toWyoming Fertilizer Recommendations; University of Wyoming: Laramie, WY, USA, 1996.

13. Lucena, J.J. Methods of diagnosis of mineral nutrition of plants a critical review. Acta Hortic. **1997**, 448, 179–192.

14. Cantarutti, R.B.; Barros, N.F.; Martinez, H.E.P.; Novais, R.F. Avaliação da fertilidade do solo e recomendação de fertilizantes. In Fertilidade do Solo; Novais, R.F., Alvarez, V., De Barros, N.F., Fontes, R.L.F., Cantarutti, R.B., Neves, J.C.L., Eds.; Socidade Brasileira de Ciência do Solo: Viçosa, Brazil, 2007; pp. 769–850.

15. Munson, R.D. Principles of plant analysis. In Handbook of Reference Methods for Plant Analysis; Kalra, Y.P., Ed.; Taylor & Francis Group: New York, NY, USA, 1998; pp. 1–24.

16. Sturgeon, R.E. Current practice and recent developments in analytical methodology for trace element analysis of soils, plants, and water. Commun. Soil Sci. Plant Anal. **2000**, 31, 1479–1512.

17. Elwali, A.M.O.; Gascho, G.J. Soil Testing, Foliar Analysis, and DRIS as Guides for Sugarcane Fertilization. Agron. J. **1984**, 76, 466–470.

18. Creste, J.E.; Echer, F.R. Establishing standards for the integrated recommendation and diagnosis system (DRIS) for irrigated bean crops. Commun. Soil Sci. Plant Anal. **2010**, 41, 1921–1933.

19. Maia, C.E. Fertilization response likelihood for the interpretation of leaf analyses. Rev. Bras. Cienc. Solo **2012**, 36, 437–445.

20. Miller, R. Nitric-Perchloric Acid Wet Digestion in an Open Vessel. In Handbook of Reference Methods for Plant Analysis; Kalra, Y.P., Ed.; CRC Press: Boca Raton, FL, USA, 1998; pp. 57–61.

21. Isaac, R.A.; Johnson, W.C., Jr. Elemental determination by inductively coupled plasma atomic emission spectroscopy. In Handbook of Reference Methods for Plant Analysis; Kalra, Y.P., Ed.; CRC Press: Boca Raton, FL, USA, 1998; pp. 165–170.

22. Weindorf, D.C.; Bakr, N.; Zhu, Y. Advances in portable X-ray fluorescence (PXRF) for environmental, pedological, and agronomic applications. Adv. Agron. **2014**, 128, 1–45.

23. Ribeiro, B.T.; Silva, S.H.G.; Silva, E.A.; Guilherme, L.R.G. Portable X-ray fluorescence (pXRF) applications intropical Soil Science. Cienc. Agrotec. **2017**, 41, 245–254.

24. US EPA: Method 6200-Field Portable X-ray Fluorescence Spectrometry for the Determination of Elemental Concentrations in Soil and Sediment. Available online: https://www.epa.gov/sites/production/files/2015-12/documents/6200.pdf (accessed on 20 January 2020).

25. Soil Survey Staff. Soil Survey Field and Laboratory Methods Manual. Soil Survey Investigations. Available online: https://www.nrcs.usda.gov/Internet/FSE_DOCUMENTS/stelprdb1244466.pdf (accessed on 20 January 2020).

26. Weindorf, D.C.; Chakraborty, S. Portable X-ray Fluorescence Spectrometry Analysis of Soils. In Methods of Soil Analysis; Hirmas, D., Madison, W.I., Eds.; Soil Science Society of America: Madison, WI, USA, 2016; pp. 1–8.

27. Zhu, Y.;Weindorf, D.C.; Zhang,W. Characterizing soils using a portable X-ray fluorescence spectrometer: 1. Soil texture. Geoderma **2011**, 167–168, 167–177.

28. Sharma, A.;Weindorf, D.C.;Wang, D.D.; Chakraborty, S. Characterizing soils via portable X-ray fluorescence spectrometer: 4. Cation exchange capacity (CEC). Geoderma **2015**, 239, 130–134.

29. de Lima, T.M.;Weindorf, D.C.; Curi, N.; Guilherme, L.R.G.; Lana, R.M.Q.; Ribeiro, B.T. Elemental analysis of Cerrado agricultural soils via portable X-ray fluorescence spectrometry: Inferences for soil fertility assessment. Geoderma **2019**, 353, 264–272.

30. Andrade, R.; Faria,W.M.; Silva, S.H.G.; Chakraborty, S.;Weindorf, D.C.; Mesquita, L.F.; Guilherme, L.R.G.; Curi, N. Prediction of soil fertility via portable X-ray fluorescence (pXRF) spectrometry and soil texture in the Brazilian Coastal Plains. Geoderma **2020**, 357, 113960.

31. Andrade, R.; Silva, S.H.G.;Weindorf, D.C.; Chakraborty, S.; Faria,W.M.; Mesquita, L.F.; Guilherme, L.R.G.; Curi, N. Assessing models for prediction of some soil chemical properties from portable X-ray fluorescence (pXRF) spectrometry data in Brazilian Coastal Plains. Geoderma **2020**, 357, 113957.

32. Silva, F.M.; Weindorf, D.C.; Silva, S.H.G.; Silva, E.A.; Ribeiro, B.T.; Guilherme, L.R.G.; Curi, N. Tropical Soil Toposequence Characterization via pXRF Spectrometry. Pedology **2019**, 83.

33. dos Santos Teixeira, A.F.; Pelegrino, M.H.P.; Faria, W.M.; Silva, S.H.G.; Gonçalves, M.G.M.; Acerbi, F.W., Jr.; Gomide, L.R.; Pádua, A.L., Jr.; de Souza, I.A.; Chakraborty, S.; et al. Tropical soil pH and sorption complex prediction via portable X-ray fluorescence spectrometry. Geoderma **2020**, 361, 114132.

34. Bachiega, P.; de Almeida, E.; Salgado, J.M.; Arruda, M.A.Z.; Lehmann, E.L.; Morzelle, M.C.; de Carvalho, H.W.P. Benchtop and Handheld Energy-Dispersive X-Ray Fluorescence (EDXRF) as Alternative for Selenium Concentration Measurement in Biofortified Broccoli Seedling. Food Anal. Method. **2019**, 12, 1520–1527.

35. Costa, G.T., Jr.; Nunes, L.C.; Gomes, M.H.F.; de Almeida, E.; de Carvalho, H.W.P. Direct determination of mineral nutrients in soybean leaves under vivo conditions by portable X-ray fluorescence spectroscopy. X-ray Spectrom. **2019**, 49, 1–10.

36. Melquiades, F.L.; Bortoleto, G.G.; Marchiori, L.F.S.; Bueno, M.I.M.S. Direct determination of sugar cane quality parameters by X-ray spectrometry and multivariate analysis. J. Agric. Food Chem **2012**, 60, 10755–10761.

37. McLaren, T.I.; Guppy, C.N.; Tighe, M.K. A Rapid and Nondestructive Plant Nutrient Analysis using Portable X-Ray Fluorescence. Soil Sci. Soc. Am. J. **2012**, 76, 1446–1453.

38. Paltridge, N.G.; Milham, P.J.; Ortiz-Monasterio, J.I.; Velu, G.; Yasmin, Z.; Palmer, L.J.; Guild, G.E.; Stangoulis, J.C.R. Energy-dispersive X-ray fluorescence spectrometry as a tool for zinc, iron and selenium analysis in whole grain wheat. Plant Soil. **2012**, 361, 261–269.

39. Paltridge, N.G.; Palmer, L.J.; Milham, P.J.; Guild, G.E.; Stangoulis, J.C.R. Energy-dispersive X-ray fluorescence analysis of zinc and iron concentration in rice and pearl millet grain. Plant Soil. **2012**, 361, 251–260.

40. Towett, E.K.; Shepherd, K.D.; Drake, B.L. Plant elemental composition and portable X-ray fluorescence (pXRF) spectroscopy: Quantification under di_erent analytical parameters. X-ray Spectrom. **2016**, 45, 117–124.

41. Sacristán, D.; Viscarra Rossel, R.A.; Recatalá, L. Proximal sensing of Cu in soil and lettuce using portable X-ray fluorescence spectrometry. Geoderma **2016**, 265, 6–11.

42. McGladdery, C.; Weindorf, D.C.; Chakraborty, S.; Li, B.; Paulette, L.; Podar, D.; Pearson, D.; Kusi, N.Y.O.; Duda, B. Elemental assessment of vegetation via portable X-ray fluorescence (PXRF) spectrometry. J. Environ. Manag. **2018**, 210, 210–225.

43. Montanha, G.S.; Rodrigues, E.S.; Marques, J.P.R.; Almeida, E.; Reis, A.R.; Carvalho, H.W.P. X-ray fluorescence spectroscopy (XRF) applied to plant science: Challenges towards in vivo analysis of plants. Metallomics **2019**, 12, 183–192.

44. Gutiérrez-Ginés, M.J.; Pastor, J.; Hernández, A.J. Assessment of field portable X-ray fluorescence spectrometry for the in situ determination of heavy metals in soils and plants. Environ. Sci. Proc. Imp. **2013**, 15, 1545–1552.

45. Sapkota, Y.; McDonald, L.M.; Griggs, T.C.; Basden, T.J.; Drake, B.L. Portable X-Ray fluorescence spectroscopy for rapid and cost-e_ective determination of elemental composition of ground forage. Front. Plant Sci. **2019**, 10, 1–9.

46. Guerra, M.B.B.; de Almeida, E.; Carvalho, G.G.A.; Souza, P.F.; Nunes, L.C.; Santos, D., Jr.; Krug, F.J. Comparison of analytical performance of benchtop and handheld energy dispersive X-ray fluorescence systems for the direct analysis of plant materials. J. Anal. Atom. Spectrom. **2014**, 29, 1667–1674.

47. Malavolta, E.; Vitti, G.C.; Oliveira, S.A. Avaliação do Estado Nutricional das Plantas: Princípios e Aplicações, 2nd ed.; Associação Brasileira para pesquisa da Potassa e do Fosfato: Piracicaba, Brazil, 1997.

48. Byers, H.L.; McHenry, L.J.; Grundl, T.J. XRF techniques to quantify heavy metals in vegetables at low detection limits. Food Chem. **2019**, 1, 100001.

49. Lavilla, I.; Filgueiras, A.V.; Bendicho, C. Comparison of digestion methods for determination of trace and minor metals in plant samples. J. Agric. Food Chem. **1999**, 47, 5072–5077.

50. Carneiro, C.; Reissmann, C.B.; Marques, R. Comparação de métodos de análise química de K, Ca, Mg e Al, em folhas de erva-mate (Ilex paraguariensis St. Hil.). Cerne **2006**, 12, 113–122.

51. Bernardi, A.C.C.; Oka, S.H.; de Souza, G.B. Comparação de técnicas analíticas para a extração de potássio de amostras de tecido vegetal com água e soluções ácidas concentrada e diluída. Eclet. Quim. **2010**, 35, 45–49.

52. Kalnicky, D.J.; Singhvi, R. Field portable XRF analysis of environmental samples. J. Hazard. Mater. **2001**, 83, 93–122.

53. Marguí, E.; Queralt, I.; Hidalgo, M. Application of X-ray fluorescence spectrometry to determination and quantitation of metals in vegetal material. TrAC Trend. Anal. Chem. **2009**, 28, 362–372.

54. Omote, J.; Kohno, H.; Toda, K. X-Ray fluorescence analysis utilizing the fundamental parameter method for the determination of the elemental composition in plant samples. Anal. Chim. Acta **1995**, 307, 117–126.

55. Kirkby, E. Introduction, Definition and Classification of Nutrients. In Marschner's Mineral Nutrition of Higher Plants; Marschner, P., Ed.; Elsevier: London, UK, 2012; pp. 3–14.

56. Epstein, E.; Bloom, A.J. Mineral Nutrition of Plants: Principles and Perspectives, 2nd ed.; Sinauer Associates Publishers: Sunderland, MA, USA, 2005.

57. Rodrigues, M.; Pavinato, P.S.; Withers, P.J.A.; Teles, A.P.B.; Herrera, W.F.B. Legacy phosphorus and no tillage agriculture in tropical oxisols of the Brazilian savanna. Sci. Total Environ. **2016**, 542, 1050–1061

58. Roy, E.D.; Willig, E.; Richards, P.D.; Martinelli, L.A.; Vazquez, F.F.; Pegorini, L.; Spera, S.A.; Porder, S. Soil phosphorus sorption capacity after three decades of intensive fertilization in Mato Grosso, Brazil. Agric. Ecosyst. Environ. **2017**, 249, 206–214.

59. Broadley, M.; Brown, P.; Cakmak, I.; Rengel, Z.; Zhao, F. Function of Nutrients: Micronutrients. In Marschner's Mineral Nutrition of Higher Plants; Marschner, P., Ed.; Elsevier: London, UK, 2012; pp. 191–248.

60. Hawkesford, M.; Horst, W.; Kichey, T.; Lambers, H.; Schjoerring, J.; Møller, I.S.; White, P. Functions of Macronutrients. In Marschner's Mineral Nutrition of Higher Plants; Marschner, P., Ed.; Elsevier: London, UK, 2012; pp. 135–189.

61. Clarkson, D.T. The Uptake and Translocation of Manganese by Plant Roots. In Manganese in Soils and Plants; Graham, R.D., Hannam, R.J., Uren, N.C., Eds.; Springer: Dordrecht, The Netherlands, 1988; pp. 101–111.

62. de Varennes, A.; Carneiro, J.P.; Goss, M.J. Characterization of manganese toxicity in two species of annual medics. J. Plant Nutr. **2001**, 24, 1947–1955.

63. Gates,W.P. Chapter 12.3 X-ray Absorption Spectroscopy. In Handbook of Clay Science; Bergaya, F., Theng, B.K.G., Lagaly, G., Eds.; Elsevier: London, UK, 2006; pp. 789–864.

64. Reidinger, S.; Ramsey, M.H.; Hartley, S.E. Rapid and accurate analyses of silicon and phosphorus in plants using a portable X-ray fluorescence spectrometer. New Phytol. **2012**, 195, 699–706.

65. Tighe, M.; Forster, N. Rapid, Nondestructive Elemental Analysis of Tree and Shrub Litter. Commun. Soil Sci. Plant Anal. **2014**, 45, 53–60.

66. Melo, L.C.A.; Silva, C.A. Influência de métodos de digestão e massa de amostra na recuperação de nutrientes em resíduos orgânicos. Quim. Nova **2008**, 31, 556–561.

67. de Carvalho, A.M.; Dantas, R.D.A.; Coelho, M.C.; Lima,W.M.; Souza, J.P.S.P.; Fonseca, O.P.; Guimarães, R., Jr. Teores de Hemiceluloses, Celulose e Lignina em Plantas de Cobertura com Potencial para Sistema Plantio Direto no Cerrado; Embrapa Cerrados: Planaltina, Brazil, 2010; pp. 1–15.

68. Kagiliery, J.; Chakraborty, S.; Acree, A.;Weindorf, D.C.; Brevik, E.C.; Jelinski, N.A.; Li, B.; Jordan, C. Rapid quantification of lignite sulfur content: Combining optical and X-ray approaches. Int. J. Coal Geol. **2019**, 216, 103336.

69. Weindorf, D.C.; Chakraborty, S.; Herrero, J.; Li, B.; Castañeda, C.; Choudhury, A. Simultaneous assessment of key properties of arid soil by combined PXRF and Vis-NIR data. Eur. J. Soil Sci. **2016**, 67, 173–183.

70. Kalcsits, L.A. Non-destructive measurement of calcium and potassium in apple and pear using handheld X-ray fluorescence. Front. Plant Sci. **2016**, 7, 1–8.

ARTICLE 3: POCKET-SIZED SENSOR TO ASSESS THE COLOR OF PLANT LEAVES

Camila Silva Borges[1], Ruby Antonieta Vega R.[1], Somsubhra Chakraborty[2], David C. Weindorf[3], Guilherme Lopes[1], Luiz Roberto Guimarães Guilherme[1], Nilton Curi[1], Bin Li[4], and Bruno Teixeira Ribeiro[1*]

[1]Department of Soil Science, Federal University of Lavras, Lavras, 37200-000, Minas Gerais State, Brazil.
[2]Agricultural and Food Engineering Department, Indian Institute of Technology Kharagpur, India.
[3]Department of Earth and Atmospheric Sciences, Central Michigan University, Mount Pleasant, Michigan, USA.
[4]Department of Experimental Statistics, Louisiana State University, Baton Rouge, LA, USA.
[*]Corresponding author. Email: brunoribeiro@ufla.br

This article was prepared in line with the guidelines of the Journal of Plant physiology, which was submitted to.

Abstract - The color of plant leaves can be assessed qualitatively by color charts or after intricate processing of digital images. This pilot study employed a novel pocket-sized sensor to obtain the color of plant leaves. In order to assess its performance, a color-dependent parameter (SPAD index) was used as dependent variable, since there is a strong correlation between SPAD index and greenness of plant leaves. A total of 1,872 fresh and intact leaves from 13 crops were analyzed using a SPAD-502 meter and scanned using the NixTM Pro color sensor. The color was assessed via RGB and CIELab systems. The full dataset was divided into calibration (70% of data) and validation (30% of data). For each crop and color pattern, multiple linear regression (MLR) analysis and multivariate modeling [least absolute shrinkage and selection operator (LASSO), and elastic net (ENET) regression]. The obtained MLR equations and multivariate models were then tested using the validation dataset based on r, R2, root mean squared error (RMSE), and mean absolute error (MAE). In both RGB and CIELab color systems, the NixTM Pro color sensor was able to differentiate crops, and the SPAD indices were successfully predicted, mainly for mango, quinoa, peach, pear, and rice crops. The correlation between SPAD and greenness is crop-dependent. Overall, the NixTM Pro color sensor revealed to be a fast, sensible and an easy way to obtain color of leaves directly in the field, constituting a reliable alternative to digital camera imagery and associated image processing.

Keywords: Nix^{TM} Pro color sensor. SPAD. Plant leaves. Chlorophyll.

Introduction

In field conditions, the color of plant leaves can be qualitatively assessed and differentiated via color charts (e.g., Munsell Color Chart for Plant Tissues, Globe Plant Color Chart, and Leaf Color Chart) (Ali et al., 2014; O'campo et al., 2015; Tao et al., 2020). The most common is the former (Munsell Color, 1977) which reports hue (color name), value (brightness), and chroma (saturation) parameters (Mizunuma et al., 2014). This is a simple and low-cost technique to obtain the color of plant leaves, however, it depends on the perception of human eyes and sunlight conditions. Color charts have been commonly employed for N management in rice (Bathia et al., 2012; Witt et al., 2005), maize (Pasuquin et al., 2012; Shukla et al., 2004; Varinderpal et al., 2011), soybean (Prilianti et al., 2014; Rorie et al., 2011), and wheat crops (Shukla et al., 2004).

Technological advancements have allowed the quantitative determination of leaf color based on images (Majer et al., 2010). Several studies have elucidated the use of digital and different images processing for a range of purposes, such as: nitrogen status assessment (Baresel et al., 2017; Errecart et al., 2012; Prilianti et al., 2014; Ravier et al., 2017; Reyes et al. 2017), weed and crop discrimination (Aitkenhead et al., 2003), leaf disease detection (Singh et al., 2020), senescence evaluation (Hu et al., 2010), and leaf water content assessment (Ge et al., 2016).

Recently the Nix™ Pro color sensor, a pocket-sized and smartphone-based multipurpose color sensor, has been launched in the market (www.nixsensor.com). This device can be operated in Android and iOS operating systems via Bluetooth. The sensor can be placed on any solid surface without the influence of external light while the color can be easily and instantaneously obtained in different color space models (e.g., RGB, CIELab, CMYK, and HEX).

The Nix™ Pro color sensor has been successfully employed in Soil and Environmental Science, for example, to determine the soil color for pedological classification purposes (Mancini et al., 2020; Stiglitz et al. 2016) and to predict the soil organic matter content (Mukhopadhyay et al., 2020; Raeesi et al. 2019). For geological and mining purposes, the Nix™ color parameters combined with portable X-ray fluorescence spectrometry data successfully predicted the S content in lignite (Kagiliery et al., 2019). To date, there is no application of the Nix™ color sensor in Plant Science.

Thus, this pilot study was carried out in order to assess the performance and sensibility of the Nix™ Pro color sensor to obtain and detect changes in the color of plant leaves. For that, several plant leaves from different crops were analyzed via Nix sensor and the obtained color parameters were used to predict the chlorophyll content as SPAD index. The Soil Plant Analysis Development (SPAD) sensor is the most common chlorophyll meter used worldwide (Manetas et al., 1998; Dong et al., 2019; Ling et al., 2011; Xiong et al., 2015; Yuan et al., 2016), and responsible for the characteristic greenness of plants (Ocampo et al., 2015). Thus, alterations of the greenness are a useful parameter for evaluation of plant conditions (Majer et al., 2010) as they provide insight about nutrient status (Singh et al., 2002), plant diseases (Patil and Bodhi, 2001) and senescence evaluation (Hu et al., 2010). Also, chlorophyll content has a strong correlation with crop productivity (Rorie et al., 2011; Wood et al., 1993). If successful prediction of SPAD is obtained, the Nix™ Pro Color Sensor can be considered an innovative, sensible and low-cost technique to assess the color of plant leaves rapidly and quantitatively.

Material and Methods

Plant materials

For this study, a total of 1,872 leaves from 13 crops were analyzed: atemoya (n = 50), common bean (n = 570), corn (n = 100), coffee (n = 128), grape (n = 100), mango (n = 47), passion fruit (n= 60), peach (n = 99), pear (n = 100), quinoa (n = 268), rice (n = 150), soybean (n = 100), and sugarcane (n =100). Table A.1 brings the scientific names and genotypes (cultivar or variety) for each selected crop. For most crops (atemoya, coffee, common bean, corn, mango, passion fruit, peach, quinoa, and rice) just one genotype was studied. For sugarcane, 57 different genotypes were randomly analyzed in the field. The selected leaves were obtained from either crop fields or greenhouse experiments (Fig. 1). For each crop, the leaves were randomly selected to obtain a large variation in the greenness. The crop fields and greenhouse experiments are in Lavras, Minas Gerais, Brazil. According to Köppen`s classification the climate is Cwa, with a mean annual temperature of 20.4º C and a mean annual rainfall of 1,460 mm (Dantas et al., 2007), with dry and cold winters and rainy and hot summers.

Data acquisition

SPAD index measurements

For the SPAD index assessment, the SPAD-502 Plus chlorophyll meter (Konica Minolta Sensing, Osaka, Japan) was used (Minolta, 1989). The leaves were divided into three portions from petiole to tip: base, middle, and apex (Fig. 1a). In the middle region, three measurements were performed (L1, L2, and L3). The SPAD value of each measurement was calculated according to Eq. 1 and the used value corresponded to the average of three measurements. Detailed information about SPAD index determination based on optical parameters using the SPAD-502 chlorophyll meter can be found in Minolta (1989), Markwell et al. (1995) and Wood et al. (1993).

$$SPAD = a\left[Log(\frac{I_{0r}}{I_r})\text{-}Log\,(\frac{I_{0f}}{I_f})\right]+b \quad (1)$$

Here, a and b are constants; I_r and I_f are electrical currents from red and infrared at the time of measurement, respectively; and I_{0r} and I_{0f} are electrical currents from red and infrared with no measurement, respectively.

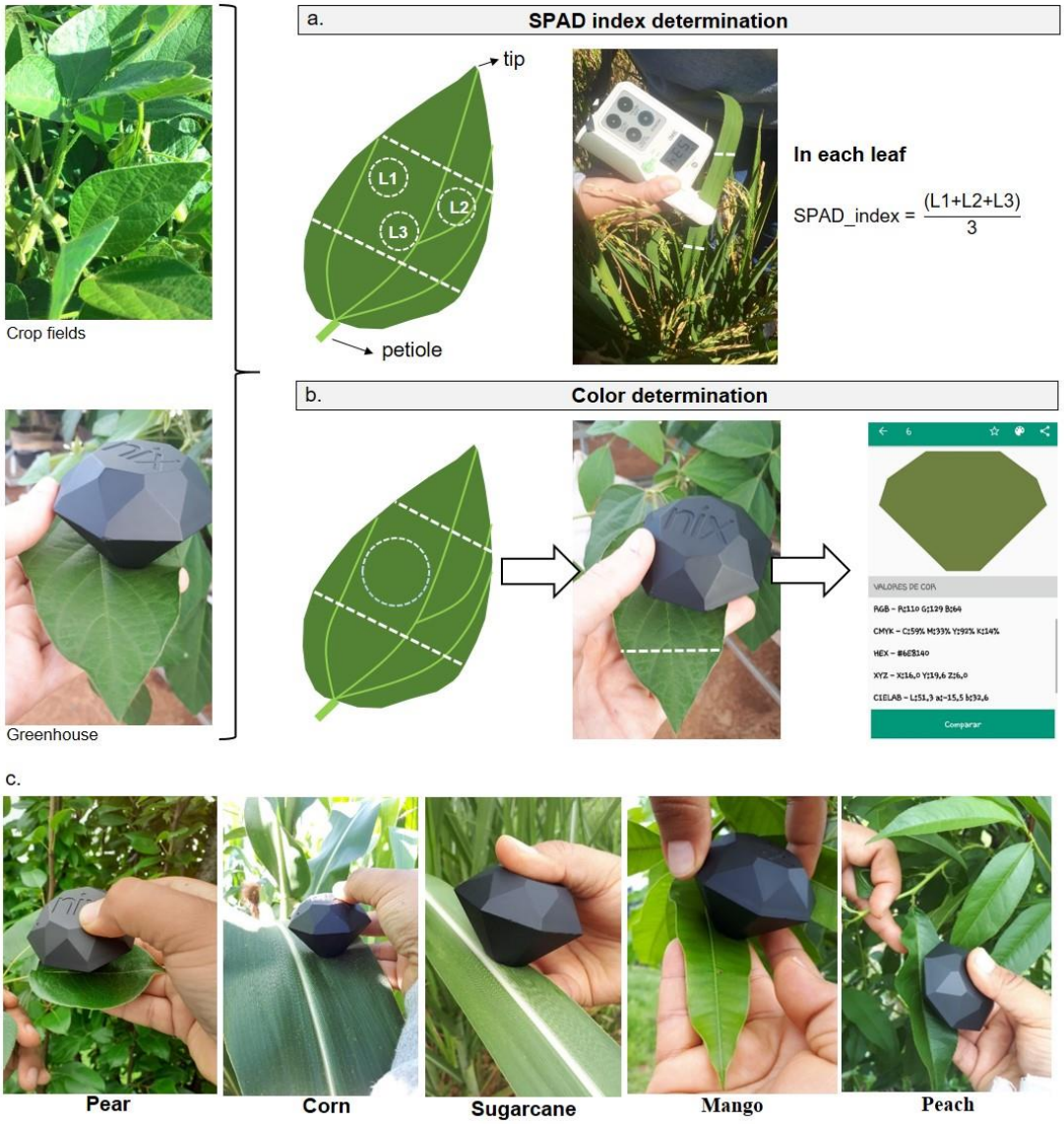

Figure 1. Details of the Soil Plant Analysis Development (SPAD) measurements (a) and color determination via Nix™ Pro Color Sensor (b and c).

Leaf color measurements

For the same leaves used to assess the SPAD index, the leaf color was obtained using the Nix™ Pro color sensor (Nix Team, Ontario, Canada) (Fig. 1b). The measurement was performed at the central region of the middle leaf portion. The Nix™ has an internal LED light source that is activated at the time of measurement. The measurement were instantaneously obtained after press the "scan" bottom of the application. So, the reflected color is captured and, by a specific model, converted into various color parameters (e.g., RGB, CIELab, HEX, CMYK, XYZ, etc.). For this work, default conditions (D50 illuminant and 2º reference angle) and RGB and CIELab color systems were selected. A detailed discussion of each color systems

can be found in Fairchild (2013) and Ohta and Robertson (2005). In the CIELab system, L means lightness ranging from black (0) to white (100); a corresponds to green-red component ranging from -128 (green) to +127 (red); b corresponds to blue-yellow component also ranging from -128 (blue) to +127 (yellow). In the RGB system, R, G, and B correspond to red, green, and blue colors, respectively. For all these parameters, the values range from 0 to 255.

Nix color measurements were performed under direct sunlight on the adaxial leaf surface. The leaves were handheld, assuring that the equipment aperture (1.5 cm of diameter) was totally covered with no influence of external light. A previous experiment using sugarcane leaves was carried out in order to check for that, where the Nix color measurements (n = 100) were performed placing the leaves on wood with different background colors (white, black, red, orange, yellow, green, blue, and violet). Results (Appendix A, Figure A.1) indicated no difference between background surface conditions and hand. Thus, holding the leaves by hand was considered a suitable and simple procedure in the field.

Statistical analyses

Descriptive statistics (minimum, maximum, mean, and median values) were calculated for SPAD index and each color parameter (R, G, B, L, a, and b). Principal component analysis (PCA) was executed to group and/or distinguish crops with similar greenness.

For each crop and color system, the SPAD index was predicted based on color parameters using multiple linear regression (MLR). MLR equations were developed for the randomly selected 70% calibration dataset. Subsequently, the obtained MLR equations were validated using 30% of the data (validation dataset). The statistical significance of MLR equations (calibration dataset) was assessed by the correlation (r) and determination (R^2) coefficients, respectively. The prediction accuracy of MLR models was assessed using root mean squared error (RMSE) (Eq. 2) and mean absolute error (MAE) (Eq. 3). Statistical procedures and graphs were implemented using Sigma Plot 14.0 (Systat Software Inc., San Jose, CA, USA) and R software (RStudio Team, 2016).

$$\text{RMSE} = \sqrt{\sum_{i=1}^{n} \frac{(\hat{Y}_i - Y_i)^2}{n}} \qquad (2)$$

Here, Y_i and $\hat{Y}_i$ indicate observed and predicted values.

$$MAE = \frac{\sum_{i=1}^{n}|\hat{y}_i - y|}{n} \quad (3)$$

Here, n, $\hat{y}_i$, and y indicate the number of samples, observed and predicted values, respectively.

Subsequently, for better interpretation of SPAD prediction via combined color parameters (R, G, B, L, a, and b) on each crop separately, a rigorous comparison between MLR, least absolute shrinkage and selection operator (LASSO), and elastic net (ENET) regression was executed. Notably, LASSO is a regularized linear regression model that can select variables and estimate coefficient simultaneously while ENET is a generalization of LASSO and ridge regression (Tibshirani, 1996; Zou and Hastie, 2005). Notably, sum squared of error (SSE_{MLR}) from MLR is expressed as (Eq. 4):

$$SSE_{MLR} = \sum (A - \hat{A})^2 \quad (4)$$

Here, A and $\hat{A}$ represent the actual response value and the predicted value, respectively. In LASSO regression, an L_1 penalty term is added to the model and causes coefficients to shrink (Tibshirani, 1996). This L_1 term aids in the feature selection during modelling and is given by Eq. 5:

$$SSE_{Lasso} = \sum (A - \hat{A})^2 + \lambda \sum |\beta| \quad (5)$$

Here, SSE_{Lasso} is the SSE_{MLR} plus the L_1 penalty term.

ENET regression combines both Ridge and LASSO penalties (Eq. 6):

$$SSE_{ENET} = \sum (A - \hat{A})^2 + \lambda \left[(1-\alpha) \sum \beta^2 + \alpha \sum |\beta| \right] \quad (6)$$

Here, SSE_{ENET} is computed from the SSE_{MLR} plus the L_2 and L_1 penalties and L_2 denotes the Ridge regression penalty. In addition to the two penalties, a mixing parameter α is also added to the model.

To achieve an objective comparison, the data for each crop was randomly split 50 times into a calibration set (75%) and validation set (25%). Each time, LASSO, ENET, and MLR were fitted on the calibration set, and the validation set was used for testing the calibration performance. The R^2 on the validation set was used to evaluate the prediction accuracy. Both

LASSO and ENET were executed using the ‘glmmet’ package in R version 3.6.2 (R Core Team, 2020).

Results and Discussion

General description of SPAD indices and color parameters

From PCA analysis it was possible to distinguish the crops based on color parameters (Fig. 2). This information is relevant for SPAD value prediction since the greenness of leaves is a property intrinsic of each plant species and the prediction models must be specific for each crop. PCA analysis also revealed that SPAD was positively influenced by a and negatively by R, G, L, and b parameters. The positive correlation observed for a parameter can be attributed to the fact that most a values were negative (99.6% of all samples). This means that all samples are in the green region. Within this region, as the a value increases the color becomes darker green (Baldevbhai and Anand, 2012; Ganesan et al., 2010). In the PCA graph (Fig. 2), from left to right the lightness increases. For example, the negative correlation observed between SPAD and R and G parameters means that the color changed (left to right) from dark-red to light-red and from dark-green to light-green, respectively. Summarily, the crops on the left side (e.g., coffee, corn, and grape) are darker green showing the highest SPAD values, corroborating the results obtained earlier for spinach (Agarwal et al., 2018), potato (Yadav et al., 2010), and barley leaves (Hu et al., 2010). The inverse correlation observed between SPAD values and R and G parameters from the RGB color system, and to L and b parameters from the CIELab color system, corroborates the results obtained by Cavallo et al. (2017), Vollmann et al. (2011) and Vesali et al. (2015). The non-influence of the B parameter on SPAD prediction was also observed by Agarwal et al. (2018).

High chlorophyll contents result in higher light absorbance, reducing the light reflection (Carter and Knapp, 2001) with a concomitant reduction in brightness and RGB values (Agarwal et al. 2018). In the CIELab system, the L parameter corresponds to lightness, ranging from black (L = 0) to white (L=100) (Baldevbhai and Anand, 2012; Hill et al., 1997). Thus, an inverse correlation between L and SPAD is also expected.

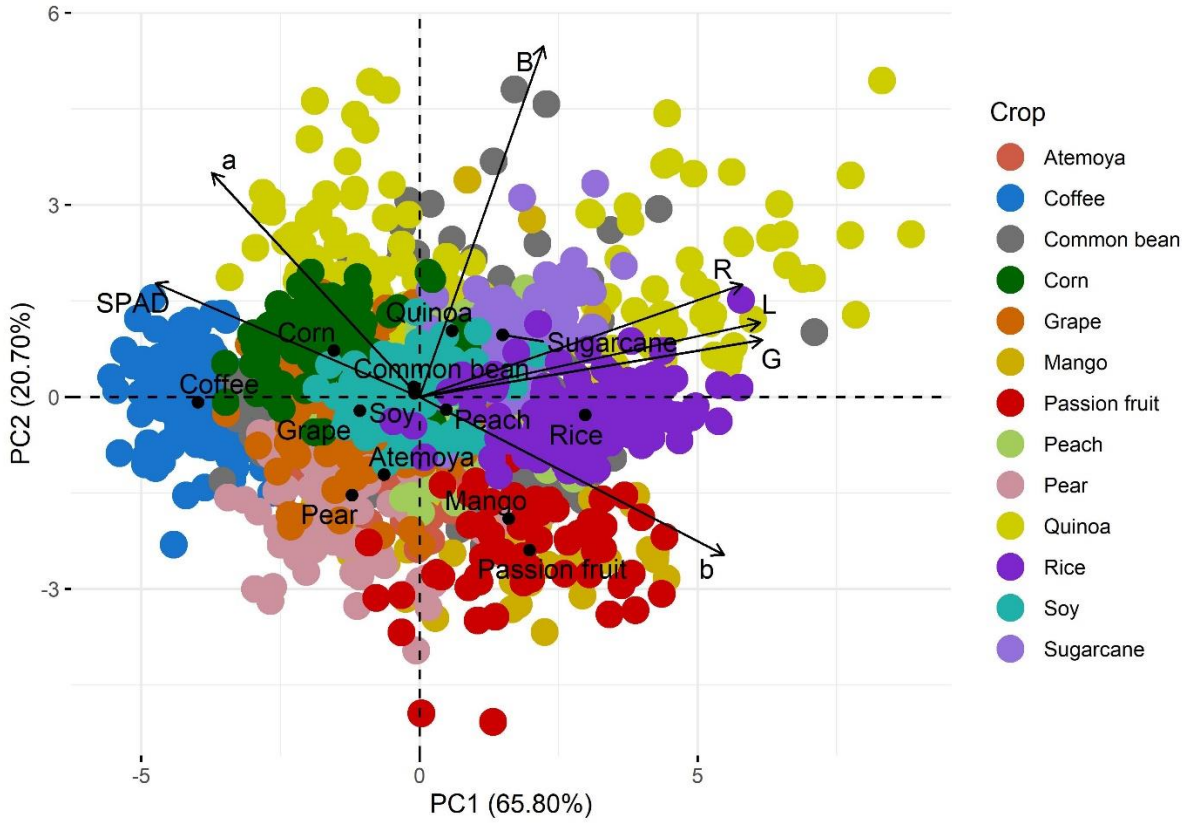

Figure 2. Principal component analysis (PCA) for differentiation of studied crops based on color parameters from RGB and CIELab systems.

Figure 3 displays a color scheme built with real values from the RGB color system for each crop. From left to right, minimum, median and maximum values for SPAD indices and color parameters are presented. As the greenness increases (from left to right) the SPAD values also increase and range from 18.0 (quinoa) to 83.0 (coffee). The largest and smallest SPAD index variation was observed for quinoa (from 18 to 79) and for soybean (33.6 to 48.1), respectively. Moreover, moderate range (21.1 to 60.6) was observed for common bean. The greenness variation obtained for each crop (Fig. 2) can be influenced by environmental aspects, nutritional, and physiological conditions of plants (Borrell et al., 2001; Xiong et al., 2015; Yang et al., 2016). This color variation for each crop is important to obtain prediction models. The chlorophyll content is highly dependent on the time of sampling and vegetative period (Karele, 2001; Reith et al., 1991), reaching maximum values close to flowering stage (Riccardi et al. 2014). Notably, changes in chlorophyll content over time were observed for corn and sugar maple (*Acer saccharum M.)* crops (Croft et al., 2014).

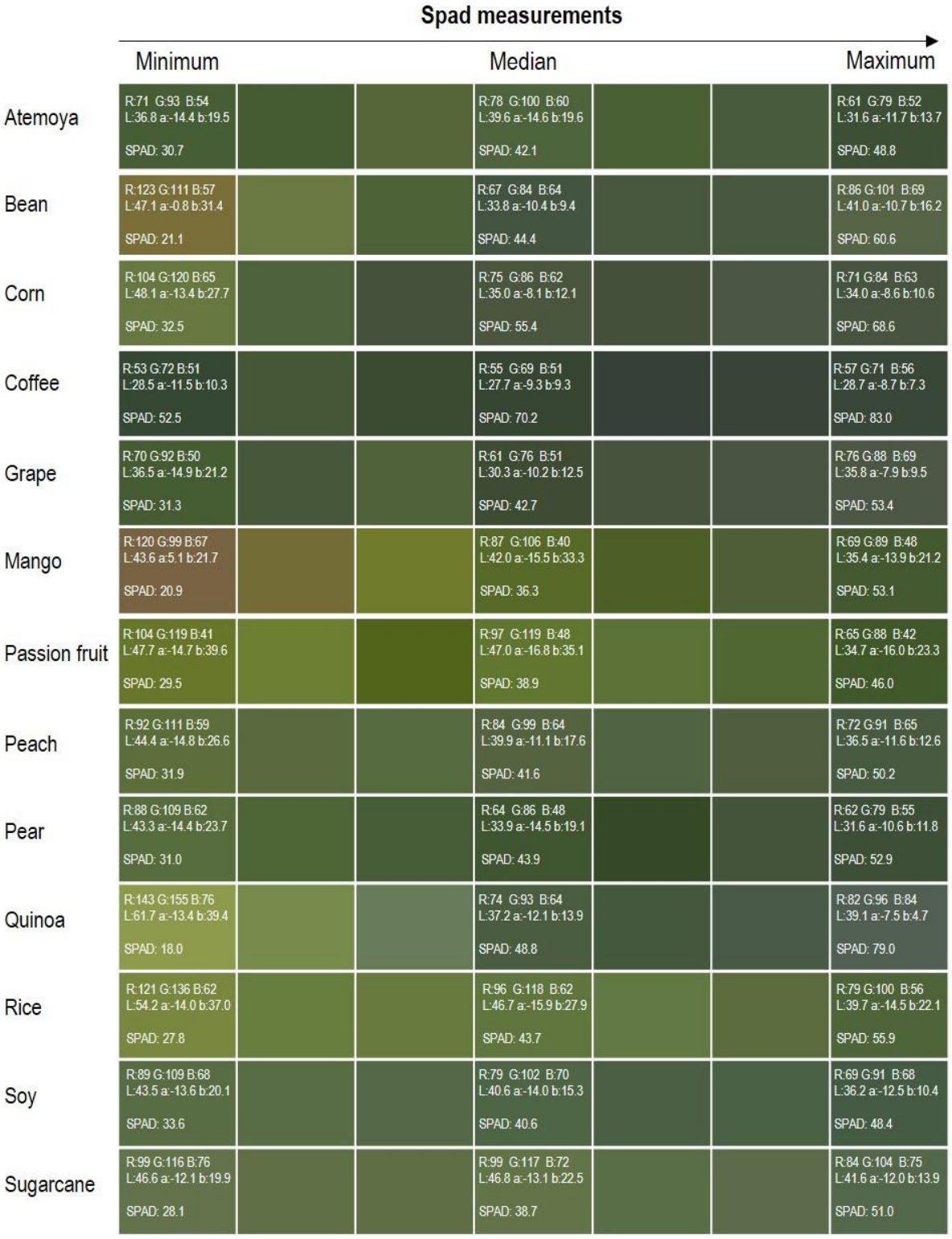

Figure 3. Soil Plant Analysis Development (SPAD) index and color parameters variation (minimum, median and maximum values) for each studied crop.

A suitable comparison of the obtained SPAD index with other studies is difficult since the chlorophyll content depends on several conditions of the leaves such as water deficit (Rolando et al., 2015; Soureshjani et al., 2019), growth stage (Karele, 2001), and nutritional

status (Barbedo et al., 2019). SPAD index is merely a conversion of optical parameters into a non-dimensional value which reflects the influence of chlorophyll on light reflectance (Markwell et al., 1995; Wood et al., 1993). The real chlorophyll content is normally expressed in μg cm^{-2}. Previous studies have confirmed a consistent correlation between SPAD index and chlorophyll content for a wide range of crop species such as rice, maize, wheat, cotton, soybean, grape, and coffee (Markwell et al., 1995; Netto et al., 2005; Steele et al., 2008; Wood et al., 1993). Ling et al. (2011) reported a mean difference between SPAD and conventional solvent-extracted chlorophyll of only 6%. For quinoa leaves chlorophyll contents ranged from 0.6 to 55.6 μg cm^{-2} (Riccardi et al., 2014). These authors proposed equations to predict the chlorophyll content based on the SPAD index. Incorporating the SPAD values obtained for quinoa leaves in this study to the equations given by Riccardi et al. (2014), predicted chlorophyll content ranged from 7.7 to 83.7 μg cm^{-2}. Nevertheless, the SPAD values obtained for common bean (26.0 to 50.2) and soybean (33.6 to 48.4) corroborated the values obtained by Darkwa et al. (2016) and Yokoyama et al. (2018), respectively.

SPAD index has strong correlation with N concentration in plant leaves and crop productivity (Lindsey et al., 2016; Shafagh-Kolvanagh et al., 2008; Yu et al., 2010). For rice, SPAD values from 35 to 48 have been associated to adequate N concentration and higher crop yields (Huang et al., 2008; Peng et al., 1996; Yang et al., 2014). In this work, SPAD values for rice leaves ranged from 27.8 to 55.9 (Fig. 3) and 94% of samples had SPAD higher than 35.0. For maize, SPAD values from 42.0 to 55.0 have been associated to the highest grain yields (Liu and Wiatrak, 2012; Rostami et al., 2008). Piekielek et al. (1995) suggested SPAD value of 52.0 as the critical level for N sufficiency. Here, 66% of samples had SPAD values higher than 52.0. Similarly, Reis et al. (2009) and Netto et al. (2005) found a close relationship between crop production, N status and SPAD values for coffee plants. The maximum N supply (300 kg ha^{-1}) corresponded to the maximum SPAD value (70.8) and foliar N content (33.3 g kg^{-1}) (Reis et al., 2009). The maximum N content of coffee leaves corresponded to a SPAD value of 94.2 (Netto et al., 2005).

SPAD indices prediction

MLR equations obtained for each color system are presented in Table 1. The highest r and R^2 values were obtained for mango (0.92) and quinoa (0.91) leaves for both RGB and CIELab

system, and the lowest for sugarcane (0.48 and 0.49 for RGB and CIELab system, respectively). The lowest r and R^2 values found for sugarcane can be attributed to the fact that 57 genotypes (cultivars) were randomly scanned in the field. Thus, the intrinsic genetic characteristic may have influenced the correlation between chlorophyll content (as SPAD index) and greenness. Although a general MLR equation has limited applications, since the greenness is a particular characteristic of each species, it yielded r and R^2 values of 0.72 and 0.52, respectively.

Table 1. Obtained equations from multiple linear regression (MLR) for prediction of SPAD index using color parameters from RGB and CIELab systems.

Crop	MLR	r	R^2
Atemoya	$SPAD_{RGB}$ = 39.79 - 0.43R + 0.10G + 0.44B	0.55	0.23
	$SPAD_{Lab}$ = 40.73 + 0.23L - 0.81a - 0.94b	0.56	0.25
Bean	$SPAD_{RGB}$ = 65.19 + 0.18R - 0.72G + 0.54B	0.80	0.64
	$SPAD_{Lab}$ = 68.87 - 0.06L + 0.68a - 0.85b	0.81	0.65
Coffee	$SPAD_{RGB}$ = 75.76 + 0.95R - 1.40G + 0.75B	0.67	0.42
	$SPAD_{Lab}$ = 81.46 + 0.54L + 2.47a - 0.57b	0.68	0.44
Corn	$SPAD_{RGB}$ = 89.07 + 0.17R - 0.90G + 0.51B	0.81	0.64
	$SPAD_{Lab}$ = 92.85 - 0.58L + 0.87a - 0.73b	0.82	0.65
Grape	$SPAD_{RGB}$ = 64.18 + 0.46R - 0.92G + 0.44B	0.81	0.64
	$SPAD_{Lab}$ = 67.47 - 0.12L + 1.22a - 0.51b	0.80	0.63
Mango	$SPAD_{RGB}$ = 66.55 - 0.46R+ 0.03G + 0.16B	**0.92**	0.82
	$SPAD_{Lab}$ = 68.33 - 0.66L -0.75a - 0.46b	**0.92**	0.82
Passion fruit	$SPAD_{RGB}$ = 37.67 - 0.52R + 0.34G + 0.19B	0.69	0.43
	$SPAD_{Lab}$ = 38.69 + 0.04L - 0.96a - 0.56b	0.68	0.43
Peach	$SPAD_{RGB}$ = 66.43 + 0.45R - 0.80G + 0.30B	0.78	0.59
	$SPAD_{Lab}$ = 71.10 - 0.20L + 1.29a - 0.27b	0.79	0.60
Pear	$SPAD_{RGB}$ = 50.15 - 0.16R - 0.22G + 0.43B	0.73	0.52
	$SPAD_{Lab}$ = 50.66 + 0.09L - 0.33a - 0.87b	0.74	0.53
Quinoa	$SPAD_{RGB}$ = 103.45 + 0.87R - 1.72G + 0.73B	**0.91**	0.82
	$SPAD_{Lab}$ = 108.99 - 0.43L + 2.15a - 0.91b	**0.91**	0.83
Rice	$SPAD_{RGB}$ = 61.89 - 0.30R - 0.25G + 0.64B	0.85	0.72
	$SPAD_{Lab}$ = 64.75 + 0.22L - 0.40a - 1.35b	0.86	0.73
Soybean	$SPAD_{RGB}$ = 38.71 + 0.37R - 0.79G + 0.76B	0.67	0.42
	$SPAD_{Lab}$ = 42.59 + 0.78L + 1.17a - 1.11b	0.68	0.44
Sugarcane	$SPAD_{RGB}$ = 42.14 - 0.67R + 0.17G + 0.54B	0.48	0.19
	$SPAD_{Lab}$ = 41.26 + 0.11L - 1.44a - 1.33b	0.49	0.20
Full dataset	$SPAD_{RGB}$ = 77.70 + 0.15R - 0.68G + 0.36B	0.71	0.50
	$SPAD_{Lab}$ = 80.68 - 0.43L + 0.62a - 0.59b	0.72	0.52

SPAD: Soil Plant Analysis Development

Considering the full dataset, the SPAD calibration model based on RGB parameters (Fig. 4a) exhibited r, R^2, RMSE and MAE values of 0.71, 0.50, 7.4, and 5.9, respectively.

Similar values were observed for the validation dataset (Fig. 4a). The SPAD prediction accuracy using the color parameters from CIELab (Fig. 4b) was almost the same as produced by the RGB system.

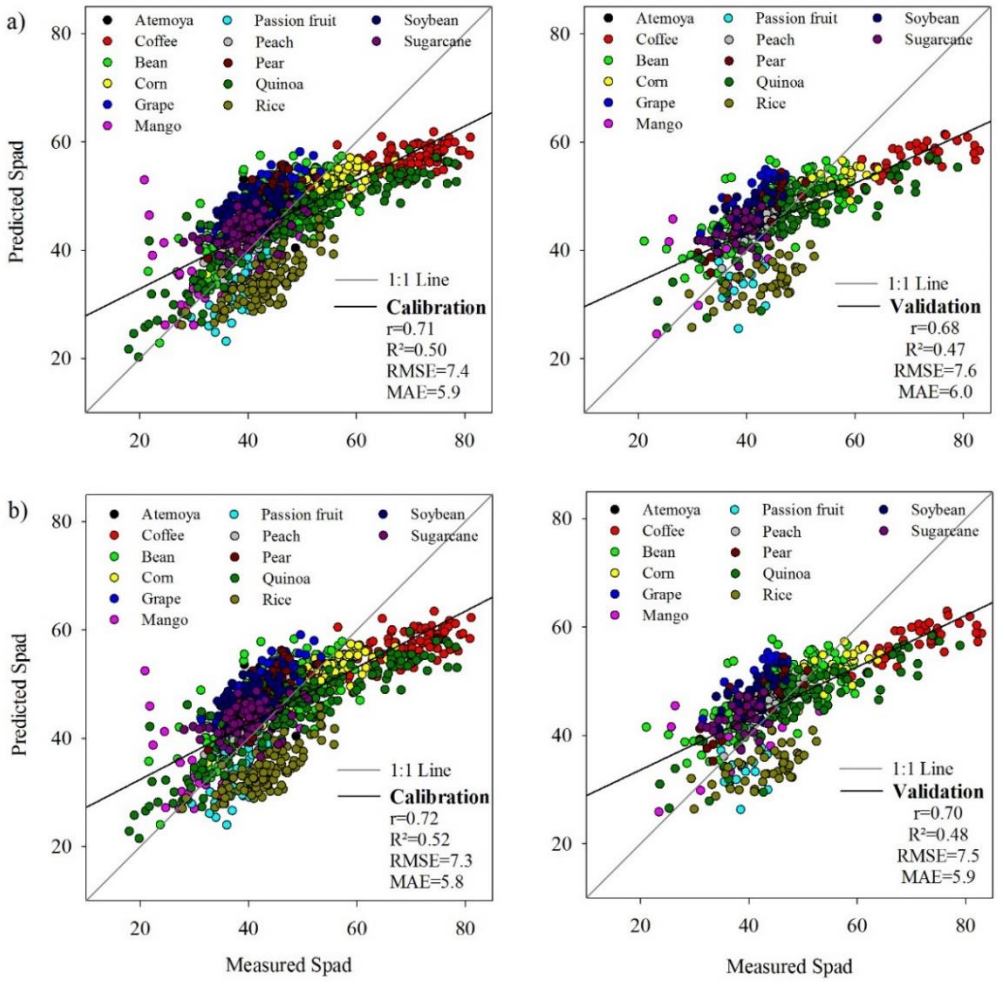

Figure 4. Prediction of SPAD index considering the full dataset for RGB (a) and CIELab (b) color systems. SPAD: Soil Plant Analysis Development.

Compared to the prediction considering the full dataset (Fig. 4), SPAD prediction for each crop using both RGB (Fig. 5) and CIELab color systems (Fig. 6) increased the r and R^2 values and decreased RMSE and MAE values. Based on R^2 values, the best prediction was observed for mango (0.90), followed by quinoa (0.77), pear (0.70), peach (0.66), and rice (0.59) leaves. The worst prediction was observed for sugarcane leaves (R^2 = 0.11). Leaf color (greenness) and chlorophyll content are closely correlated and so the use of color parameters for chlorophyll content prediction has been widely tested in previous studies (Gitelson et al. 2003; Karcher and Richardson, 2003; Vesali et al. 2015; Yao and Luo, 2012).

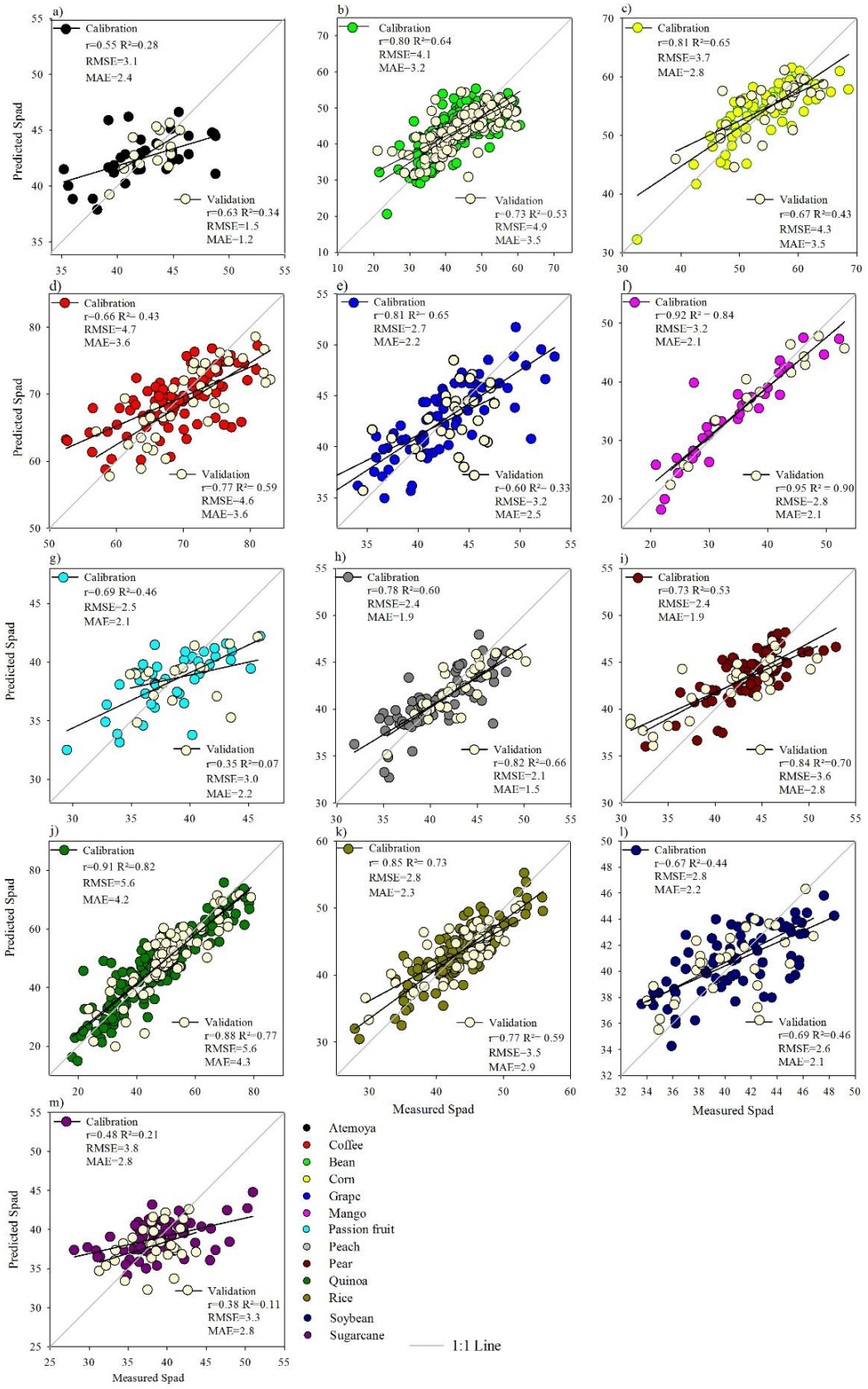

Figure 5. Prediction of SPAD index for each crop using the color parameters from RGB system. SPAD: Soil Plant Analysis Development.

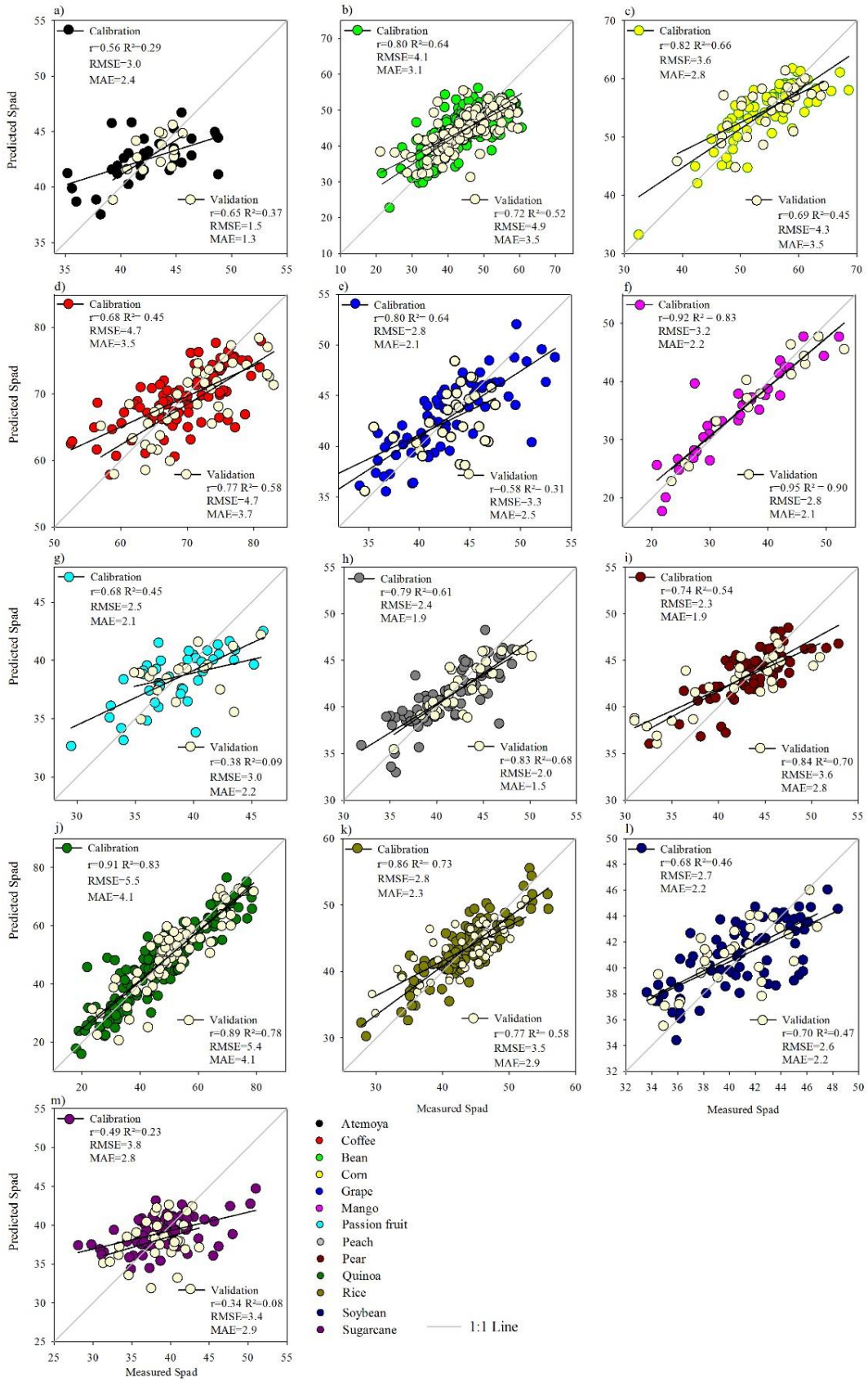

Figure 6. Prediction of SPAD index for each crop using the color parameters from CIELab system. SPAD: Soil Plant Analysis Development.

Yadav et al. (2010) also employed a MLR model for chlorophyll content prediction in potato leaves. However, instead of simply using R, G, and B values, the authors used the mean brightness and mean brightness ratio [R/(R+G+B)]. The best predictive model was obtained using the mean brightness ratio (RMSE = 6.6) which was attributed to the RGB dependence on light intensity and subsequently solved by normalization. In this study, there was no effect of light intensity on color components, since it was acquired under constant illumination. Notably, the Nix^{TM} Pro color sensor emits the same light intensity in all scanning conditions.

Dey et al. (2018) used the same RGB-based approach for SPAD index prediction for betel (*Piper betle L.*) where the most accurate model used the R and B parameters in an MLR equation and yielded an RMSE value of 5.53. Agarwal et al. (2018), compared the capacity of six different color systems to predict the SPAD values of spinach leaves and achieved the lowest RMSE (2.68) and the highest R^2 (0.86) for the CIELab color system. In the present work, the RGB and CIELab color systems yielded almost the same model generalization for all evaluated crops, corroborating the findings obtained by Hu et al. (2010). RGB color parameters provided the lowest RMSE values for coffee (4.6), grape (3.2), and sugarcane (3.3) (Fig. 5), while the CIELab parameters yielded the lowest RMSE value for peach (2.0) and quinoa (5.4) (Fig. 6). Previous studies have reported the better performance of machine learning algorithms compared to simple MLR analysis for leaf chlorophyll content prediction. For corn, Vesali et al. (2015) observed an increase in R^2 value and a decrease in RMSE value using a neural network model compared to a multiple linear model. Similarly, Liu et al. (2010) using spectral indices as inputs observed R^2 of 0.71 when using a multiple regression model and of 0.90 when applied a neural network for rice. Despite that, when used together in a linear combination in this study, the R, G, B and L, a, and b parameters were able to reasonably predict the SPAD values (Figs. 5 and 6).

The boxplots of validation R^2 based on 50 replications for each crop on three methods (LASSO, ENET , and MLR) revealed that three crops (atemoya, passion fruit, and sugarcane) had many negative R^2 values and the median of the R^2 was close to zero (Fig. 7). These results indicated that fitting a linear regression may not be prudent for these three crops and thus subsequent calculation and comparisons were made for the remaining 10 crops. The relative validation R^2 on the rest 10 crops was plotted in Fig. 8. Notably, relative validation R^2 was calculated by scaling validation R^2 values within each iteration where the maximum obtained R^2 was given a value of 1. Consequently, the smaller R^2 values indicated reduced model performance. Results indicated that ENET performed best in most crops (e.g., coffee, corn, mango, pear, rice, and soy) and very close to MLR in bean, grape, peach, and quinoa. Although

MLR produced the worst performance, it produced values within 0.8 (in terms of validation R^2) in most trials.

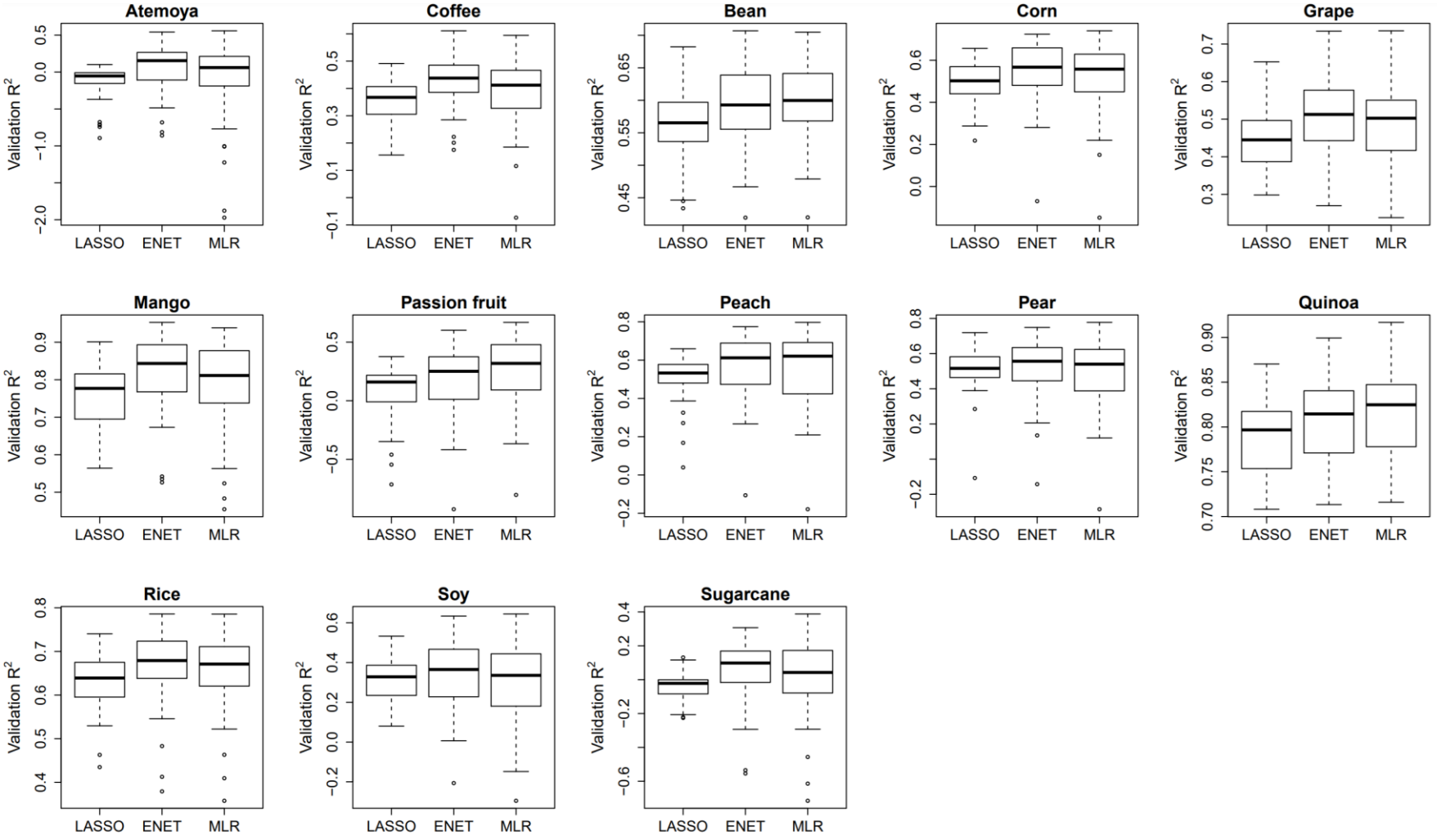

Figure 7. Validation R^2 based on 50 replications for each crop on three multivariate methods

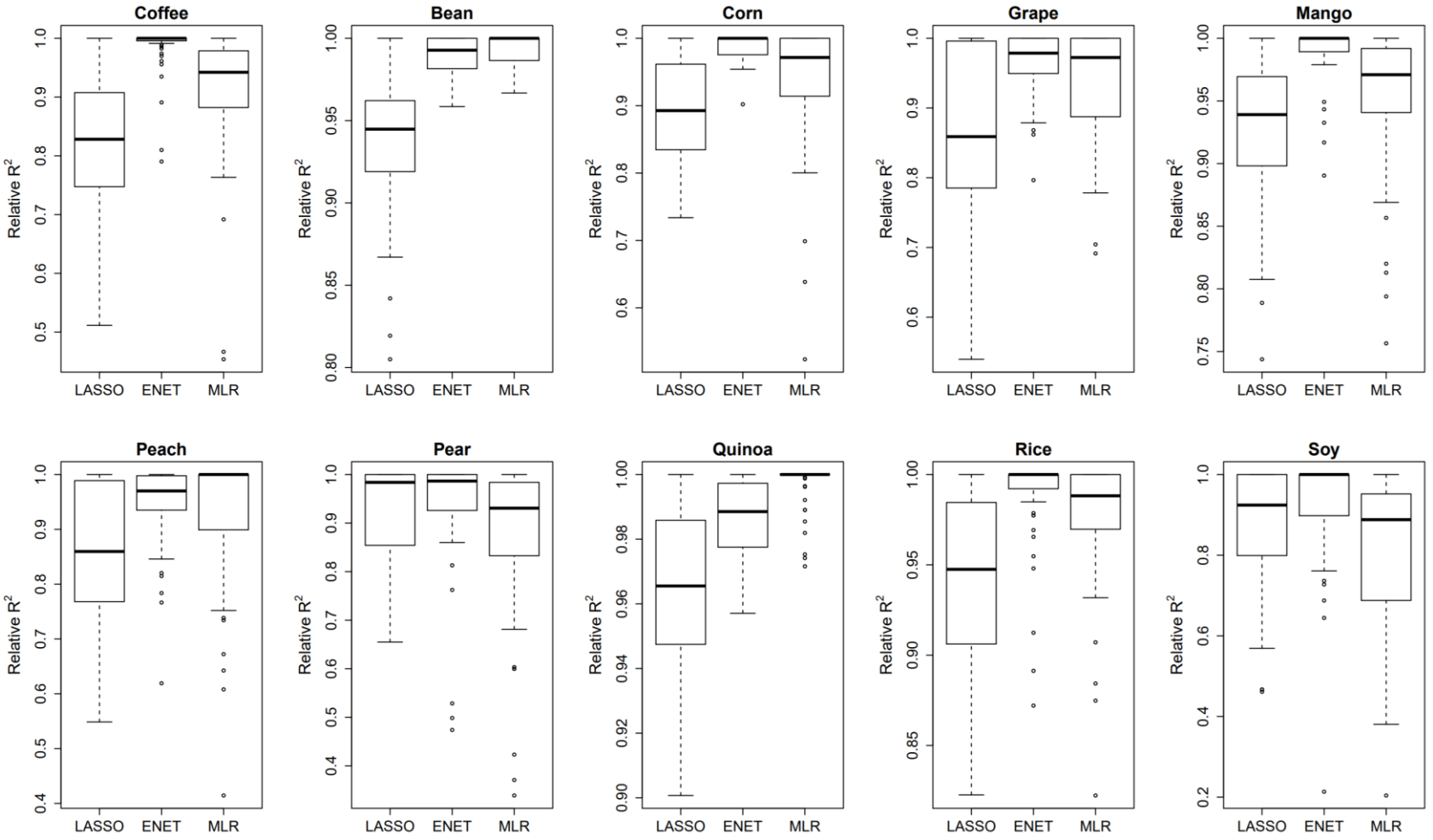

Figure 8. The relative validation R^2 based on 50 replications for 10 crops using three multivariate methods.

Plotting the LASSO model coefficients for interpretation purposes (Fig. A.2) suggested which variables should be used for subsequent MLR models. For example, for coffee, the model should include a and b parameters. Subsequently, Fig. 9 exhibits the MLR model prediction plots using LASSO selected parameters and indicated reasonable model performance.

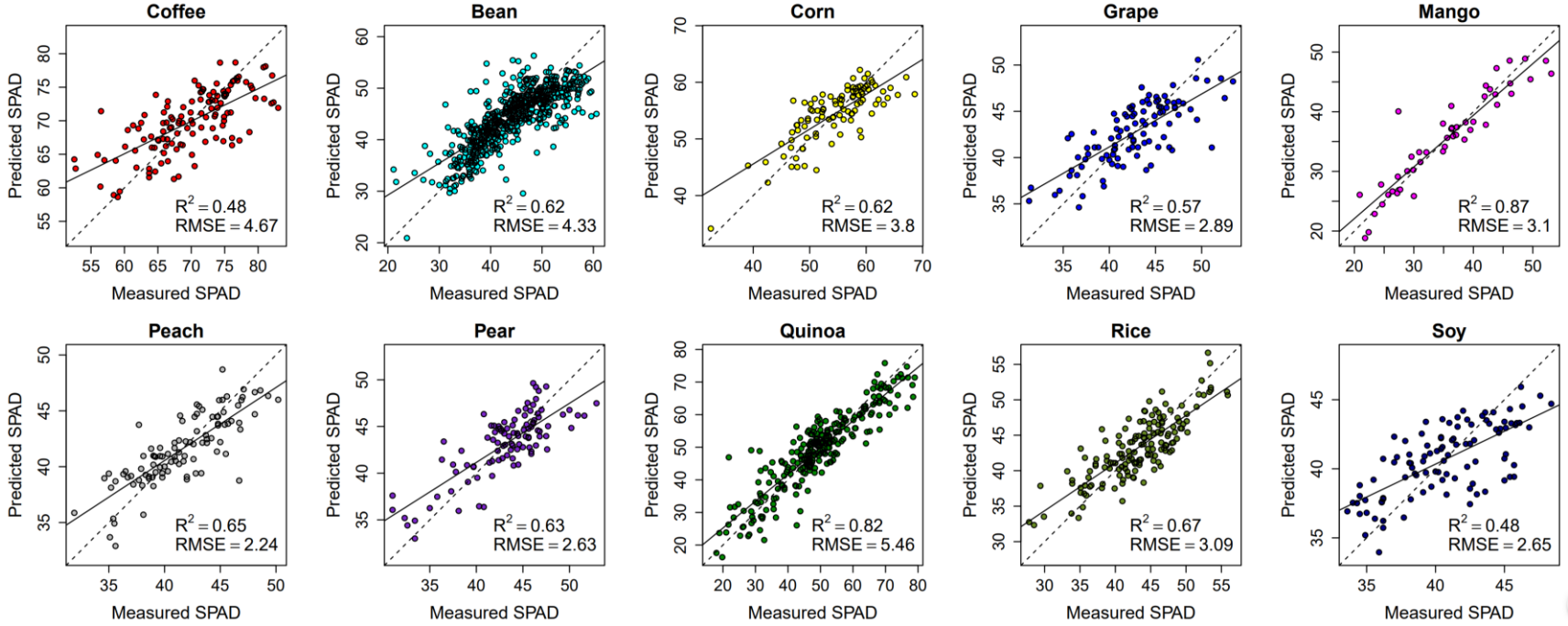

Figure 9. MLR-SPAD prediction plots using all LASSO selected parameters for 10 crops.

Summarily, the use of Nix™ Pro color sensor for rapid and cost-effective assessment of plant leaves is promising. Future works involving soil environmental conditions, such as water availability, fertility, texture, structure, effective depth and drainage, nutritional conditions (e.g., N and Mg contents) and physiological aspects of plants (e.g., vigor and productivity) using the pocket-sized color sensor are encouraged. For example, Singh et al. (2002) proposed threshold leaf color greenness for N fertilization purposes using merely color charts. This approach can be greatly benefited by digital color parameters easily obtained using in-field sensors (Bang et al., 2020).

Conclusions

The Nix™ Pro color sensor revealed to be an easy, fast, sensible and accurate tool to obtain the color of plant leaves in the field. In this pilot study, based on color parameters from both RGB and CIELab color systems, a color-dependent parameter (SPAD index) was satisfactorily predicted using multiple linear regression, mainly for mango, quinoa, peach, pear, and rice leaves. Further, while combining all color parameters, the ENET model produced better prediction accuracy for most crops. Since the color parameters are easily obtained in a quantitative manner, the Nix™ Pro color sensor is a better option for color acquisition than conventional digital cameras or smartphones. Also, the color parameters from Nix™ Pro color sensor can work as auxiliary data to confirm and/or validate color obtained by using advanced remote sensing technologies. From this work, several other applications and calibrations can be performed for different plant species and environmental conditions worldwide, for example, to estimate the real chlorophyll content, N and Mg contents, and many factors influencing the nutritional status of plants, based exclusively on color parameters from Nix™ Pro color sensor. Also, color data can be combined to other sensors such as portable X-ray fluorescence spectrometer (pXRF) and laser-induced breakdown spectroscopy (LIBS) producing results even better.

Acknowledgements

The authors thank the following Brazilian research funding agencies: National Council for Scientific and Technological Development (CNPq); Coordination for the Improvement of Higher Education Personnel (CAPES); and Research Foundation of Minas Gerais State (FAPEMIG). Dr. Bruno T. Ribeiro thanks the PrInt-Capes Program (Grant number

888887.363577/2019-00) for support with this project while working as visiting professor at Texas Tech University, USA.

Appendix A

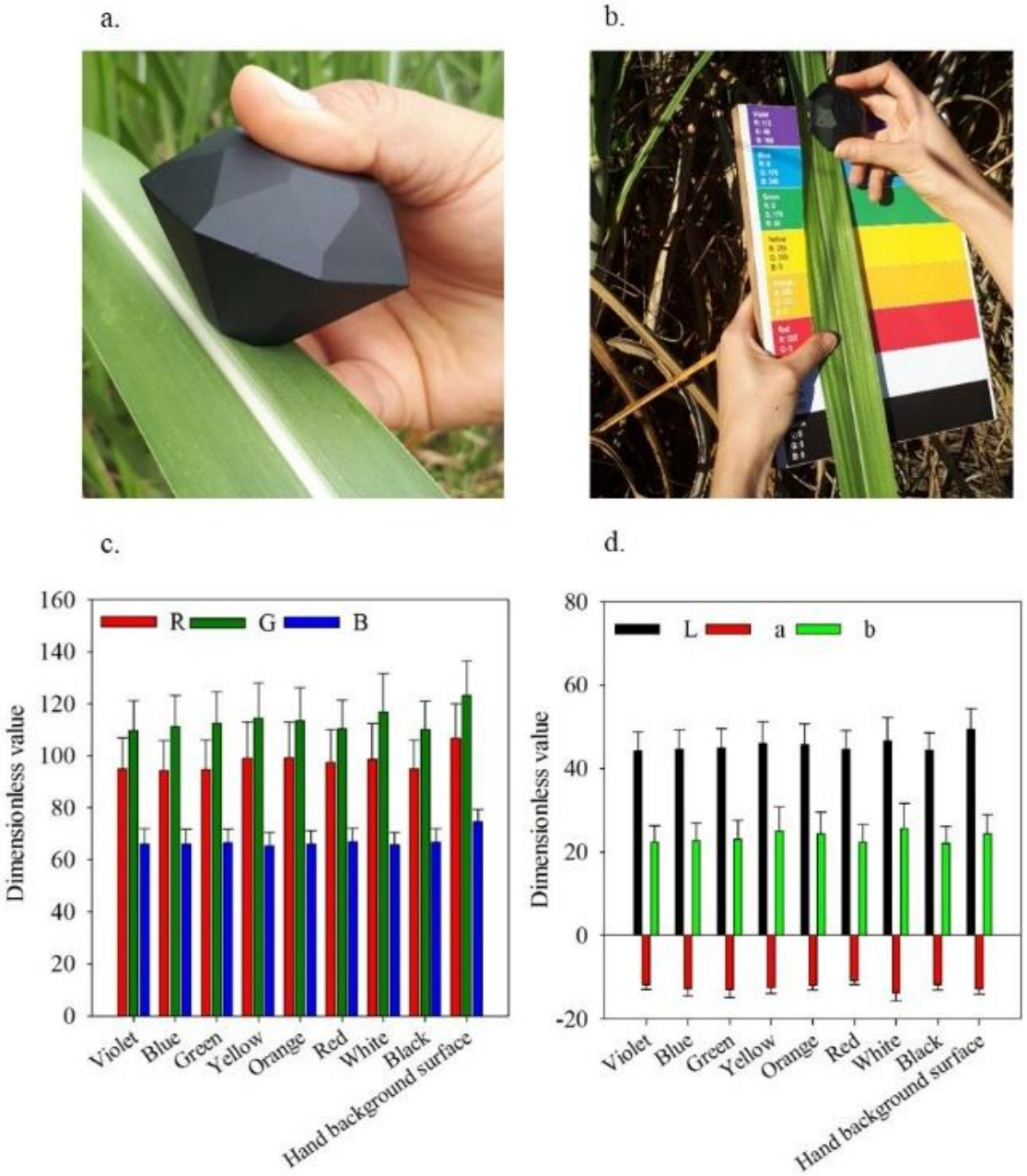

Figure A.1. Assessing the effect of background conditions to obtain the color of plant leaves using Nix™ Pro Color Sensor. (a) Holding the sugarcane leaf by hands assuring no influence of external light. (b) Assessing the color on different background surfaces. Comparison of different background surfaces and hands in the RGB (c) and CIELab (d) color systems. Error bars indicate the standard deviation (n = 20).

Observation: There was not significant difference between solid background surface having different colors and handheld.

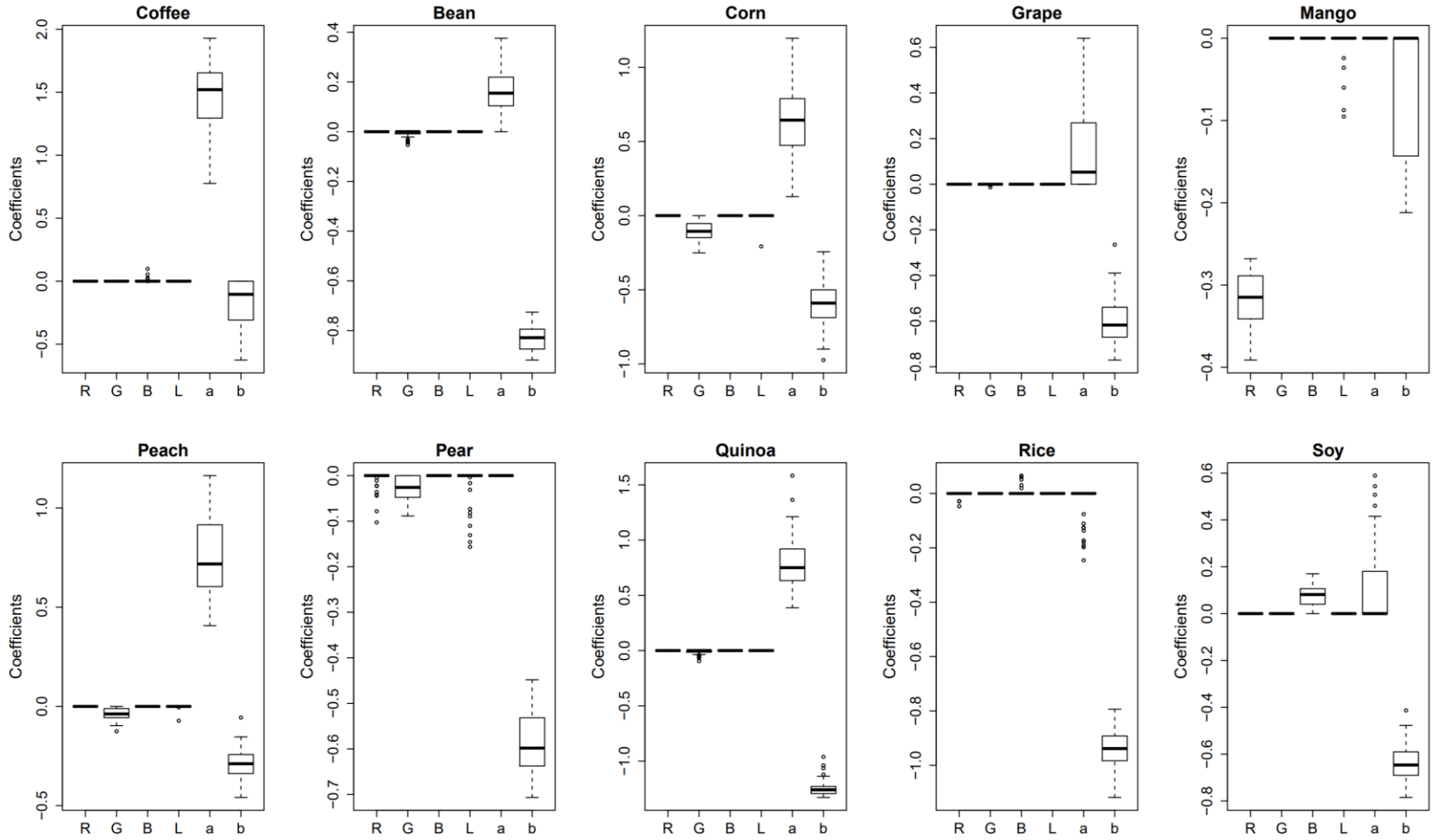

Figure A.2. LASSO model coefficients for all six Nix Pro color parameters.

References

Agarwal, A., Dutta Gupta, S., 2018. Assessment of spinach seedling health status and chlorophyll content by multivariate data analysis and multiple linear regression of leaf image features. Comput. Eletron. Agr. 152, 281–289. https://doi.org/10.1016/j.compag.2018.06.048

Aitkenhead, M.J., Dalgetty, I.A., Mullins, C.E., McDonald, A.J.S., Strachan, N.J., 2003. Weed and crop discrimination using image analysis and artificial intelligence methods. Comput. Eletron. Agr. 39, 157–171. https://doi.org/10.1016/S0168-1699(03)00076-0

Ali, A.M., Thind, H.S., Sharma, S., Varinderpal-Singh., 2014. Prediction of dry direct-seeded rice yields using chlorophyll meter, leaf color chart and GreenSeeker optical sensor in northwestern India. Field Crop Res. 161, 11–15. https://doi.org/10.1016/j.fcr.2014.03.001

Baldevbhai, P.J., Anand, R.S., 2012. Color image segmentation for medical images using L*a*b* color space. Journal of Electronics and Communication Engineering 1, 24–45. https://doi.org/10.9790/2834-0122445

Bang, T.C., Husted, S., Laursen, K.H., Persson, D.P., Schjoerring, J.K., 2020. The molecular-physiological functions of mineral macronutrients and their consequences for deficiency symptoms in plants. New Phytol. 229, 2446-2469. https://doi.org/ 10.1111/nph.17074

Barbedo, J.G.A., 2019. Detection of nutrition deficiencies in plants using proximal images and machine learning: A review. Comput. Eletron. Agr. 162, 482–492. https://doi.org/10.1016/j.compag.2019.04.035

Baresel, J.P., Rischbeck, P., Hu, Y., Kipp, S., Hu, Y., Barmeier, G., Mistele, B., 2017. Use of a digital camera as alternative method for non-destructive detection of the leaf chlorophyll content and the nitrogen nutrition status in wheat. Comput. Eletron. Agr. 140, 25–33. https://doi.org/10.1016/j.compag.2017.05.032

Borrell, A., Hammer, G., Van Oosterom, E., 2001. Stay-green: A consequence of the balance between supply and demand for nitrogen during grain filling. Ann. Appl. Biol. 138, 91–95. https://doi.org/10.1111/j.1744-7348.2001.tb00088.x

Carter, G.A., Knapp, A.K., 2001. Leaf optical properties in higher plants: Linking spectral characteristics to stress and chlorophyll concentration. Am. J. Bot. 88, 677–684. https://doi.org/10.2307/2657068

Cavallo, D.P., Cefola, M., Pace, B., Logrieco, A.F., Attolico, G., 2017. Contactless and non-destructive chlorophyll content prediction by random forest regression: A case study on fresh-cut rocket leaves. Comput. Eletron. Agr. 140, 303–310. https://doi.org/10.1016/j.compag.2017.06.012

Croft, H., Chen, J.M., Zhang, Y., 2014. Temporal disparity in leaf chlorophyll content and leaf area index across a growing season in a temperate deciduous forest. Int. J.Appl. Earth Obs. 33, 312–320. https://doi.org/10.1016/j.jag.2014.06.005

Dantas, A.A.A., Carvalho, L.G. de, Ferreira, E., 2007. Classificação e tendências climáticas em

Lavras, MG. Cienc. Agrotec. 31, 1862–1866. https://doi.org/10.1590/s1413-70542007000600039

Darkwa, K., Ambachew, D., Mohammed, H., Asfaw, A., Blair, M.W., 2016. Evaluation of common bean (*Phaseolus vulgaris L.*) genotypes for drought stress adaptation in Ethiopia. Crop J. 4, 367–376. https://doi.org/10.1016/j.cj.2016.06.007

Dey, A.K., Guha, P., Sharma, M., Meshram, M.R., 2018. Development of a RGB-based model for predicting SPAD value and chlorophyll content of betel leaf (*Piper betle L.*). J. Mech. Cont. & Math. Sci, 13, 1–16.

Dong, T., Shang, J., Chen, J.M., Liu, J., Quian, B., Ma, B., Morrison, M.J., Zhang, C., Liu, Y., Shi, Y., Pan, H., Zhou, G., 2019. Measuring crop leaf chlorophyll concentration. Remote Sens. 11, 2706. https://doi.org/10.3390/rs11222706

Errecart, P.M., Agnusdei, M.G., Lattanzi, F.A., Marino, M.A., 2012. Leaf nitrogen concentration and chlorophyll meter readings as predictors of tall fescue nitrogen nutrition status. Field Crop Res. 129, 46–58. https://doi.org/10.1016/j.fcr.2012.01.008

Fairchild, M.D., 2013. Color Appearance Models, 3rd ed. John Wiley & Sons, Ltd, West Sussex, England.

Ganesan, P., Rajini, V., Rajkumar, R.I., 2010. Segmentation and edge detection of color images using CIELAB Color Space and Edge detectors, in: International Conference on Emerging Trends in Robotics and Communication Technologies. Institute of Electrical and Eletronics Engineers, Chennai, India, pp. 393–397. https://doi.org/10.1109/INTERACT.2010.5706186

Ge, Y., Bai, G., Stoerger, V., Schnable, J.C., 2016. Temporal dynamics of maize plant growth, water use, and leaf water content using automated high throughput RGB and hyperspectral imaging. Comput. Eletron. Agr. 127, 625–632. https://doi.org/10.1016/j.compag.2016.07.028

Gitelson, A.A., Gritz, Y., Merzlyak, M.N., 2003. Relationships between leaf chlorophyll content and spectral reflectance and algorithms for non-destructive chlorophyll assessment in higher plant leaves. J. Plant Physiol. 160, 271–282. https://doi.org/10.1078/0176-1617-00887

Hill, B., Roger, T., Vorragen, F.W., 1997. Comparative analysis of the quantization of color spaces on the basis of the CIELAB color-difference formula. ACM T. Graphic. 16, 109–154. https://doi.org/10.1145/248210.248212

Hu, H., Liu, H.Q., Zhang, H., Zhu, J.H., Yao, X.G., Zhang, X. Bin, Zheng, K.F., 2010. Assessment of chlorophyll content based on image color analysis, comparison with SPAD-502, in: 2nd International Conference on Information Engineering and Computer Science. Institute of Electrical and Eletronics Engineers, Wuhan, China, pp. 1–3. https://doi.org/10.1109/ICIECS.2010.5678413

Huang, J., He, F., Cui, K., Buresh, R.J., Xu, B., Gong, W., Peng, S., 2008. Determination of optimal nitrogen rate for rice varieties using a chlorophyll meter. Field Crop Res. 105, 70–

80. https://doi.org/10.1016/j.fcr.2007.07.006

Kagiliery, J., Chakraborty, S., Acree, A., Weindorf, D.C., Brevik, E.C., Jelinski, N.A., Li, B., Jordan, C., 2019. Rapid quantification of lignite sulfur content: Combining optical and X-ray approaches. Int. J. Coal Geol. 216 https://doi.org/10.1016/j.coal.2019.103336.

Karcher, D.E., Richardson, M.D., 2003. Turfgrass science. Crop Sci. 43, 943–951. https://doi.org/10.2135/cropsci2003.9430

Karele, I., 2001. Chlorophyll content distribution in leaves, stems, and ears in winter wheat. In: Horst, W.J., Schenk, M.K., Bürkert, A., Claassen, N., Flessa, H., Frommer, W.B., Goldbach, H., Olfs, H.-W., Römheld, V., Sattelmacher, B., Schmidhalter, U., Schubert, S., von Wirén, N., & Wittenmayer, L. (Eds.), Plant Nutrition Food Security and Sustainability of Agro-Ecosystems through Basic and Applied Research. Kluwer Academic Publishers, The Netherlands, pp. 720–721. https://doi.org/10.1007/0-306-47624-x_349

Lindsey, A.J., Steinke, K., Rutan, J., Thomison, P.R., 2016. Relationship of DGCI and SPAD values to corn grain yield in the Eastern Corn Belt. Crop, Forage & Turfgrass Management, 2, 1-9. https://doi.org/10.2134/cftm2015.0184

Ling, Q., Huang, W., Jarvis, P., 2011. Use of a SPAD-502 meter to measure leaf chlorophyll concentration in *Arabidopsis thaliana*. Photosynth. Res. 107, 209–214. https://doi.org/10.1007/s11120-010-9606-0

Liu, K., Wiatrak, P., 2012. Corn production response to tillage and nitrogen application in dry-land environment. Soil Till. Res. 124, 138–143. https://doi.org/10.1016/j.still.2012.05.017

Liu, M., Liu, X., Li, M., Fang, M., Chi, W., 2010. Neural-network model for estimating leaf chlorophyll concentration in rice under stress from heavy metals using four spectral indices. Biosyst. Eng. 106, 223–233. https://doi.org/10.1016/j.biosystemseng.2009.12.008

Majer, P., Sass, L., Horváth, G.V., Hideg, E. 2010. Leaf hue measurements offer a fast, high-throughput initial screening of photosynthesis in leaves. J. Plant Physiol. 167, 74-76. https://doi:10.1016/j.jplph.2009.06.015

Mancini, M., Weindorf, D.C., Chakraborty, S., Silva, S.H.G., dos Santos Teixeira, A.F., Guilherme, L.R.G., Curi, N., 2019. Tracing tropical soil parent material analysis via portable X-ray fluorescence (pXRF) spectrometry in Brazilian Cerrado. Geoderma 337, 718–728. https://doi.org/10.1016/j.geoderma.2018.10.026

Manetas, Y., Grammatikopoulos, G., Kyparissis. 1998. The use of the portable, non-destructive, spad-502 (minolta) chlorophyll meter with leaves of varying trichome density and anthocyanin content. J. Plant. Physiol. 153, 513-516. https://doi.org/10.1016/S0176-1617(98)80182-X

Markwell, J., Osterman, J.C., Mitchell, J.L., 1995. Calibration of the Minolta SPAD-502 leaf chlorophyll meter. Photosynth. Res. 46, 467–472. https://doi.org/10.1007/BF00032301

Minolta Camera Co., Ltda., 1989. Manual for chlorophyll meter SPAD 502. Osaka, Minolta, Radiometric Instruments divisions. 22p.

Mizunuma, T., Mencuccini, M., Wingate, L., Ogée, J., Nichol, C., Grace, J., 2014. Sensitivity of colour indices for discriminating leaf colours from digital photographs. Methods Ecol. Evol. 5, 1078–1085. https://doi.org/10.1111/2041-210X.12260

Mukhopadhyay, S., Chakraborty, S., Bhadoria, P.B.S., Li, B., Weindorf, D.C., 2020. Assessment of heavy metal and soil organic carbon by portable X-ray fluorescence spectrometry and NixPro™ sensor in landfill soils of India. Geoderma Regional, 20, e00249. https://doi.org/10.1016/j.geodrs.2019.e00249

Netto, A.T., Campostrini, E., De Oliveira, J.G., Bressan-Smith, R.E., 2005. Photosynthetic pigments, nitrogen, chlorophyll a fluorescence and SPAD-502 readings in coffee leaves. Sci. Hortic. 104, 199–209. https://doi.org/10.1016/j.scienta.2004.08.013

Ocampo, A.L.P. de, Albo, J.B., Ocampo, K.J. de., 2015. Image Analysis of foliar greenness for quantifying relative plant health. International Research Journal on Innovations in Engineering, Science and Technology 1, 27–31.

Ohta, N., Robertson, A.R., 2005. Colorimetry Fundamentals and Applications. John Wiley & Sons, Ltd, West Sussex, England. https://doi.org/10.1002/0470094745

Pasuquin, J.M., Saenong, S., Tan, P.S., Witt, C., Fisher, M.J., 2012. Evaluating N management strategies for hybrid maize in Southeast Asia. Field Crop Res. 134, 153–157. https://doi.org/10.1016/j.fcr.2012.06.004

Patil, S.B., Bodhe, S.K., 2011. Leaf disease severity measurement using image processing. International Journal of Engineering and Technology 3, 297–301.

Peng, S., Garcia, F. V., Laza, R.C., Sanico, A.L., Visperas, R.M., Cassman, K.G., 1996. Increased N-use efficiency using a chlorophyll meter on high-yielding irrigated rice. Field Crop Res. 47, 243–252. https://doi.org/10.1016/0378-4290(96)00018-4

Piekielek, W.P., Fox, R.H., Toth, J.D., Macneal, K.E., 1995. Use of a chlorophyll meter at the early dent stage of corn to evaluate nitrogen sufficiency. Agron. J. 87, 403–408. https://doi.org/10.2134/agronj1995.00021962008700030003x

Prilianti, K.R., Yuwono, S.P., Adhiwibawa, M.A.S., Prihastyanti, M.N.P., Limantara, L., Brotosudarmo, T.H.P., 2014. Automatic leaf color level determination for need based fertilizer using fuzzy logic on mobile application: A model for soybean leaves, in: 6th International Conference on Information Technology and Electrical Engineering. Institute of Electrical and Eletronics Engineers, Yogyakarta, Indonesia, pp. 1–6. https://doi.org/10.1109/ICITEED.2014.7007895

Raeesi, M., Zolfaghari, A.A., Yazdani, M.R., Gorji, M., Sabetizade, M., 2019. Prediction of soil organic matter using an inexpensive colour sensor in arid and semiarid areas of Iran. Soil Res. 57, 276–286. https://doi.org/10.1071/SR18323

Ravier, C., Quemada, M., Jeuffroy, M.H., 2017. Use of a chlorophyll meter to assess nitrogen nutrition index during the growth cycle in winter wheat. Field Crop Res. 214, 73–82. https://doi.org/10.1016/j.fcr.2017.08.023

R Core Team., 2020. R: A Language and Environment for Statistical Computing. R Foundation for Statistical Computing. Vienna, Austria. Available online https://www.r-project.org/. (Verified on 13 May 2020).

Reis, A.R., Favarin, J.L., Malavolta, E., Júnior, J.L., Moraes, M.F., 2009. Photosynthesis, chlorophylls, and SPAD readings in coffee leaves in relation to nitrogen supply. Commun. Soil Sci. Plan. 40, 1512–1528. https://doi.org/10.1080/00103620902820373

Reyes, J.F., Correa, C., Zúñiga, J., 2017. Reliability of different color spaces to estimate nitrogen SPAD values in maize. Comput. Eletron. Agr. 143, 14–22. https://doi.org/10.1016/j.compag.2017.09.032

Riccardi, M., Mele, G., Pulvento, C., Lavini, A., 2014. Non-destructive evaluation of chlorophyll content in quinoa and amaranth leaves by simple and multiple regression analysis of RGB image components. Photosynth. Res. 120, 263–272. https://doi.org/10.1007/s11120-014-9970-2

Rolando, J.L., Ramírez, D.A., Yactayo, W., Monneveux, P., Quiroz, R., 2015. Leaf greenness as a drought tolerance related trait in potato (*Solanum tuberosum L.*). Environ. Exp. Bot. 110, 27–35. https://doi.org/10.1016/j.envexpbot.2014.09.006

Rorie, R.L., Purcell, L.C., Mozaffari, M., Karcher, D.E., Andy King, C., Marsh, M.C., Longer, D.E., 2011. Association of "Greenness" in corn with yield and leaf nitrogen concentration. Agron. J. 103, 529–535. https://doi.org/10.2134/agronj2010.0296

Rostami, M., Koocheki, A.R., Mahallati, M.N., Kafi, M., 2008. Evaluation of chlorophyll meter (SPAD) data for prediction of nitrogen status in corn (*Zea mays L.*). Am.-EUrasian J. Agric. Environ. 3, 79–85.

Shafagh-Kolvanagh, J., Zehtab-Salmasi, S., Javanshir, A., Moghaddam, M., Nasab, A.D.M., 2008. Effects of nitrogen and duration of weed interference on grain yield and SPAD (chlorophyll) value of soybean (*Glycine max (L.) Merrill*). J. Food Agric. Environ. 6, 368–373.

Shukla, A.K., Ladha, J.K., Singh, V.K., Dwivedi, B.S., Balasubramanian, V., Gupta, R.K., Sharma, S.K., Singh, Y., Pathak, H., Pandey, P.S., Padre, A.T., Yadav, R.L., 2004. Calibrating the leaf color chart for nitrogen management in different genotypes of rice and wheat in a systems perspective. Agron. J. 96, 1606–1621. https://doi.org/10.2134/agronj2004.1606

Singh, B., Singh, Y., Ladha, J.K., Bronson, K.F., Balasubramanian, V., Singh, J., Khind, C., 2002. Chlorophyll meter - and leaf color chart-based nitrogen management for rice and wheat in Northwestern India. Agron. J. 94, 821–829.

Singh, J.P., Pradhan, C., Das, S.C., 2020. Image processing and machine learning techniques to detect and classify paddy leaf diseases: A Review. In: Swain, D., Pattnaik, P.K., & Gupta, P.K. (Eds.), Machine Learning and Information Processing. Springer Nature Singapore Pte Ltd., Singapore, pp. 161–172. https://doi.org/10.1007/978-981-15-1884-3_4

Soureshjani, H.K., Nezami, A., Kafi, M., Tadayon, M., 2019. Responses of two common bean (*Phaseolus vulgaris L.*) genotypes to deficit irrigation. . Agr. Water Manage. 213, 270–279. https://doi.org/10.1016/j.agwat.2018.09.038

Steele, M.R., Gitelson, A.A., Rundquist, D.C., 2008. A comparison of two techniques for nondestructive measurement of chlorophyll content in grapevine leaves. Agron. J. 100, 779–782. https://doi.org/10.2134/agronj2007.0254N

Stiglitz, R., Mikhailova, E., Post, C., Schlautman, M., Sharp, J., 2016. Evaluation of an inexpensive sensor to measure soil color. Comput. Eletron. Agr. 121, 141–148. https://doi.org/10.1016/j.compag.2015.11.014

Tao, M., Ma, X., Huang, X., Liu, C., Deng, R., Liang, K., Qi, L., 2020. Smartphone-based detection of leaf color levels in rice plants. Comput. Eletron. Agr. 173, 105431. https://doi.org/10.1016/j.compag.2020.105431

Tibshirani, R., 1996. Regression shrinkage and selection via the lasso. J. Roy. Stat. Soc. B Met. 58, 267-288. https://doi.org/10.1111/j.2517-6161.1996.tb02080.x

Varinderpal, S., Yadvinder, S., Bijay, S., Thind, H.S., Kumar, A., Vashistha, M., 2011. Calibrating the leaf colour chart for need based fertilizer nitrogen management in different maize (*Zea mays L.*) genotypes. Field Crop Res. 120, 276–282. https://doi.org/10.1016/j.fcr.2010.10.014

Vesali, F., Omid, M., Kaleita, A., Mobli, H., 2015. Development of an android app to estimate chlorophyll content of corn leaves based on contact imaging Comput. Eletron. Agr. 116, 211–220. https://doi.org/10.1016/j.compag.2015.06.012

Vollmann, J., Walter, H., Sato, T., Schweiger, P., 2011. Digital image analysis and chlorophyll metering for phenotyping the effects of nodulation in soybean. Comput. Eletron. Agr. 75, 190–195. https://doi.org/10.1016/j.compag.2010.11.003

Witt, C., Pasuquin, J.M.C., Mutters, R., Buresh, R.J., 2005. New leaf color chart for effective nitrogen management in rice. Better Crops, 89, 36–39.

Wood, C.W., Reeves, D.W., Himelrick, D.G., 1993. Relationships between chlorophyll meter readings and leaf chlorophyll concentration, N status, and crop yield: A review. . P. Ag. Soc. Nz. 23, 1–9.

Xiong, D., Chen, J., Yu, T., Gao, W., Ling, X., Li, Y., Peng, S., Huang, J., 2015. SPAD-based leaf nitrogen estimation is impacted by environmental factors and crop leaf characteristics. Sci. Rep. 5, 1–12. https://doi.org/10.1038/srep13389

Yadav, S.P., Ibaraki, Y., Gupta, S.D., 2010. Estimation of the chlorophyll content of micropropagated potato plants using RGB based image analysis. Plant Cell Tiss. Org. 100, 183–188. https://doi.org/10.1007/s11240-009-9635-6

Yang, D., Li, M., Liu, Y., Chang, L., Cheng, H., Chen, J., Chai, S., 2016. Identification of quantitative trait loci and water environmental interactions for developmental behaviors

of leaf greenness in wheat. Front. Plant Sci. 7, 1–16. https://doi.org/10.3389/fpls.2016.00273

Yang, H., Yang, J., Lv, Y., He, J., 2014. SPAD values and nitrogen nutrition index for the evaluation of rice nitrogen status. Plant Prod. Sci. 17, 81–92. https://doi.org/10.1626/pps.17.81

Yao, X., Luo, W., 2012. Foliar image color features for rubber nitrogen deficiency status analysis. Adv. Mat. Res. 488–489, 1674–1679. https://doi.org/10.4028/www.scientific.net/AMR.488-489.1674

Yokoyama, A.H., Ribeiro, R.H., Balbinot Junior, A.A., Franchini, J.C., Debiasi, H., Zucareli, C., 2018. Índices de área foliar e SPAD da soja em função de culturas de entressafra e nitrogênio e sua relação com a produtividade. Revista de Ciências Agrárias, 41, 953–962. https://doi.org/10.19084/RCA18153

Yu, H., Wu, H.S., Wang, Z.J., 2010. Evaluation of SPAD and Dualex for in-season corn nitrogen status estimation. Acta Agronomica Sinica 36, 840–847. https://doi.org/10.1016/S1875-2780(09)60051-1

Yuan, Z., Cao, Q., Zhang, K., Ata-Ul-Karim, S.T., Tan, Y., Zhu, Y., Cao, W., Liu, X., 2016. Optimal leaf positions for SPAD meter measurement in rice. Front. Plant Sci. 7, 1–10. https://doi.org/10.3389/fpls.2016.00719

Zou, H., Hastie, T., 2005. Regularization and variable selection via the elastic net. J. Roy. Stat. Soc. B Met. 67, 301-320. https://doi.org/10.1111/j.1467-9868.2005.00503.x

FINAL CONSIDERATIONS

Environment and sustainable agricultural development requires the adoption of new methods and technologies. In this context, the use of sophisticated and portable sensors in the agricultural and environmental sciences is a reality. Nowadays, smart farming technologies have been gradually incorporated several sensors in the production system. In this work, the potential of portable X-ray fluorescence spectrometry (pXRF) for soil and plant characterization was reinforced. It was demonstrated that pXRF was efficient to assess the total elemental composition of an important wet ecosystem in the Brazilian Savannah. From this work, further studies in the field can be carried out contributing to still scarce inventory of wetland soils from Cerrado biome. Regarding plants, the determination of macro- and micronutrients in ground and sieved plant material via pXRF is really promising. Now, the great challenge and contribution will be to obtain the nutritional condition of plants directly in the field. Undoubtedly, this approach will contribute to the best management practices of soil and foliar fertilization. Excess or deficiency of a given plant nutrient could be easily assessed in seconds. To the best of our knowledge, this work showed for the first time the potential of a pocket-sized sensor to obtain the color of plant leaves, and several other studies can be performed to predict nutritional and physiological conditions of plants combining to other sensors able to assess the elemental composition and reflectance properties. Finally, it is believed that this doctoral thesis contributed to: "*Let's bring the lab to the field*".